12-2010

ELUCIDATING FUNCTIONAL ROLES FOR MYOGENIN IN ADULT SKELETAL MUSCLE METABOLISM, EXERCISE CAPACITY, AND REGENERATION

Jesse Flynn

ELUCIDATING FUNCTIONAL ROLES FOR MYOGENIN IN ADULT SKELETAL MUSCLE METABOLISM, EXERCISE CAPACITY, AND REGENERATION

by

Jesse Michael James Flynn, B.S.

APPROVED:

_____
William Klein, Ph.D.
Supervisory Professor

_____
James Martin, M.D., Ph.D.

_____
Michael Galko, Ph.D.

_____
Elsa Flores, Ph.D.

_____
John Putkey, Ph.D.

APPROVED:

_____
George Stancel, Ph.D.
Dean, The University of Texas
Graduate School of Biomedical Sciences at Houston

ELUCIDATING FUNCTIONAL ROLES FOR MYOGENIN IN ADULT SKELETAL MUSCLE METABOLISM, EXERCISE CAPACITY, AND REGENERATION

A

DISSERTATION

Presented to the Faculty of
The University of Texas
Health Science Center at Houston
And
The University of Texas
M. D. Anderson Cancer Center
Graduate School of Biomedical Sciences
in Partial Fulfillment

of the Requirements

for the Degree of

DOCTOR OF PHILOSOPHY

by

Jesse Michael James Flynn, B.S.

Houston, Texas

August, 2010

Acknowledgements

I thank my mentor, William Klein, PhD for his guidance, patience, and support over the years both professionally and personally. I owe Bill a great debt of gratitude for developing my critical thinking skills. I thank the members of the Klein laboratory for their assistance, advice, and camaraderie. Thanks to my former and current committee members, James Martin, MD, PhD, Michael Galko, PhD, Elsa Flores, PhD, John Putkey, PhD, Miles Wilkinson, PhD, Yi-Ping Li, PhD, and Zhimin Lu, PhD. Their constructive criticism and advice have been instrumental in my development as a scientist.

I thank Eric Meadows and Melanie Ramón for being true friends. Thanks also to my parents, Kerry and Patti Flynn for their love and support over my entire life.

I thank my wife, Amy Elisabeth Flynn for more than can be expressed in words. Because of her, I can be who I am and have become more than I thought I could.

ELUCIDATING FUNCTIONAL ROLES FOR MYOGENIN IN ADULT SKELETAL MUSCLE METABOLISM, EXERCISE CAPACITY, AND REGENERATION

Publication No._____

Jesse Michael James Flynn, Ph. D.

Supervisory Professor: William Klein, Ph.D.

The four basic helix-loop-helix myogenic transcription factors, myogenin, Myf5, MRF4, and MyoD are critical for embryonic skeletal muscle development. Myogenin is necessary for the terminal differentiation of myoblasts into myofibers during embryogenesis, but little is known about the roles played by myogenin in adult skeletal muscle function and metabolism. Furthermore, while metabolism is a well-studied physiological process, how it is regulated at the transcriptional level remains poorly understood. In this study, my aim was to determine the function of myogenin in adult skeletal muscle metabolism, exercise capacity, and regeneration. To investigate this, I utilized a mouse strain harboring the $Myog^{flox}$ allele and a Cre recombinase transgene, enabling the efficient deletion of myogenin in the adult mouse. $Myog^{flox/flox}$ mice were stressed physically through involuntary treadmill running and by breeding them with a strain harboring the Duchenne's muscular dystrophy (DMD^{mdx}) allele. Surprisingly, *Myog*-deleted animals exhibited an enhanced capacity for exercise, running farther and faster

than their wild-type counterparts. Increased lactate production and utilization of glucose as a fuel source indicated that *Myog*-deleted animals exhibited an increased glycolytic flux. Hypoglycemic *Myog*-deleted mice no longer possessed the ability to outrun their wild-type counterparts, implying the ability of these animals to further deplete their glucose reserves confers their enhanced exercise capacity. Moreover, *Myog*-deleted mice exhibited an enhanced response to long-term exercise training. The mice developed a greater proportion of type 1 oxidative muscle fibers, and displayed increased levels of succinate dehydrogenase activity, indicative of increased oxidative metabolism. *Mdx:Myog*-deleted mice exhibited a similar phenotype, outperforming their *mdx* counterparts, although lagging behind wild-type animals. The morphology of muscle tissue from *mdx:Myog*-deleted mice appears to mimic that of *mdx* animals, indicating that myogenin is dispensable for adult skeletal muscle regeneration. Through global gene expression profiling and quantitative (q)RT-PCR, I identified a unique set of putative myogenin-dependent genes involved in regulating metabolic processes. These data suggest myogenin's functions during adulthood are distinctly different than those during embryogenesis, and myogenin acts as a high-level transcription factor regulating metabolic activity in adult skeletal muscle.

TABLE OF CONTENTS

LIST OF ILLUSTRATIONS

List of Tables

ABBREVIATIONS

Bdh1	3-hydroxybutyrate dehydrogenase-type 1
bHLH	Basic helix-loop-helix
CK	Creatine Kinase
DMD	Duchenne muscular dystrophy
Dpyd	dihydropyrimidine dehydrogenase
F1,6BP	fructose-1,6-bisphosphate
F6P	fructose-6-phosphate
Fbxo32	F-box protein 32
Glut4	Glucose transporter 4
Gys	glycogen synthase
HDAC4	histone deacetylase 4
MRF	Myogenic Regulatory Factor
myHC	Myosin heavy chain
nNOS	neuronal nitric oxide synthase
Pc	pyruvate carboxylase
PFK	phosphofructokinase
PFK1	6-phosphofructo-1-kinase
PFK2	phosphofructokinase 2
Pfkfb3	6-phosphofructo-2-kinase/fructose-2,6-biphosphatase 3
SDH	succinate dehydrogenase

TCR	Transcriptional control region
Trim63	Tripartite motif-containing 63
qRT-PCR	Quantitative Real-Time Polymerase Chain Reacton

CHAPTER I:

Myogenin regulates adult skeletal muscle metabolism and exercise capacity

INTRODUCTION:

The myogenic regulatory factors (MRFs), MyoD [1], Myf5 [2], MRF4 [3-5], and myogenin [6, 7], are basic helix-loop-helix (bHLH) transcription factors best known for regulating skeletal muscle development during the embryonic stages of life [8]. While their functions during adult life are less well known, persistent expression of these factors into adulthood suggests they play a significant role during this time. During embryonic development, Myf5 and MyoD are required for the earlier stages of myoblast determination. In the absence of Myf5, postnatal (P)0 pups exhibit seemingly normal skeletal muscle at birth, but die soon thereafter due to improper rib development [9, 10]. MyoD-null mice are viable and display normal skeletal muscle. In the absence of both Myf5 and MyoD, P0 pups posses no skeletal muscle or skeletal muscle stem cells [11]. Myogenin is required for the latter stages of myoblast differentiation. *Myog*-null mice die perinatally due to severe skeletal muscle deficiency [12]. However, adult myogenin conditional knock-out mice deleted at P1 are viable with normal muscle, although they have 37% less body mass [13]. This suggests that myogenin is dispensable for postnatal development and survival, but plays a role in overall body homeostasis.

Skeletal muscle is composed of a highly complex and organized arrangement of structures designed for contraction and movement. (Figure 1)

Figure 1

Components and structural characteristics of skeletal muscle. (A) Illustration of a whole muscle cross section broken down into myofibers. (B) Illustration of a myofiber cross section broken down into myofibrils. (C) Structure of a sarcomere and the organization of its components. (D) Diagram of proteins comprising the thick and thin filaments of a sarcomere.

A. **B.**

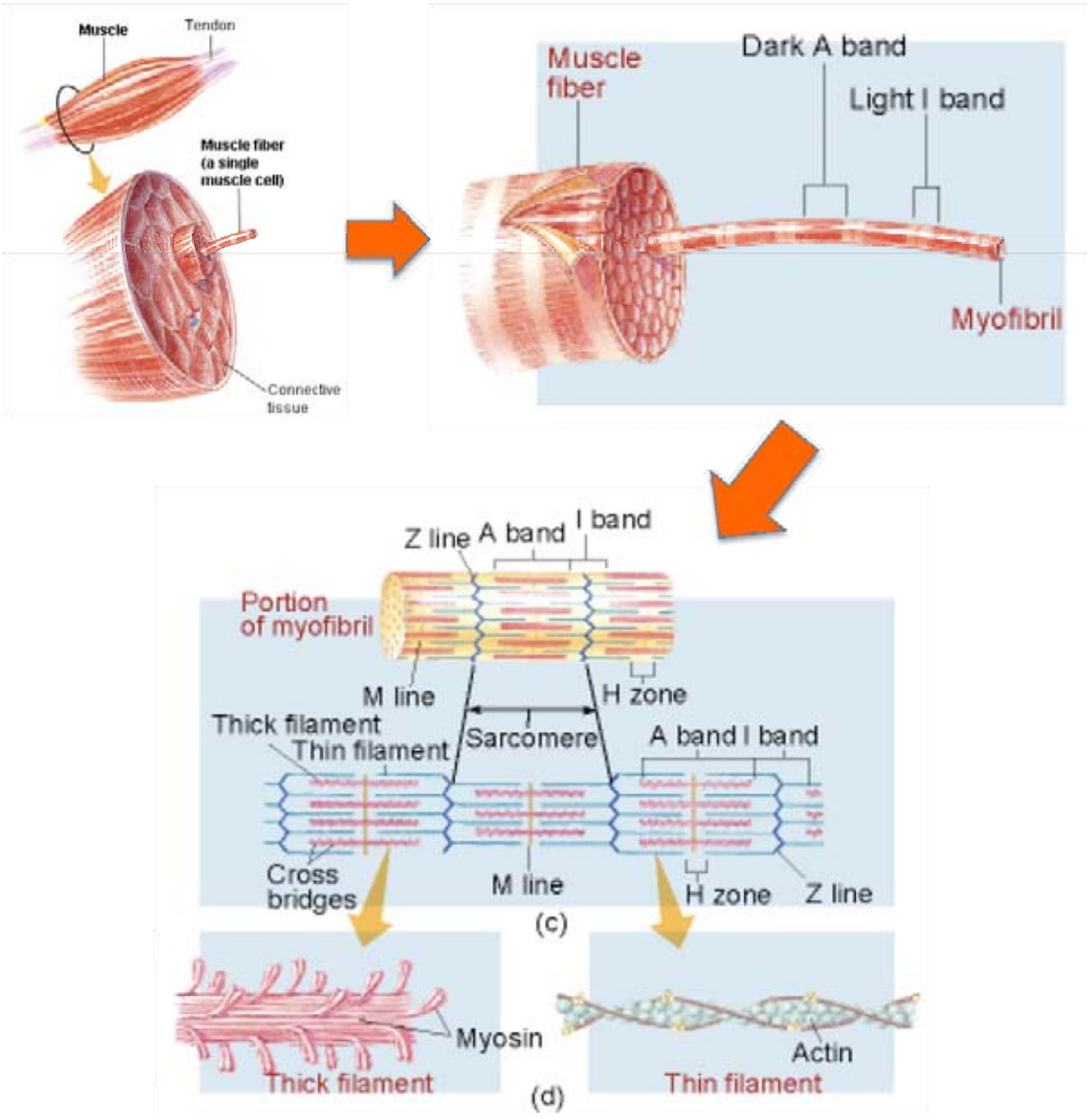
Muscle
Tendon
Muscle fiber (a single muscle cell)
Connective tissue
Muscle fiber
Dark A band
Light I band
Myofibril
Z line
A band
I band
Portion of myofibril
M line
H zone
Thick filament
Thin filament
Sarcomere
A band
I band
Cross bridges
M line
H zone
Z line
(c)
Myosin
Thick filament
Actin
Thin filament
(d)

[for review, see 14]. Muscles are composed of numerous muscle fibers. Each fiber is further broken down to individual myofibrils. Myofibrils contain the functional contraction unit of skeletal muscle, the sarcomere. Sarcomeres are composed of thick myosin filaments in between thin actin filaments and are linked from end to end by the Z line. Myosin filaments contain thick globular heads with an actin-binding site and a Myosin ATPase site. Actin filaments are enwrapped by tropomyosin and troponin. Tropomyosin functions to conceal actin's myosin binding site. Troponin is composed of three polypeptide units which bind actin, tropomyosin, and Ca^{2+}. It functions to secure tropomyosin's location over actin's myosin binding site. During contraction, Ca^{2+} is released from the sarcoplasmic reticulum surrounding the muscle fibers and binds to troponin. Troponin then undergoes a conformational change causing tropomyosin to shift positions and expose actin's myosin binding site. ATP-bound myosin then binds to actin, and through the dephosphorylation of ATP to ADP, the myosin head shifts toward the center of the sarcomere. This is called the actomyosin crossbridge, or power stroke. The power stroke brings the actin filaments closer together causing contraction. Relaxation is then achieved by the active transport of Ca^{2+} back in to the sarcoplasmic reticulum via a Ca^{2+} – ATPase pump. This ultimately causes tropomyosin to shift back to its resting position and cover actin's myosin binding sites. This well-developed arrangement of factors provides a foundation through which motion and exercise can be performed.

All vertebrate organisms posses a wide variety of skeletal muscle fibers designed to support the skeletal system that are specialized to maintain body posture as well as perform a myriad of movements and functions [15]. Depending on which myosin heavy chain (myHC) isoform is expressed, they are categorized as types 1, 2A, and 2B [16]. Expression of a particular MyHC isoform dictates the contraction speed for a given fiber [17, 18]. Type 1 fibers, expressing MyHC type 1, contract the slowest while fiber types 2A and 2B contract more rapidly. The endurance of a fiber is largely dependent on the rate by which ATP can be supplied by the tissue during contraction to complete the power stroke cycle [14]. ATP is produced in skeletal muscle via both glycolysis and the citric acid cycle. Glucose is acquired by the intramuscular conversion of glycogen to glucose or can be transported into the muscle from the liver via the blood stream by transporter factors such as Glucose Transporter 4 (Glut4). Glucose is first metabolized anaerobically via glycolysis in the cytoplasm. This process quickly produces 2 net ATP molecules and is the primary source for ATP in the absence of oxygen. Glucose is converted to two pyruvic acid molecules, which then enter the citric acid cycle to undergo oxidative phosphorylation in the mitochondria. This is the primary source for ATP in the presence of oxygen and produces 36 net ATP per glucose molecule.

The rate limiting steps for the production of ATP are regulated by metabolic enzymes. Oxidative enzymes found in Type 1 and 2A fibers supply a slow but constant store of ATP by aerobically metabolizing pyruvic acid derived from glucose furnished by the blood stream. Glycolytic enzymes more prevalent

in type 2B fibers quickly and anaerobically metabolize glucose derived from glycogen supplied by the muscle fiber. This mode of ATP production quickly exhausts glycogen reserves and is only sustainable for short bursts of energy. Thus, oxidative type 1 and 2A fibers are more resistant to fatigue and are required for endurance and skeletal support whereas glycolytic type 2B fibers fatigue more quickly and are utilized for rapid bursts of speed and strength.

Environmental pressures can incite drastic phenotypic alterations in existing mature adult skeletal muscle fibers [19]. Experimentally induced modifications in contraction activity are also known to incite fiber type shifts [20, 21]. These conversions demand tremendous alterations in physical activity for extensive periods of time [22]. As a result, significant modifications in fiber character are often not observed in mammalian exercise training studies [23]. Thus long term studies are necessary for determining experimental effects on skeletal muscle function.

Myogenin has previously been implicated in multiple aspects of mature skeletal muscle function. Denervated adult muscle tissue expresses increased levels of myogenin [24, 25]. However, *Myog*-deleted adult mice are known to be resistant to neurogenic muscle atrophy due to the downregulation of proteolytic factors [26]. These studies provide a link between myogenin and mature muscle fiber turnover. *Myog* mRNA is preferentially expressed in adult slow-twitch (type 1) muscle fibers while *MyoD* transcripts are of greater abundance in fast-twitch (type 2) fibers [27]. Furthermore, the overexpression of myogenin in mature skeletal muscle tissue has been shown to incite shifts in enzymatic activity from

glycolytic to oxidative metabolism [28]. Thus myogenin makes for a good candidate gene to study when investigating the regulatory roles of MRF's in adult exercise and metabolism.

The recent generation of a mouse strain harboring the *Myog*^{flox} allele and a Cre recombinase transgene allow for the study of myogenin in the adult mouse. In the present study, *Myog*-deleted adult mice exhibited an enhanced capacity for exercise in response to physical stress and were able to further deplete their glucose stores before reaching exhaustion. Furthermore, these animals displayed an enhanced response to exercise training when given long-term access to running wheels. Global gene expression analysis reveals alterations in the expression of metabolic enzymes in the absence of myogenin. Shifts in metabolic enzyme content may be contributing to the conferment of these observed phenomena.

RESULTS:

Tamoxifen injection of adult *Myog*$^{flox/flox}$:Cre+ mice results in efficient deletion of *Myog*

A mouse strain harboring the *Myog*^{flox} allele and a Cre recombinase transgene was recently generated in the Klein laboratory [29]. While efficient deletion of *Myog* from the genome of these animals during the embryonic and perinatal stages of life had already been achieved, this had never been attempted during adult life. A single injection of tamoxifen at a dose of 10 mg/40 g of body weight was found to result in a greater than 90% deletion of genomic DNA (Figure 2A). *Myog* transcript levels were determined to be less than 5% of their wild-type counterparts (Figure 2B).

Myog-deleted adult mice exhibit an enhanced capacity for exercise and oxidative metabolism under low-intensity stress conditions

To determine the exercise capacity for *Myog*-deleted mice under low-intensity stress conditions, adult *Myog*-deleted mice were run to exhaustion at a slow, constant speed of 20m/min at 0° incline (Figure 3). These conditions are designed to assess endurance since they primarily employ the use of type 1 slow twitch muscle fibers and oxidative metabolism.

Wild-type mice (tamoxifen-injected Myog$^{flox/flox}$) ran on average 4,000 meters before reaching exhaustion whereas their *Myog*-deleted counterparts ran almost 10,000 meters (Figure 4), a significant 2.4 fold difference. Remarkably, some of these animals ran for more than ten hours before reaching exhaustion.

Figure 2

Efficient deletion of *Myog* in the adult mouse. (A) A single tamoxifen injection at 10mg/40g body weight results in >90% deletion of Myog from $Myog^{flox/flox}$;Cre+ mice (Myog-deleted, n=10; wild-type n=10). Green bar represents *Myog*-deleted values. Red bar represents wild-type control values. Error bars represent one standard deviation (**P*<0.05). (B) *Myog* transcript levels are also reduced by over 95% in $Myog^{flox/flox}$;Cre+ mice. Green bar represents *Myog*-deleted values (n=3). Red bar represents wild-type control values (n=3). Error bars represent one standard deviation (**P*<0.05).

A.

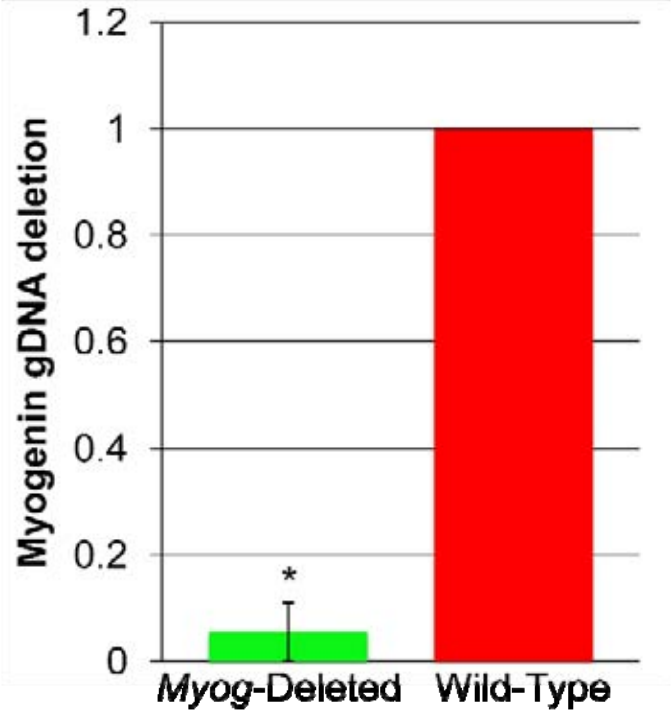
Myogenin gDNA deletion
1.2
1
0.8
0.6
0.4
0.2
0
*
Myog-Deleted
Wild-Type

B.

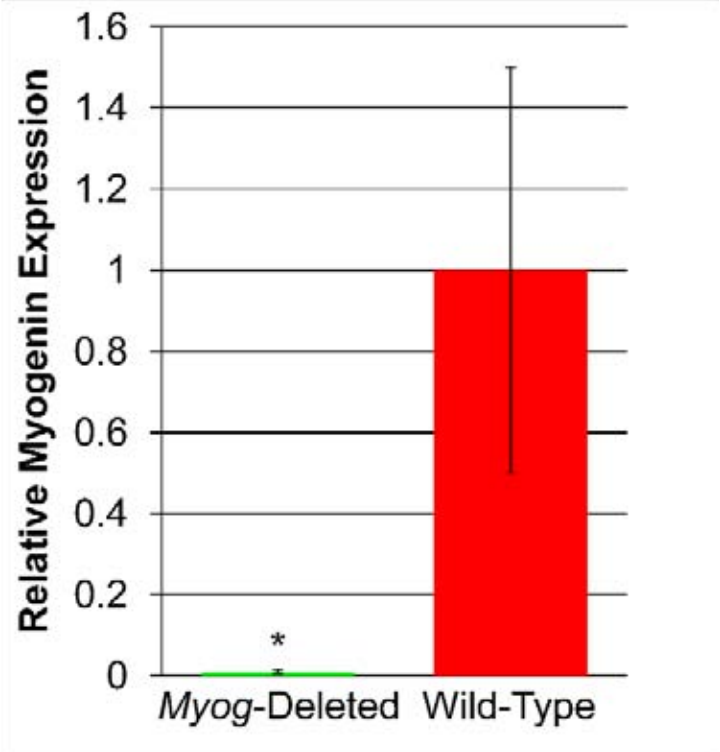
Relative Myogenin Expression
1.6
1.4
1.2
1
0.8
0.6
0.4
0.2
0
*
Myog-Deleted
Wild-Type

Figure 3

Representation of low- and high-intensity treadmill exercise regimens. The low-intensity regimen (in blue) maintains a constant speed of 20m/min until exhaustion, resulting in the mice running the same distance over any given period of time after the initial warm up period. This regimen is designed to employ primarily oxidative metabolism. The high-intensity regimen (in red) entails increasing the speed of the treadmill by 2m/min every 2 minutes until exhaustion. This results in the mice running ever increasing distances over a given two minute period as time goes on. This regimen is designed to employ glycolytic metabolism.

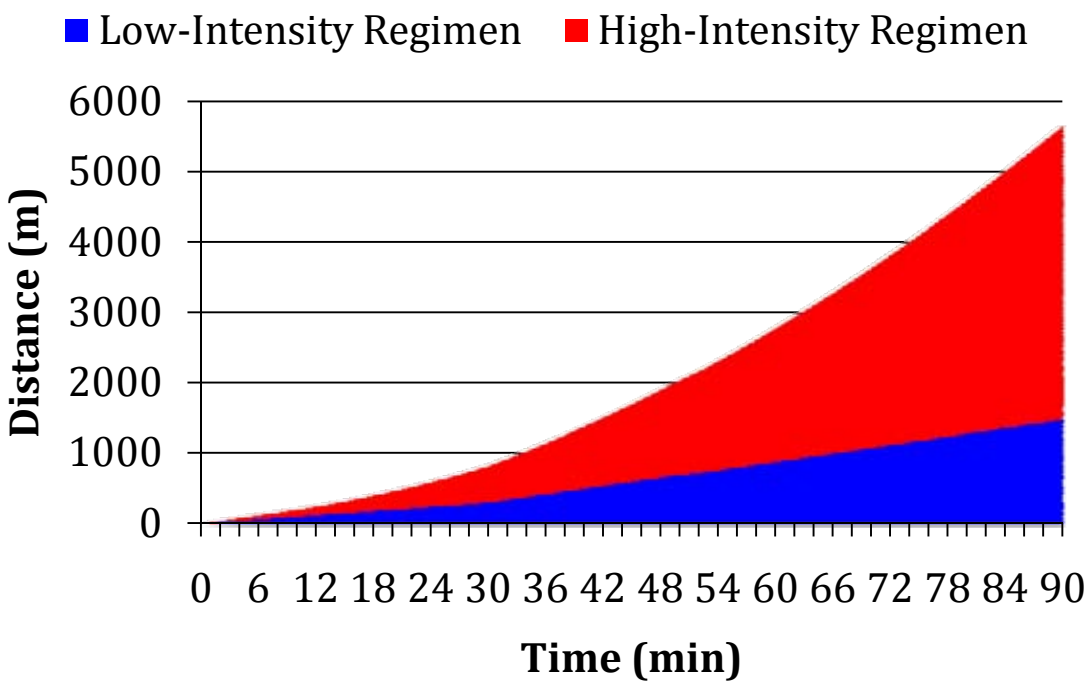
Low-Intensity Regimen
High-Intensity Regimen
Distance (m)
6000
5000
4000
3000
2000
1000
0
0 6 12 18 24 30 36 42 48 54 60 66 72 78 84 90
Time (min)

Figure 4

Enhanced exercise capacity in *Myog*-deleted mice during the low-intensity exercise regimen. *Myog*-deleted mice ran 2.4 fold more than the wild-type control group under the low-intensity exercise regimen (*Myog*-deleted, n=4; wild-type n=5). Green bar represents *Myog*-deleted values. Red bar represents wild-type control values. Error bars represent one standard deviation (*P<0.05).

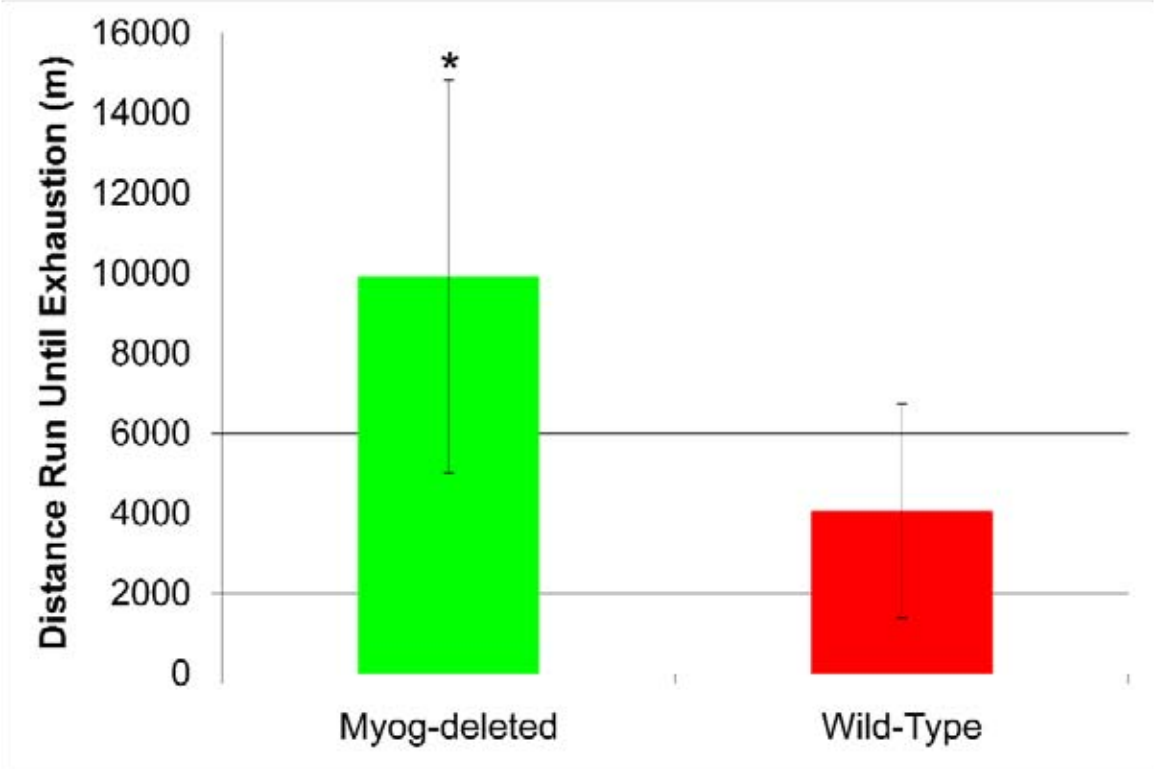
Distance Run Until Exhaustion (m)
16000
14000
12000
10000
8000
6000
4000
2000
0
*
Myog-deleted
Wild-Type

To begin investigating the observed difference in exercise capacity, blood lactate and glucose levels were recorded at baseline and exhaustion to gain insight to the metabolic processes at work. Lactate is a product of glycolysis, and increased lactate at exhaustion is a commonly used indicator of glycolytic metabolism. In contrast, unchanged lactate levels would be expected during the use of oxidative metabolism [30]. Under aerobic endurance conditions such as these, glucose accessed via the blood stream would be the expected fuel source whereas glucose converted from glycogen in the muscle would be primarily utilized during anaerobic stress conditions such as high-intensity sprinting.

Baseline blood lactate levels were virtually identical between the wild-type and *Myog*-deleted groups and increased only slightly at exhaustion (Figure 5). These constant blood lactate levels were consistent with the employment of oxidative metabolism during this aerobic, low-intensity exercise regimen. Blood glucose levels for both wild-type and *Myog*-deleted mice were virtually equal at baseline but were both dramatically decreased at exhaustion (Figure 6). Decreased blood glucose levels are also consistent with the use of oxidative metabolism during this assay. Moreover, blood glucose levels of *Myog*-deleted mice were less than half that of their wild-type counterparts at exhaustion. The data implied that *Myog*-deleted mice were able to further deplete their glucose stores before reaching exhaustion and utilized this as a source of energy. This may give *Myog*-deleted mice a competitive advantage by conferring upon them an enhanced capacity for exercise.

Figure 5

Blood lactate levels in *Myog*-deleted and wild-type mice at baseline and after running to exhaustion under the low-intensity exercise regimen. At baseline, blood lactate levels were virtually equal between the *Myog*-deleted and wild-type groups at approximately 3 mmol/L (*Myog*-deleted, n=4; wild-type n=5). At exhaustion, blood lactate levels for both groups only modestly increased from baseline and were virtually equal between the Myog-deleted and wild-type groups at approximately 4.5 mmol/L. Green bars represent *Myog*-deleted values. Red bars represent wild-type control values. Error bars represent one standard deviation.

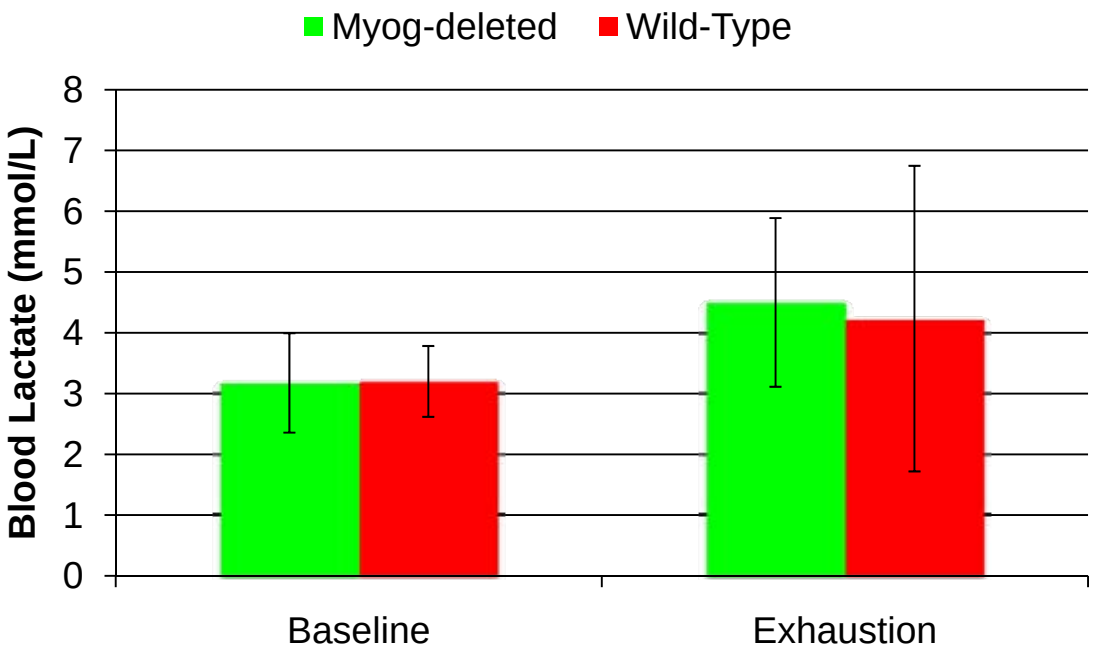
Myog-deleted
Wild-Type
Blood Lactate (mmol/L)
8
7
6
5
4
3
2
1
0
Baseline
Exhaustion

Figure 6

Blood glucose levels in *Myog*-deleted and wild-type mice at baseline and after running to exhaustion under the low-intensity exercise regimen. At baseline, blood glucose levels were virtually equal between the *Myog*-deleted and wild-type groups at approximately 150 mg/dL (*Myog*-deleted, n=4; wild-type n=5). At exhaustion, blood glucose values were significantly reduced for both groups. However, Myog-deleted values were significantly less than wild-type control values. Green bars represent *Myog*-deleted values. Red bars represent wild-type control values. Error bars represent one standard deviation (*$P<0.05$).

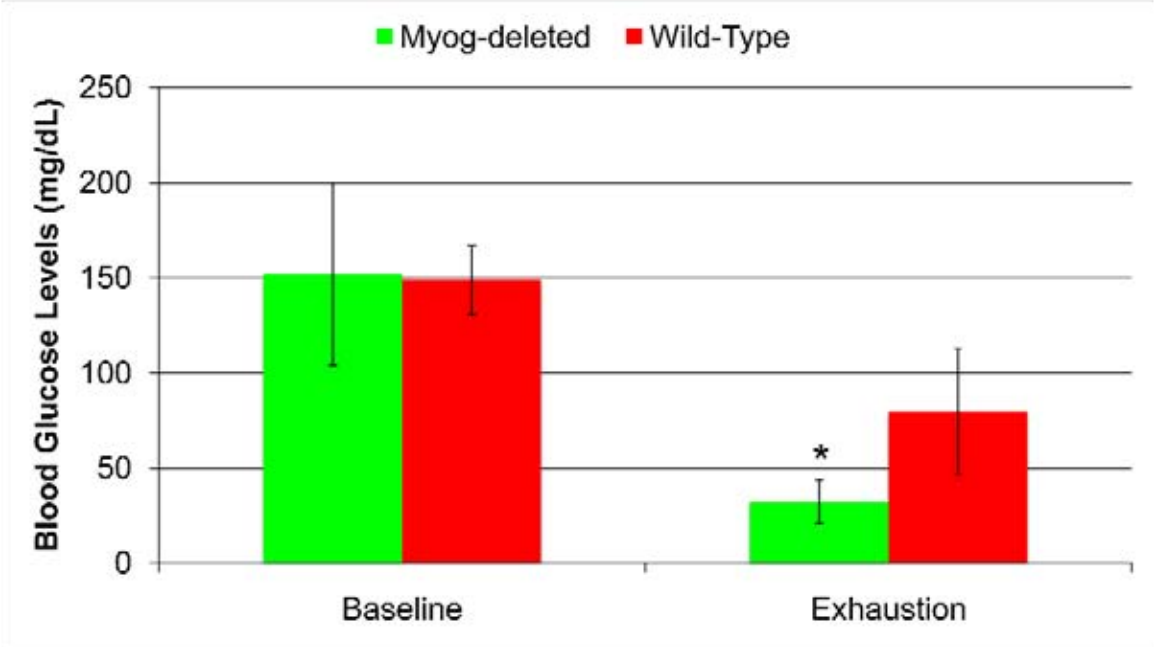
Myog-deleted
Wild-Type
Blood Glucose Levels (mg/dL)
250
200
150
100
50
0
*
Baseline
Exhaustion

To investigate metabolic and physiological changes in the muscle fibers of *Myog*-deleted mice, analyses were performed to determine fiber type proportions, expression levels of succinate dehydrogenase (SDH), transcript abundance of genes regulating fatty acid metabolism, and metabolic enzyme activity levels.

Fiber typing analysis indicated there was no difference in the proportions of type 1 and type 2 muscle fibers between wild-type and *Myog*-deleted mice (Figure 7). This was expected as these mice had not been exposed to long-term training conditions. Transcript levels for Myosins 1, 2A, and 2B were also determined to be equal between the two groups in the gastrocnemius muscle (Figure 8). SDH is a component of the mitochondrial electron transport chain, and its prevalence is an indicator of overall mitochondrial activity and the aerobic potential of muscle fibers. Assays for SDH revealed equal levels of activity in both groups (Figure 9). No differences were detected in the transcript levels of a panel of genes regulating fatty acid metabolism and Glut4 (Figure 10). Furthermore, assays detecting the enzymatic activities for a panel of both oxidative and glycolytic enzymes determined there to be no differences between the wild-type and *Myog*-deleted groups in either the slow twitch soleus muscle or the fast twitch extensor digitorum longus muscle (Figure 11). Thus, *Myog*-deleted adult mice outran their wild-type counterparts under slow, oxidative conditions but did not display the typical characteristic changes commonly associated with enhanced aerobic exercise capacity.

Figure 7

Fiber type proportion in *Myog*-deleted and wild-type mice run to exhaustion under the low-intensity regimen. *Myog*-deleted and wild-type mice did not exhibit a significant difference in the proportions of Type 1 and Type 2 muscle fibers in the soleus muscle (*Myog*-deleted, n=3; wild-type n=3). Green bar represents *Myog*-deleted values. Red bar represents wild-type control values. Error bars represent one standard deviation.

Myog-deleted

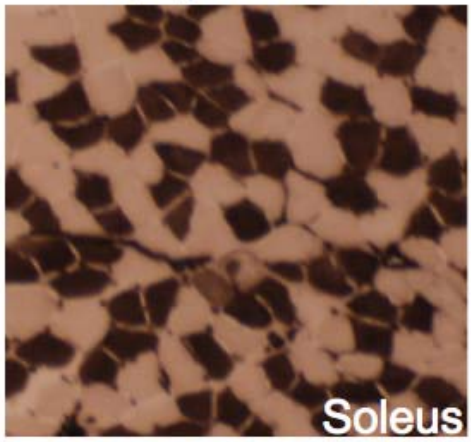

Wild-Type

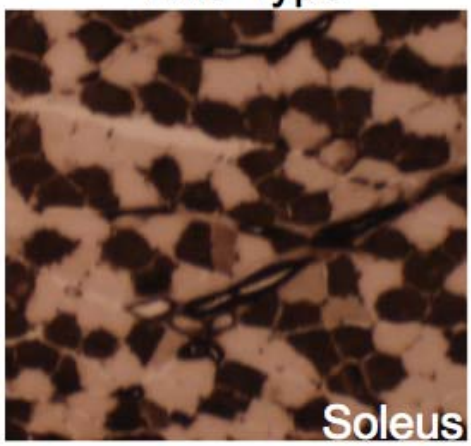

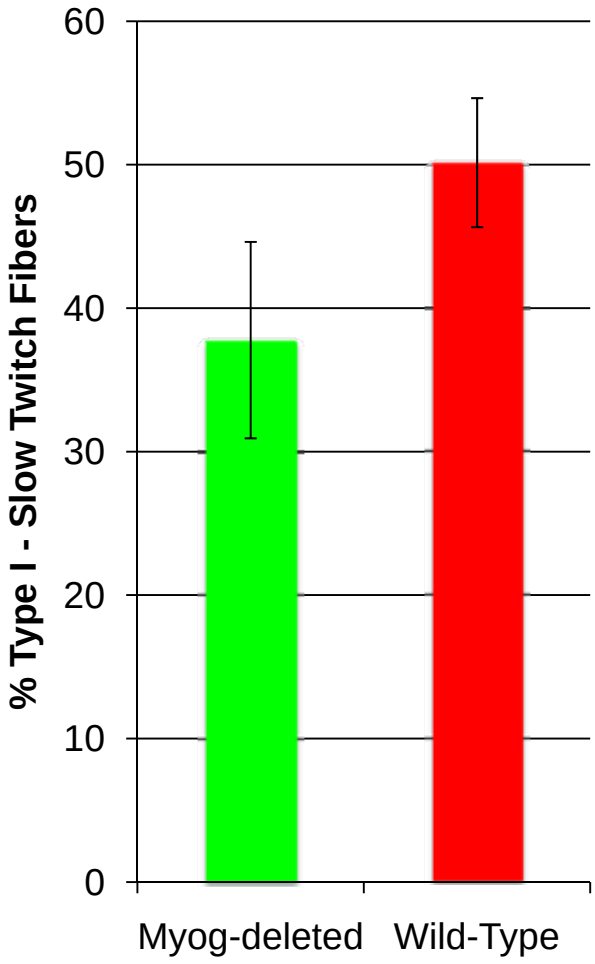

Figure 8

Transcript expression levels of Myosins Type 1, 2A, and 2B. *Myog*-deleted and wild-type mice did not exhibit a significant difference in the expression of these factors in the Gastrocnemius muscle (*Myog*-deleted, n=3; wild-type n=3). Green bars represent *Myog*-deleted values. Red bars represent wild-type control values. Error bars represent one standard deviation.

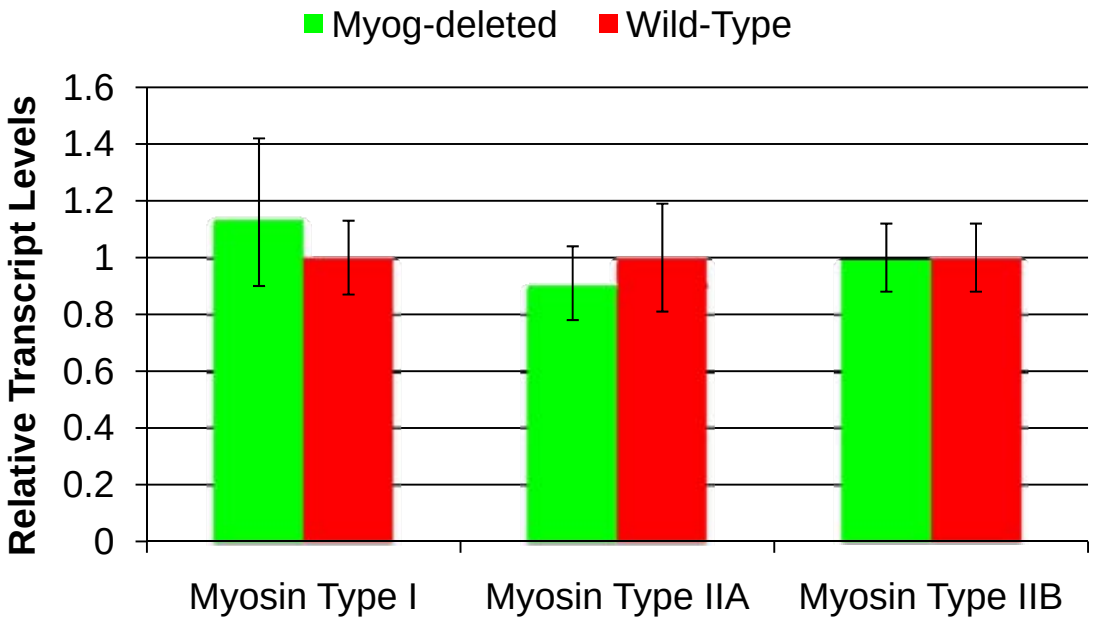
Myog-deleted
Wild-Type
Relative Transcript Levels
1.6
1.4
1.2
1
0.8
0.6
0.4
0.2
0
Myosin Type I
Myosin Type IIA
Myosin Type IIB

Figure 9

Succinate dehydrogenase (SDH) activity in *Myog*-deleted and wild-type mice run to exhaustion under the low-intensity regimen. *Myog*-deleted and wild-type mice did not exhibit a significant difference in SDH activity in the Gastrocnemius muscle (*Myog*-deleted, n=3; wild-type n=3). Green bar represents *Myog*-deleted values. Red bar represents wild-type control values. Error bars represent one standard deviation.

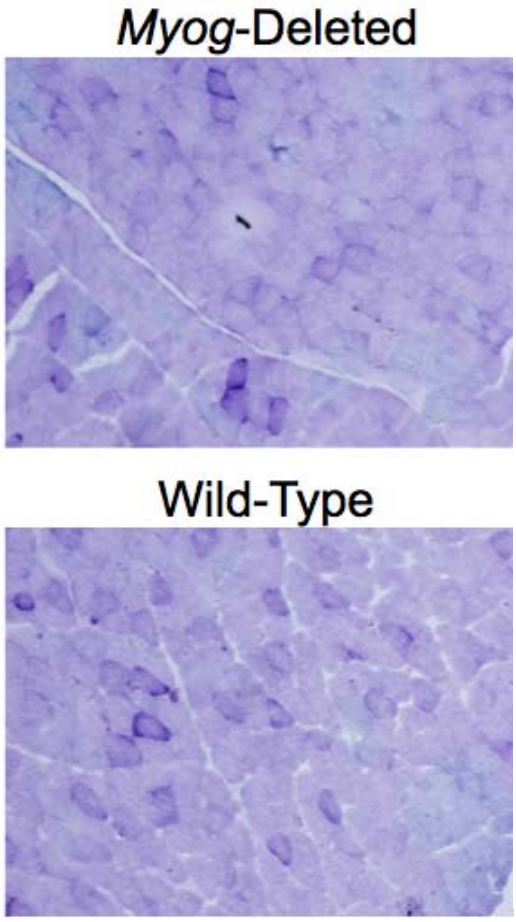
Myog-Deleted
Wild-Type

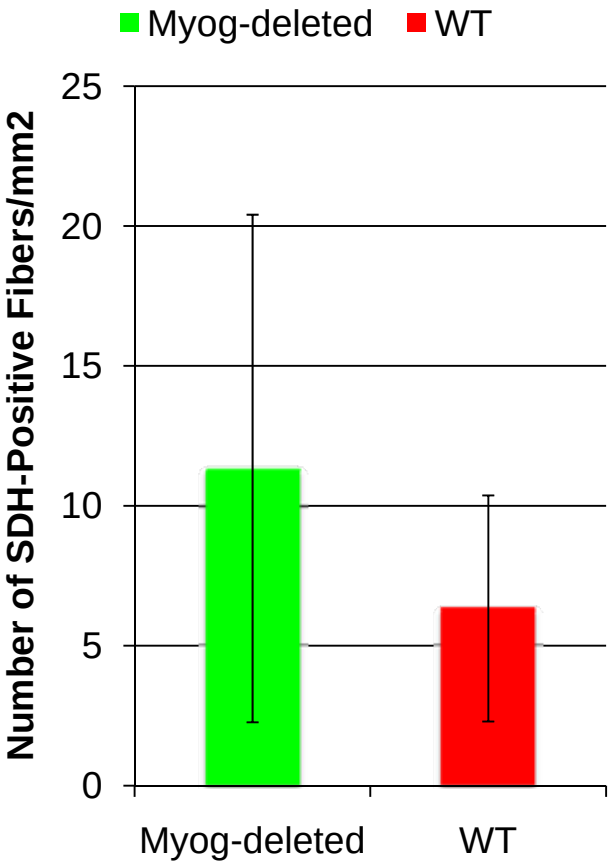
Myog-deleted
WT
Number of SDH-Positive Fibers/mm2
25
20
15
10
5
0
Myog-deleted
WT

Figure 10

Transcript expression levels of genes regulating fatty acid metabolism. *Myog*-deleted and wild-type mice did not exhibit a significant difference in the expression of these factors in the Gastrocnemius muscle (*Myog*-deleted, n=3; wild-type n=3). Green bars represent *Myog*-deleted values. Red bars represent wild-type control values. Error bars represent one standard deviation. From left to right: Acc2 - Acetyl-Coenzyme A carboxylase beta, CD36 - Cluster of Differentiation 36, Cox8b - Cytochrome C oxidase subunit 8b, Cpt-1 - Carnitine Palmitoyltransferase I, Glut4 - Glucose Transporter Type 4, Ppar-a - Peroxisome Proliferator-Activated Receptor Alpha, Ppar-g - Peroxisome Proliferator-Activated Receptor Gamma, UCP2 - Mitochondrial Uncoupling Protein 2, UCP3 - Mitochondrial Uncoupling Protein 3.

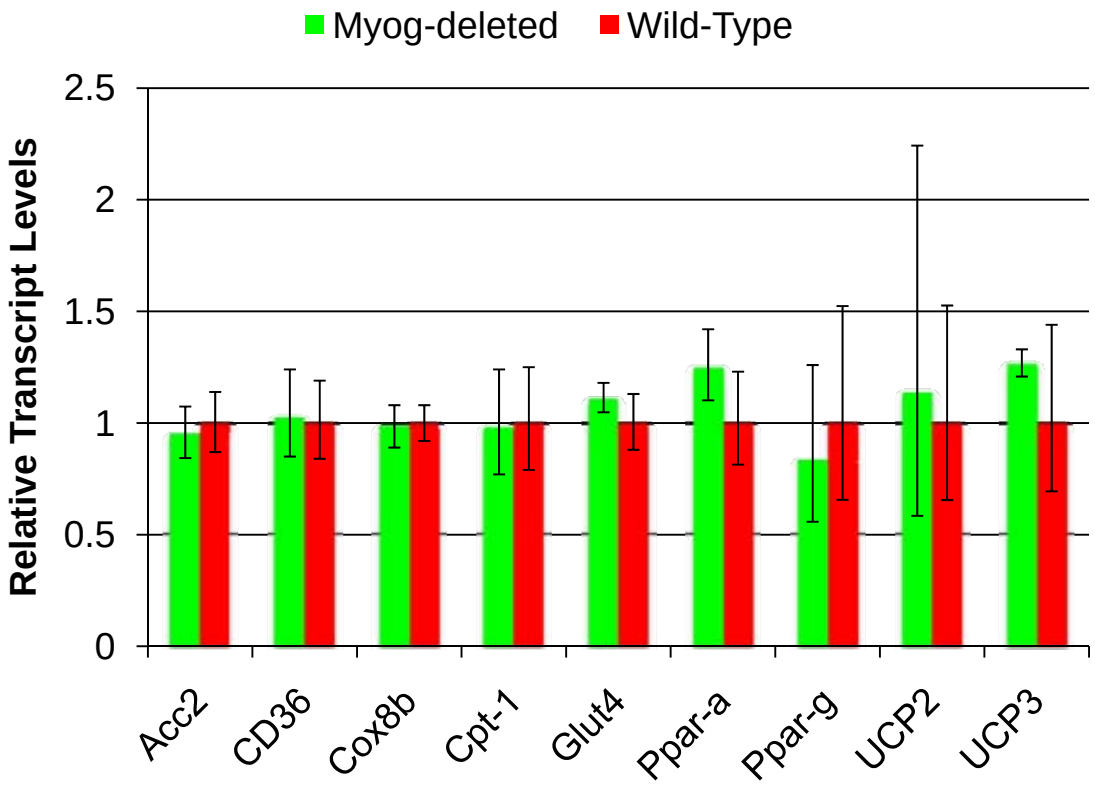
Myog-deleted
Wild-Type
Relative Transcript Levels
2.5
2
1.5
1
0.5
0
Acc2
CD36
Cox8b
Cpt-1
Glut4
Ppar-a
Ppar-g
UCP2
UCP3

Figure 11

Enzymatic activity levels of factors regulating glycolytic and oxidative metabolism. *Myog*-deleted and wild-type mice did not exhibit any significant differences in enzymatic activity for the factors tested in the Soleus or Extensor Digitorum Longus muscles (*Myog*-deleted, n=3; wild-type n=3). Green bars represent *Myog*-deleted values. Red bars represent wild-type control values. Error bars represent one standard deviation.

Glycolytic enzymes activities: Soleus Muscle

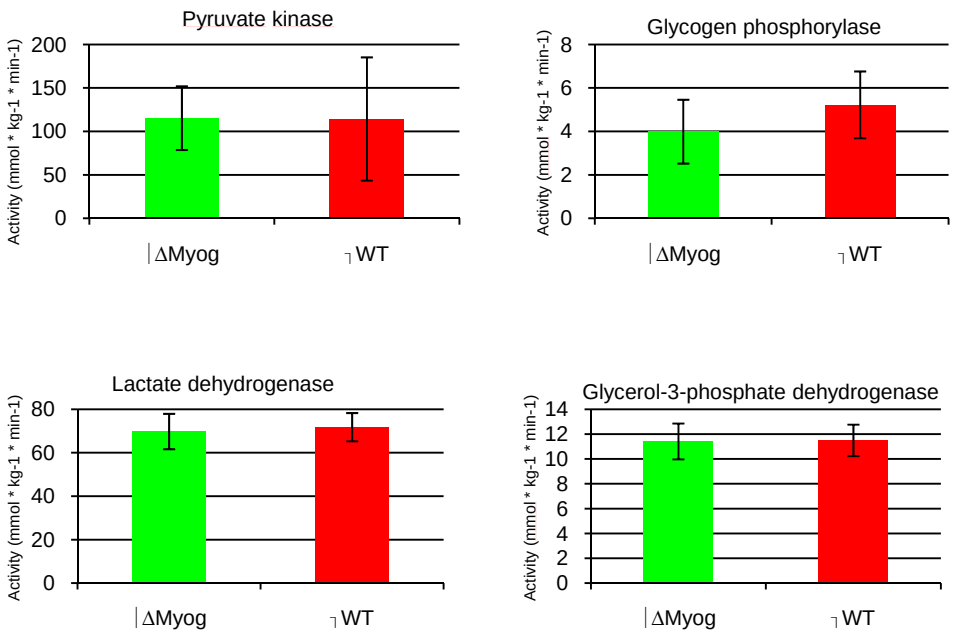

Glycolytic enzymes activities: extensor digitorum longus (EDL) muscle

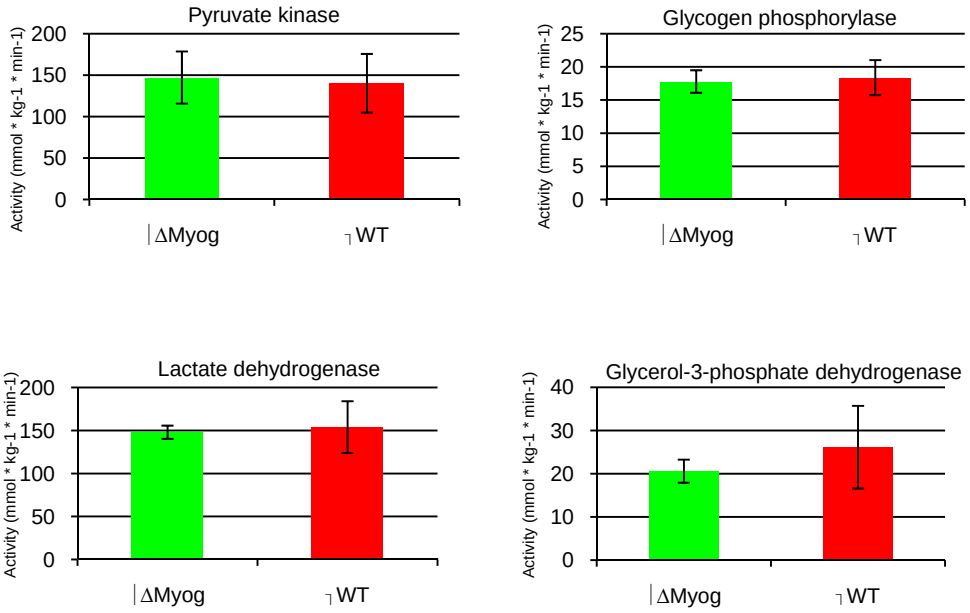

Oxidative enzymes activities: soleus muscle

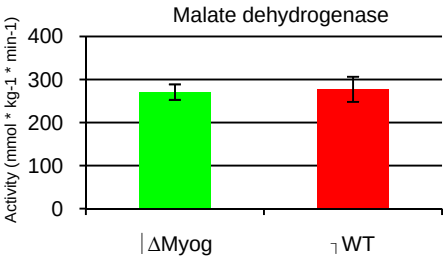

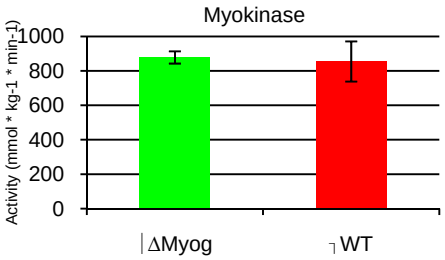

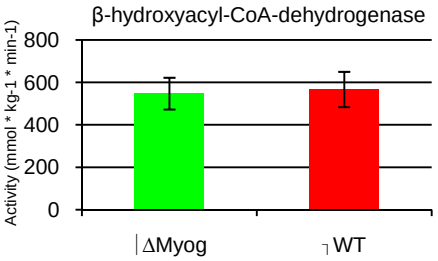

Oxidative enzymes activities: extensor digitorum longus (EDL) muscle

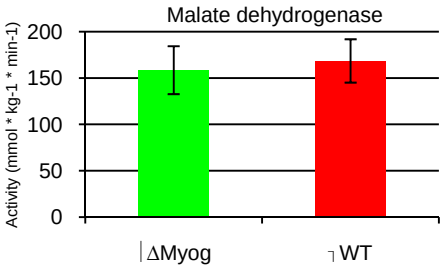

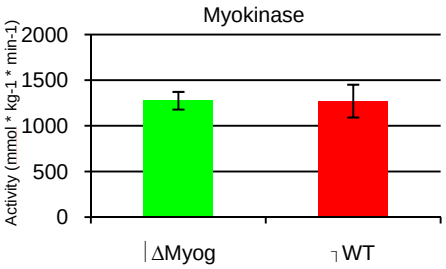

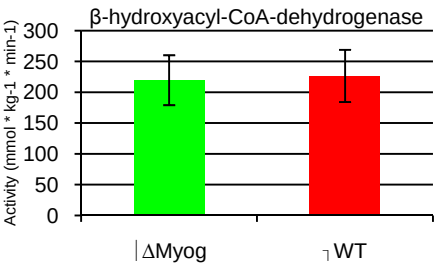

Myog-deleted adult mice exhibit an enhanced capacity for exercise and glycolytic metabolism under high-intensity stress conditions

To determine the exercise capacity for *Myog*-deleted mice under high-intensity stress conditions, adult animals were run at consistently increasing speeds to exhaustion at 10° incline (Figure 2). These conditions are designed to assess the sprinting aptitude of the mice and employ the use of fast twitch muscle fibers and glycolytic metabolism.

Myog-deleted mice ran on average 36% more than their wild-type counterparts 14 days post-deletion (Figure 12). The appearance of the phenotype at this early time point implied the enhanced exercise capacity was due to more sudden changes in fiber composition such as alterations in metabolic enzyme expression levels as opposed to long term modifications such as shifts in fiber type proportions.

At six months post-deletion, *Myog*-deleted mice ran 1.6 fold more than their wild-type counterparts over the course of 12 separate experiments conducted during consecutive days (Figure 13). This indicated the phenotype persists over the long term and suggested the difference in exercise capacity increased over time.

Blood lactate levels increased dramatically in both groups at exhaustion (Figure 14). Increased blood lactate levels were consistent with the use of glycolytic metabolism during this high-intensity exercise regimen. Moreover, *Myog*-deleted levels were 52% higher than that of their wild-type counterparts at exhaustion. However, at the wild-type exhaustion point, blood lactate levels of

Figure 12

Enhanced exercise capacity in *Myog*-deleted mice during the high-intensity exercise regimen. *Myog*-deleted mice ran 36% more than the wild-type control group under high-intensity exercise conditions at 14 days post-deletion (*Myog*-deleted, n=24; wild-type n=24). Green bar represents *Myog*-deleted values. Red bar represents wild-type control values. Error bars represent one standard deviation (*P<0.05).

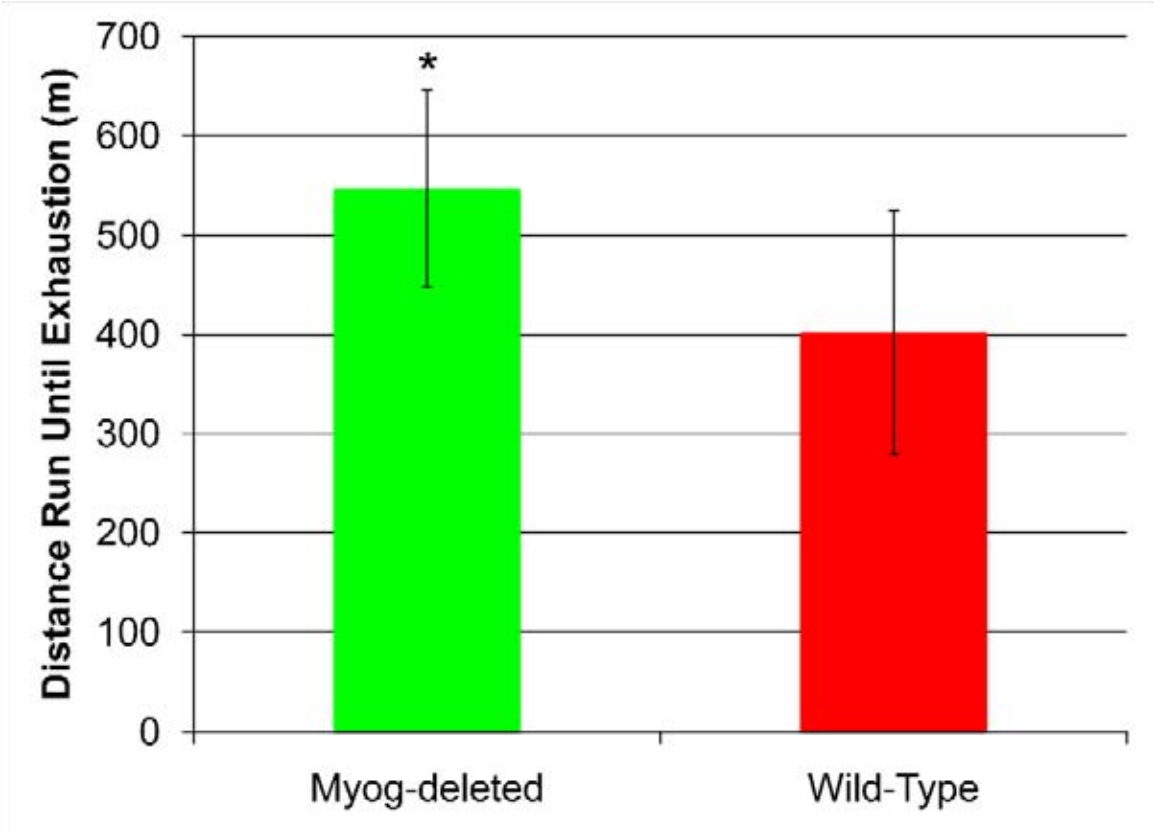
Distance Run Until Exhaustion (m)
700
600
500
400
300
200
100
0
*
Myog-deleted
Wild-Type

Figure 13

Enhanced exercise capacity in *Myog*-deleted mice during the high-intensity exercise regimen. *Myog*-deleted mice ran an average of 57% more than the wild-type control group under high-intensity exercise conditions at 6 months post-deletion for 12 consecutive days (*Myog*-deleted, n=8; wild-type n=7). Green bar (A) and green line (B) represent *Myog*-deleted values. Red bar (A) and red line (B) represent wild-type control values. Error bars represent one standard deviation (*$P<0.05$).

A.

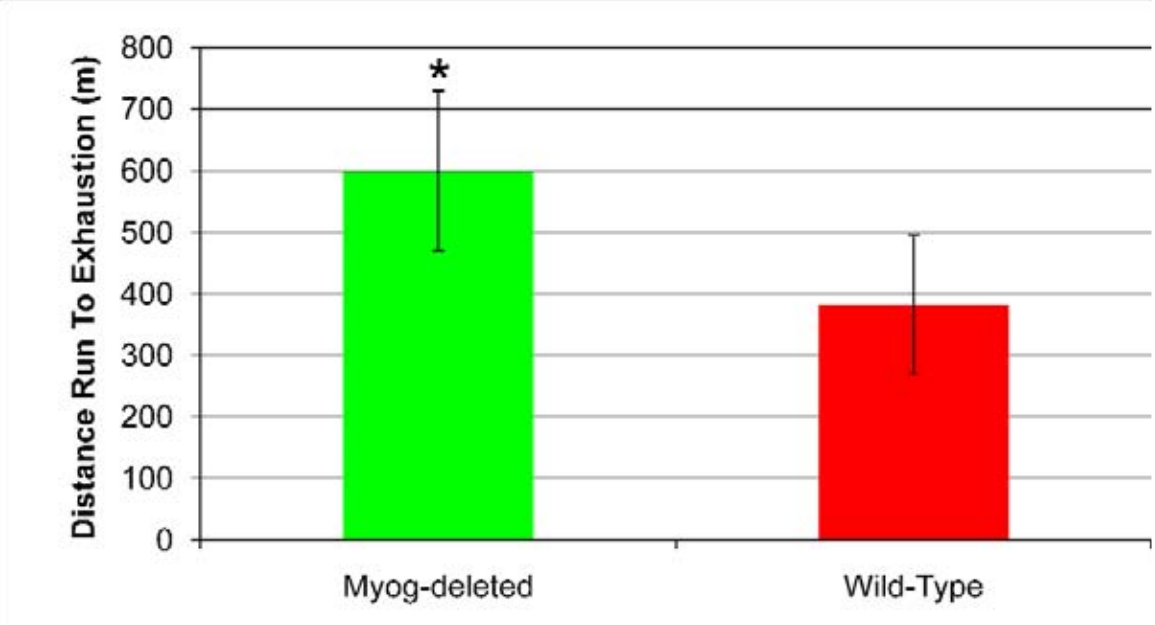
Distance Run To Exhaustion (m)
800
700
600
500
400
300
200
100
0
*
Myog-deleted
Wild-Type

B.

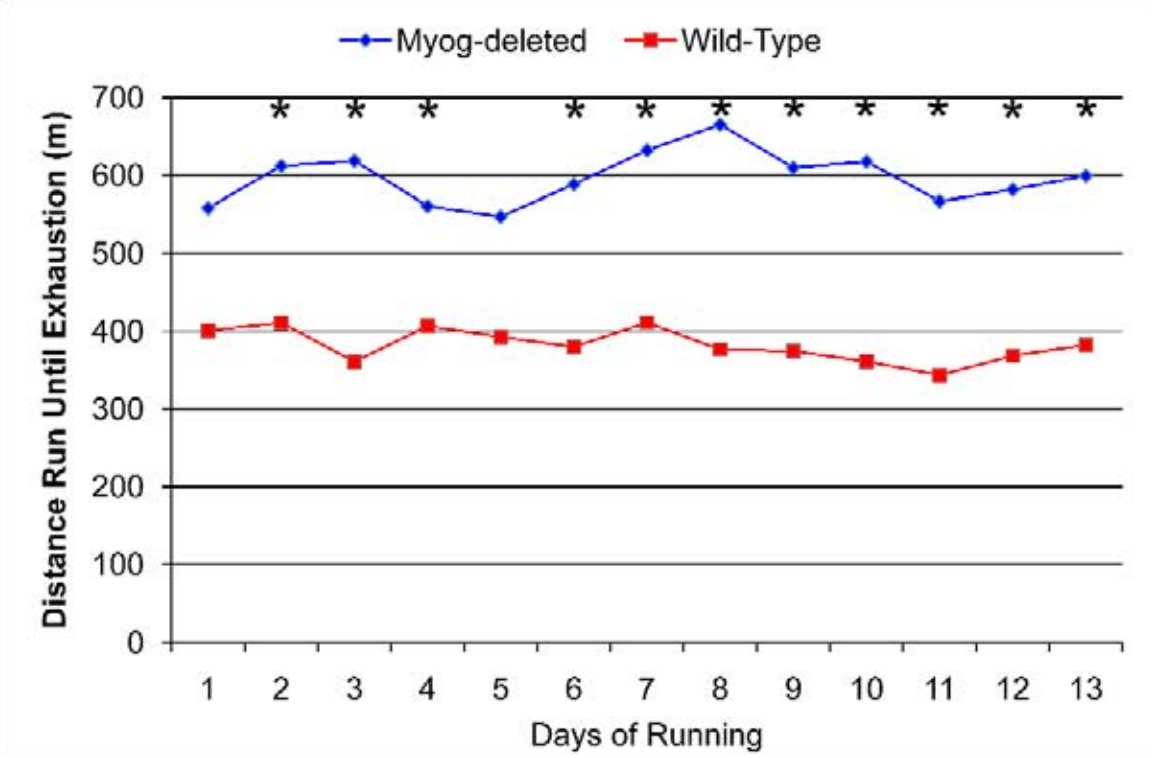
Myog-deleted
Wild-Type
Distance Run Until Exhaustion (m)
700
600
500
400
300
200
100
0
* * * * * * * * * * *
1 2 3 4 5 6 7 8 9 10 11 12 13
Days of Running

Figure 14

Blood lactate levels in *Myog*-deleted and wild-type mice at baseline and after running to exhaustion under the high-intensity exercise regimen. Wild-type blood lactate levels at exhaustion were increased by 168% over the baseline values. At the wild-type exhaustion time point, there was no significant increase in the *Myog*-deleted group. *Myog*-deleted blood lactate values at exhaustion had increased by 305% over the baseline values. These levels were also 50% greater than the wild-type blood lactate values at exhaustion (*Myog*-deleted, n=8; wild-type n=7). Green bars represent *Myog*-deleted values. Red bars represent wild-type control values. Error bars represent one standard deviation (*$P<0.05$).

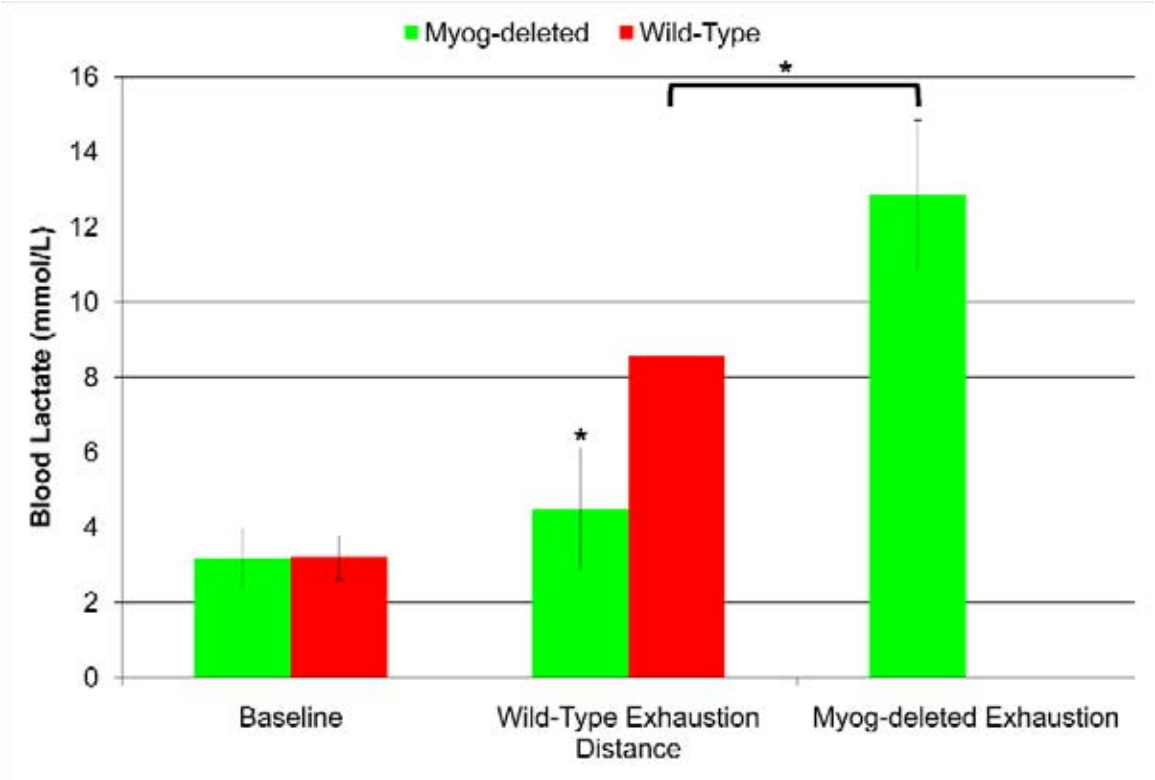
Myog-deleted
Wild-Type
Blood Lactate (mmol/L)
16
14
12
10
8
6
4
2
0
*
*
Baseline
Wild-Type Exhaustion Distance
Myog-deleted Exhaustion

Myog-deleted mice were significantly less than that of the wild-type group. These data suggested that *Myog*-deleted mice did not build up lactate as quickly and possessed a higher lactate concentration threshold before reaching exhaustion. This may be expected as previous studies have shown that lactate production may actually retard muscle acidosis.

Blood glucose levels at exhaustion remained constant for the wild-type group but decreased by 33% for *Myog*-deleted mice (Figure 15). Constant blood glucose levels in the wild-type group suggested the use of glycolytic metabolism during this high-intensity exercise regimen. The decrease in blood glucose for *Myog*-deleted mice indicated that these animals were able to further tap into their glycogen reserves and utilize this as a fuel source to power their glycolytic metabolism. Increased utilization of glucose might be conferring the observed enhanced exercise capacity.

Hypoglycemic *Myog*-deleted adult mice no longer exhibit an enhanced capacity for exercise and glycolytic metabolism under high-intensity stress conditions

To determine if the ability of *Myog*-deleted mice to further deplete their glycogen stores was responsible for the observed enhanced exercise capacity, mice were fasted to deplete their glycogen reserves and run on a daily basis until no difference in running capacity was observed between the *Myog*-deleted and wild-type groups. Baseline and exhaustion blood lactate and glucose levels were then recorded. After 96 hours of fasting, *Myog*-deleted mice reached

Figure 15

Blood glucose levels in *Myog*-deleted and wild-type mice at baseline and after running to exhaustion under the high-intensity exercise regimen. Wild-type blood glucose levels at exhaustion were unchanged from the baseline values. *Myog*-deleted values at that same time point showed a general downward trend, but the difference was not significant. *Myog*-deleted blood glucose levels at exhaustion were significantly reduced from their baseline values (*Myog*-deleted, n=8; wild-type n=7). Green bars represent *Myog*-deleted values. Red bars represent wild-type control values. Error bars represent one standard deviation (*$P<0.05$).

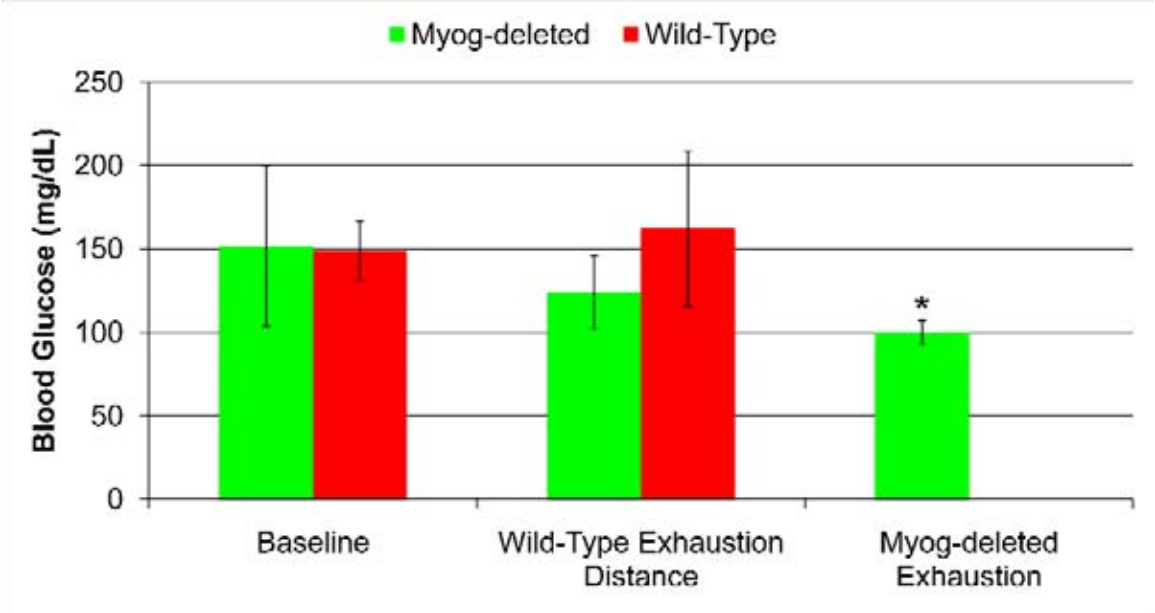
Myog-deleted
Wild-Type
Blood Glucose (mg/dL)
250
200
150
100
50
0
*
Baseline
Wild-Type Exhaustion Distance
Myog-deleted Exhaustion

exhaustion 10% faster than their wild-type counterparts. Thus, they no longer displayed an enhanced capacity for exercise at this point (Figure 16).

Baseline blood glucose levels of mice fasted for 96 hours were approximately half those of the same mice under normal dietary conditions, indicating that their glycogen stores had been depleted (Figure 17). Blood lactate levels at exhaustion were approximately twice that of baseline for both wild-type and *Myog*-deleted mice, but there was no longer a difference between the two groups (Figure 18). This suggested the glycolytic metabolism of *Myog*-deleted mice was no longer enhanced under hypoglycemic conditions. Blood glucose levels at exhaustion were not significantly altered from the fasting baseline for either group (Figure 17). Furthermore, there was no longer a difference between the two groups. These data implied that because glucose levels were already depleted before exhaustion, *Myog*-deleted mice were no longer able to further access their glycogen stores as a source of additional energy and thus ran the same distance as wild-type mice.

After 96 hours of fasting, normal dietary conditions were restored. After ten days of recovery, by which time glucose levels would be recovered, the *Myog*-deleted group again ran significantly more than their wild-type counterparts showing an enhanced capacity for exercise.

***Myog*-deleted mice exhibit an enhanced response to exercise training**

To determine the ability of *Myog*-deleted animals to respond to exercise training, mice were housed in cages with unrestricted access to exercise wheels

Figure 16

High intensity running under fasting conditions. After 96 hours of fasting, Myog-deleted mice ran slightly less than their wild-type counterparts before reaching exhaustion. Ten days after receiving their food back, *Myog*-deleted mice once again exhibited an enhanced capacity for exercise, running significant more than wild-type mice. Green line represents *Myog*-deleted values. Red line represents wild-type control values. Blue line represents fold change (*Myog*-deleted/Wild-type). Error bars represent one standard deviation (*$P<0.05$).

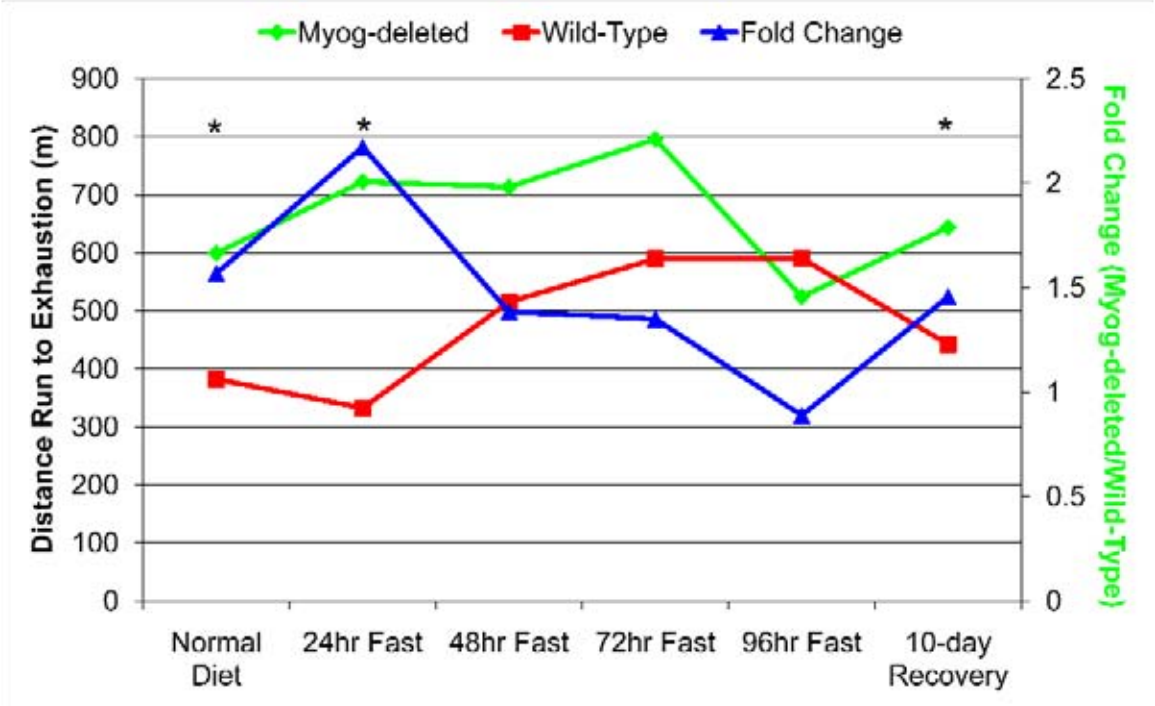
Myog-deleted
Wild-Type
Fold Change
Distance Run to Exhaustion (m)
Fold Change (Myog-deleted/Wild-Type)
900
800
700
600
500
400
300
200
100
0
2.5
2
1.5
1
0.5
0
*
*
*
Normal Diet
24hr Fast
48hr Fast
72hr Fast
96hr Fast
10-day Recovery

Figure 17

Blood glucose levels in *Myog*-deleted and wild-type mice under fasting conditions at baseline and after running to exhaustion under the high-intensity exercise regimen. Myog-deleted and wild-type blood glucose levels under fasting conditions at baseline were approximately half that of the fed baseline levels, indicating these animals were hypoglycemic. At exhaustion, there was no significant decrease in blood glucose for either group, and there was no difference between the two groups. Green bars represent *Myog*-deleted values. Red bars represent wild-type control values. Error bars represent one standard deviation.

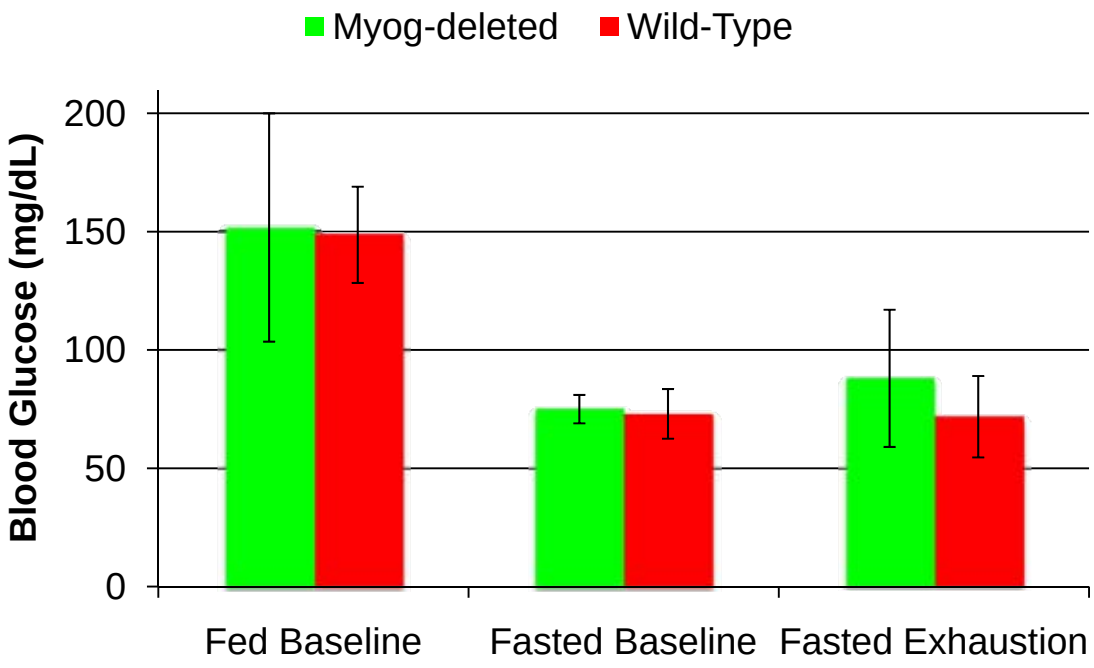
Myog-deleted
Wild-Type
Blood Glucose (mg/dL)
200
150
100
50
0
Fed Baseline
Fasted Baseline
Fasted Exhaustion

Figure 18

Blood lactate levels in *Myog*-deleted and wild-type mice under fasting conditions at baseline and after running to exhaustion under the high-intensity exercise regimen. At exhaustion, blood lactate levels in *Myog*-deleted and wild-type mice were both approximately twice that of baseline values, but there was no longer a difference between the two groups. Green bars represent *Myog*-deleted values. Red bars represent wild-type control values. Error bars represent one standard deviation (*$P<0.05$).

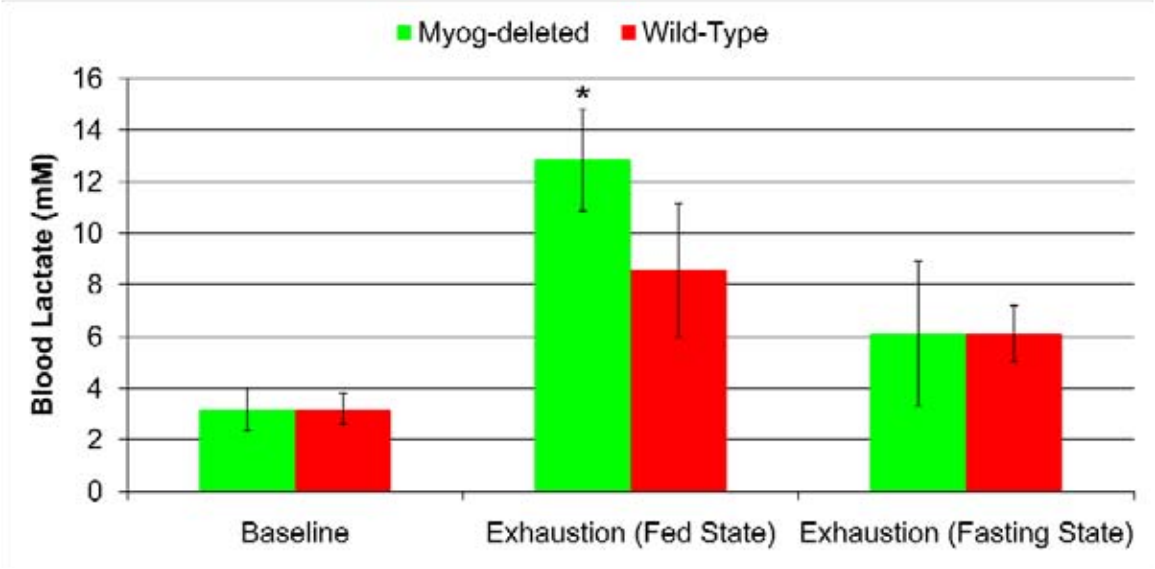
Myog-deleted
Wild-Type
Blood Lactate (mM)
16
14
12
10
8
6
4
2
0
*
Baseline
Exhaustion (Fed State)
Exhaustion (Fasting State)

outfitted with a mechanism allowing for the application of a loaded resistance for a period of six months and then subjected to the high-intensity exercise regimen. Adaptation to exercise is a long-term process and is generally accompanied by fiber type changes, increased mitochondrial content, and an improved capillary to fiber ratio [31].

Under resistance-free conditions on the running wheels, wild-type and *Myog*-deleted mice ran virtually equal distances (Figure 19). When a 1 kg loaded resistance was added to the wheels, *Myog*-deleted mice ran on average 32% farther than their wild-type counterparts for 19 consecutive days. While compelling, this trend toward increased voluntary running was not statistically significant.

Trained wild-type mice, those housed in exercise cages for the previous six months, ran 1.8 fold farther to exhaustion under the high-intensity exercise regimen than untrained mice, while trained *Myog*-deleted mice ran 2.2 fold farther to exhaustion than their untrained counterparts (Figure 20). Thus, the exercise capacity of trained *Myog*-deleted mice increased by an additional 21% as compared to wild-type animals. This implied myogenin indirectly regulated the pathways controlling long-term metabolic and physiological processes in the muscle fibers.

To investigate the metabolic and physiological changes as a result of training in the muscle fibers of these animals, histological analyses were performed to determine fiber type proportions and overall SDH activity. Both wild-type and *Myog*-deleted groups displayed increases in type 1 muscle fibers

Figure 19

Voluntary wheel running under no resistance and 1kg loaded resistance conditions. Under no resistance conditions at 4 to 5 months post-deletion, wild-type and *Myog*-deleted mice exhibited no differences in voluntary running over the course of 18 consecutive days of running. Under a 1kg loaded resistance at 5 to 6 months post-deletion, *Myog*-deleted mice exhibited a nonstatistical trend toward increased running as compared to the wild-type group over 18 consecutive days of running. Green bars represent *Myog*-deleted values (n=11). Red bars represent wild-type control values (n=11). Error bars represent one standard deviation (*$P<0.05$).

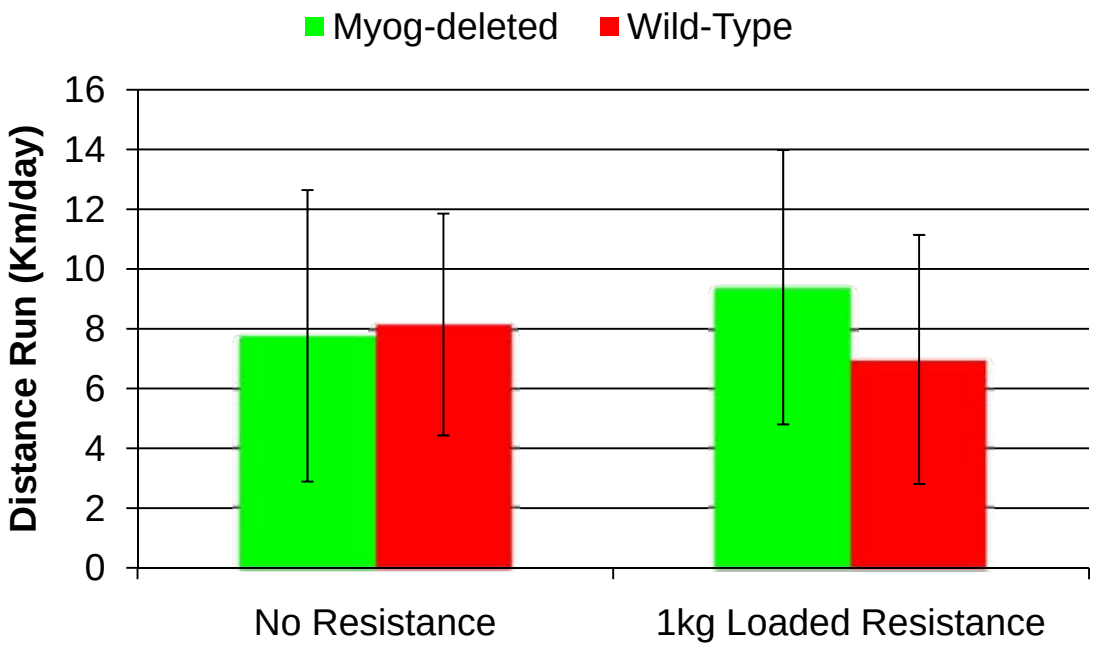
Myog-deleted
Wild-Type
Distance Run (Km/day)
16
14
12
10
8
6
4
2
0
No Resistance
1kg Loaded Resistance

Figure 20

Enhanced response to exercise training in *Myog*-deleted mice. After 6 months of exercise training on voluntary running wheels, both wild-type and *Myog*-deleted mice exhibited increased running capacities under the high-intensity exercise regimen. When making a comparison between the untrained and trained values for each genotype, *Myog*-deleted mice displayed significantly greater gains in running capacity over the wild-type group (Untrained *Myog*-deleted, n=8; Trained Myog-deleted, n=11; Untrained wild-type, n=7; Trained wild-type, n=10). Green bars represent *Myog*-deleted values (n=11). Red bars represent wild-type control values (n=11). Error bars represent one standard deviation (*$P<0.05$).

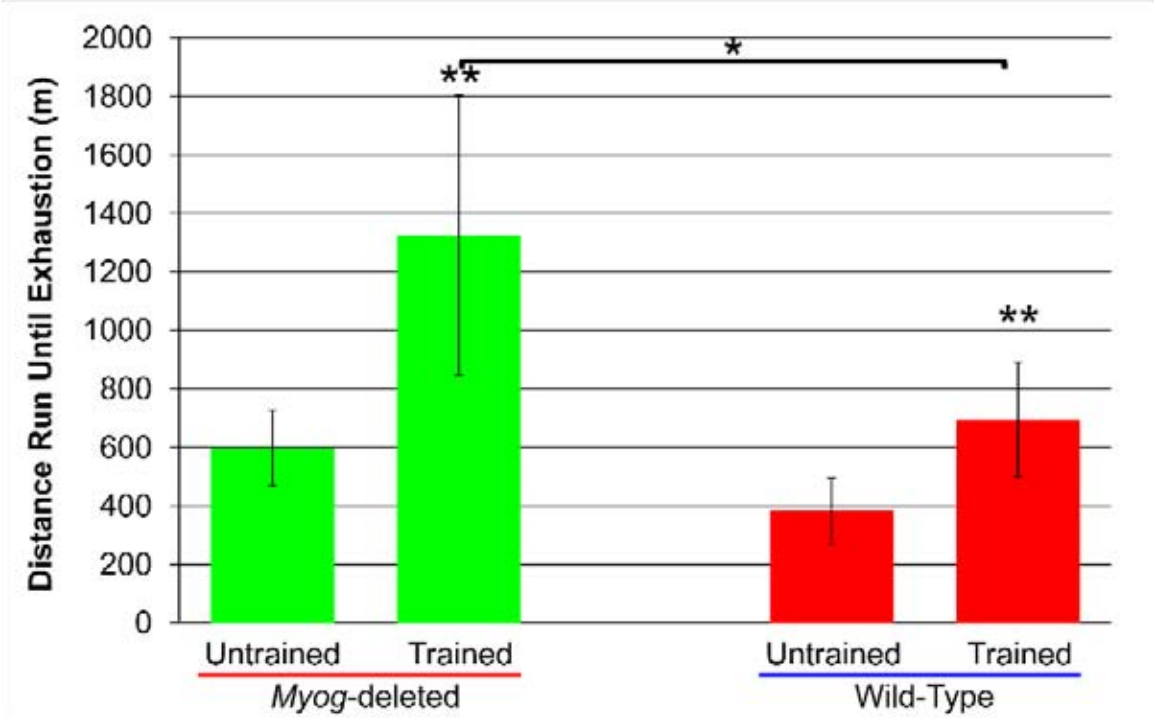
Distance Run Until Exhaustion (m)
2000
1800
1600
1400
1200
1000
800
600
400
200
0
**
*
**
Untrained
Trained
Untrained
Trained
Myog-deleted
Wild-Type

after training (Figure 21), but this gain was greater in the *Myog*-deleted animals, causing the difference between the wild-type and *Myog*-deleted groups after training to be statistically significant. This shift in fiber type proportions suggested the loss of myogenin promoted gradual changes in MyHC isoform expression and fiber contraction speed. Determination of SDH activity revealed significantly more positive fibers in the gastrocnemius for both the wild-type and *Myog*-deleted groups after training (Figure 22). However, this gain was greater in the *Myog*-deleted animals, causing the difference between the wild-type and *Myog*-deleted groups after training to be statistically significant. Further increased SDH levels suggested that these fibers possesed an increase in number and distribution of mitochondria and had greater overall oxidative potential.

Myogenin may regulate genes controlling metabolic processes

To begin establishing a basis for elucidating the mechanisms driving enhanced exercise capacity, putative myogenin gene targets were identified in adult skeletal muscle via global gene expression profiling followed by qRT-PCR. Hybridization with adult wild-type and *Myog*-deleted probes identified multiple genes with altered expression in the absence of myogenin (Table 1). Genes regulating metabolic processes including 6-phosphofructo-2-kinase/fructose-2,6-biphosphatase 3 (Pfkfb3), pyruvate carboxylase (Pc), dihydropyrimidine dehydrogenase (Dpyd), and 3-hydroxybutyrate

Figure 21

Increased proportion of type 1 muscle fibers in hindlimb muscle of trained *Myog*-deleted mice. Untrained wild-type and *Myog*-deleted mice exhibited no significant differences in type 1 muscle fibers (dark fibers). After 6 months of continuous training in voluntary running wheels, trained *Myog*-deleted mice displayed significantly more type 1 muscle fibers over the trained wild-type group. Green bars represent *Myog*-deleted values (n=3). Red bars represent wild-type control values (n=3). Error bars represent one standard deviation (*$P<0.05$).

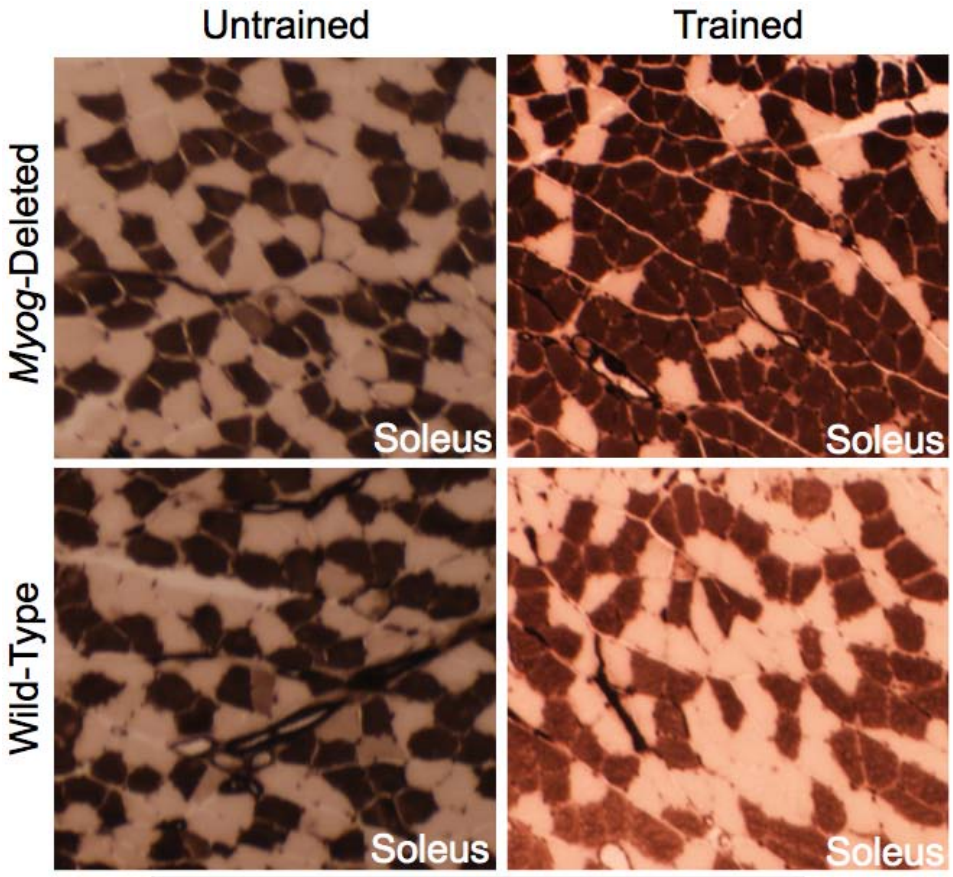
Untrained
Trained
Myog-Deleted
Wild-Type
Soleus
Soleus
Soleus
Soleus

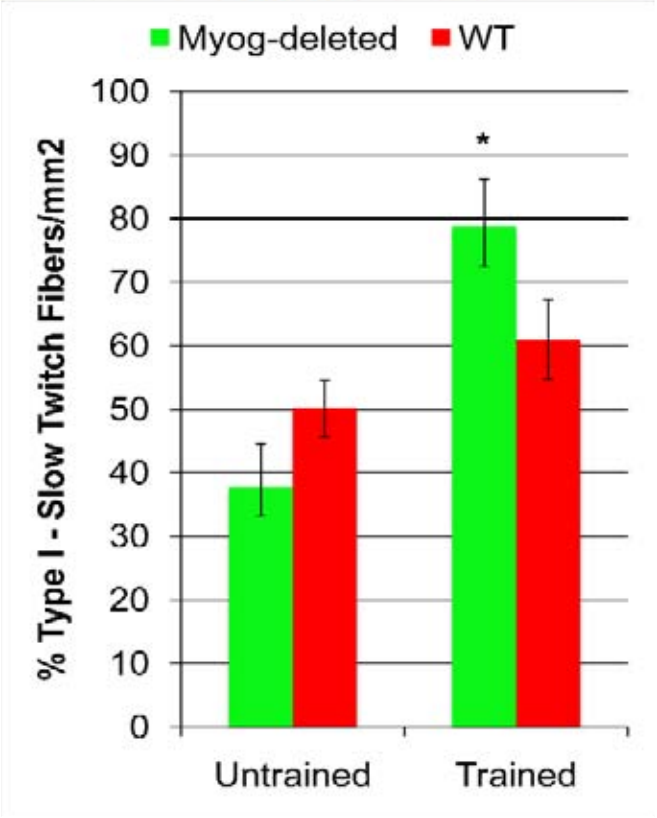
Myog-deleted
WT
% Type I - Slow Twitch Fibers/mm2
100
90
80
70
60
50
40
30
20
10
0
*
Untrained
Trained

Figure 22

Increased proportion of succinate dehydrogenase (SDH) positive fibers in hindlimb muscle of trained *Myog*-deleted mice. Untrained wild-type and *Myog*-deleted mice exhibited no significant differences in SDH positive muscle fibers. After 6 months of continuous training in voluntary running wheels, trained *Myog*-deleted mice displayed significantly more SDH positive muscle fibers over the trained wild-type group. Green bars represent *Myog*-deleted values (n=3). Red bars represent wild-type control values (n=3). Error bars represent one standard deviation (*$P<0.05$).

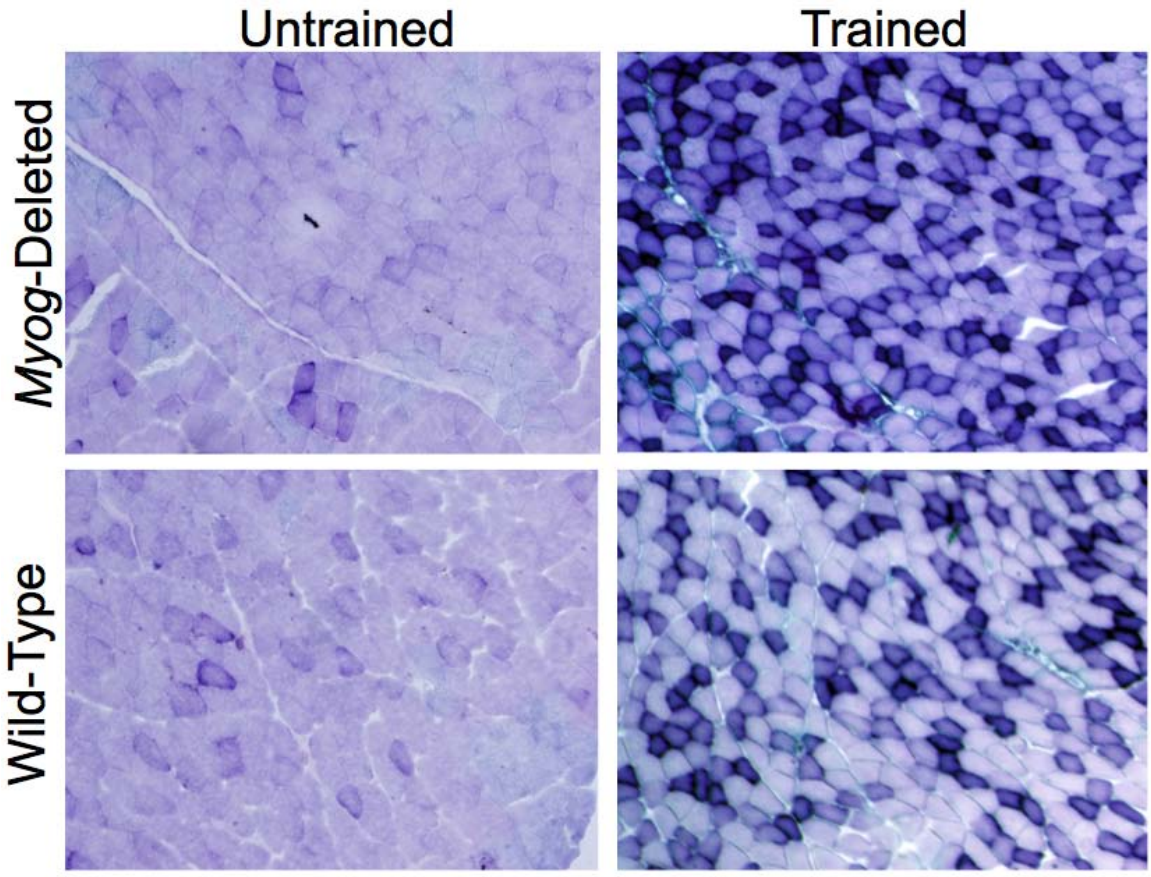
Untrained
Trained
Myog-Deleted
Wild-Type

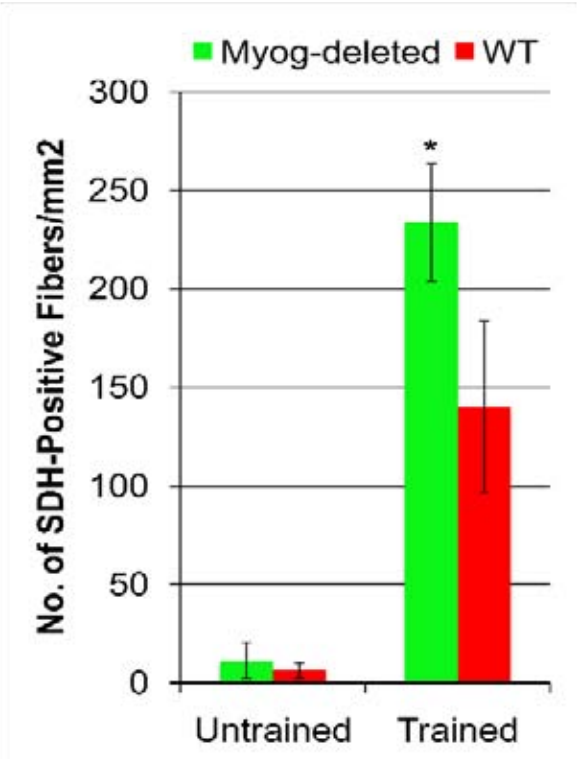
Myog-deleted
WT
No. of SDH-Positive Fibers/mm2
300
250
200
150
100
50
0
*
Untrained
Trained

Table 1

Genes identified to have significantly altered expression in the absence of myogenin. Global gene expression profiling via microarray analysis identified numerous genes involved in metabolism and signal transduction (Myog-deleted n=3, wild-type n=3). Alterations of 1.4 fold or more were considered to be significant.

Fold change	Regulation	Gene Symbol	Gene Title	Biological Process
2.4	down	Rfx7	regulatory factor X, 7	regulation of transcription, DNA-dependent
1.8	down	Rhobtb1	Rho-related BTB domain containing 1	small GTPase mediated signal transduction
1.8	down	Rhpn2	rhophilin, Rho GTPase binding protein 2	signal transduction
1.7	down	Myog	myogenin	regulation of transcription, DNA-dependent
1.6	down	Htra1	HtrA serine peptidase 1	regulation of cell growth /// proteolysis /// negative regulation of transforming growth factor beta receptor signaling pathway /// negative regulation of BMP signaling pathway
1.6	down	Gpx3	glutathione peroxidase 3	glutathione metabolic process /// response to oxidative stress /// hydrogen peroxide catabolic process /// protein homotetramerization /// protein homotetramerization /// oxidation reduction
1.6	down	Zscan21	zinc finger and SCAN domain containing 21	transcription /// regulation of transcription, DNA-dependent /// multicellular organismal development /// spermatogenesis /// cell differentiation /// positive regulation of transcription, DNA-dependent /// oogenesis
1.5	down	Pcx	pyruvate carboxylase	gluconeogenesis /// oxaloacetate metabolic process /// metabolic process /// lipid biosynthetic process
1.4	up	Bmp5	bone morphogenetic protein 5	skeletal system development /// ossification /// multicellular organismal development /// pattern specification process /// cell differentiation /// growth /// cartilage development
1.6	up	Pfkfb3	6-phosphofructo-2-kinase/fructose-2,6-biphosphatase 3	fructose metabolic process /// fructose 2,6-bisphosphate metabolic process /// metabolic process
1.8	up	Mpa2l	macrophage activation 2 like	immune response
1.9	up	Dpyd	dihydropyrimidine dehydrogenase	'de novo' pyrimidine base biosynthetic process /// pyrimidine base catabolic process /// uracil catabolic process /// thymidine catabolic process /// UMP biosynthetic process /// metabolic process /// oxidation reduction
2.0	up	Bdh1	3-hydroxybutyrate dehydrogenase, type 1	metabolic process /// oxidation reduction

dehydrogenase-type 1 (Bdh1) were shown to be significantly altered in *Myog*-deleted mice. These changes in gene expression levels were verified by qRT-PCR (Figure 23). In the absence of myogenin, this assay confirmed that the expression levels of multiple genes regulating metabolic processes in glycolysis were altered. The gene expression profiling analysis will provide a starting point from which to determine the underlying basis for enhanced exercise capacity in *Myog*-deleted mice.

Figure 23

Transcript expression levels of genes identified to be altered in the absence of myogenin. qRT-PCR confirms the altered expression of genes in *Myog*-deleted mice identified during global gene expression profiling via microarray analysis. Green bars represent *Myog*-deleted values (n=3). Red bars represent wild-type control values (n=3). Error bars represent one standard deviation (*$P<0.05$; **P<.01).

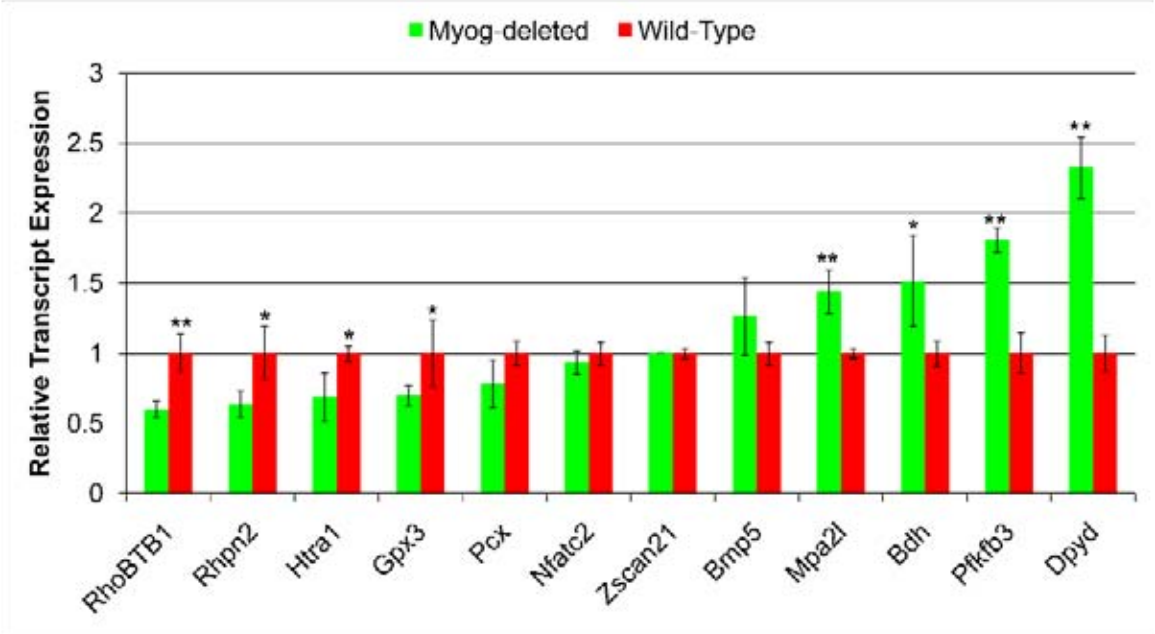
Myog-deleted
Wild-Type
Relative Transcript Expression
3
2.5
2
1.5
1
0.5
0
RhoBTB1
Rhpn2
Htra1
Gpx3
Pcx
Nfatc2
Zscan21
Bmp5
Mpa2l
Bdh
Pfkfb3
Dpyd

DISCUSSION:

The role of myogenin in regulating embryonic skeletal muscle differentiation has been thoroughly investigated. The results presented here identify new functions for myogenin in response to exercise stress and demonstrate that *Myog*-deleted adult mice possess an enhanced capacity for exercise soon after deletion. These mice display increased levels of lactate build-up at exhaustion and are able to further tap into glycogen reserves for energy production that wild-type mice are unable to access. The data suggest that the loss of myogenin abruptly alters metabolic processes in adult mice, thus conferring their enhanced capacity for exercise. When given access to a means of training over time, these shifts in metabolic processes translate into the acceleration of changes in muscle fibers to induce rapid shifts in fiber type and mitochondrial activity. The results provide evidence indicating that myogenin regulates metabolic homeostasis during adult life and may negatively regulate exercise performance. These findings are particularly striking, because myogenin is known to be vital for muscle growth and development during embryonic and postnatal life. Furthermore, the results are consistent with findings in the literature suggesting that the myogenin:MyoD expression ratio regulates fiber phenotype [27]. *MyoD* transcripts have been shown to selectively accumulate in fast twitch muscle fibers. In *Myog*-deleted mice, this ratio is presumably tipped in favor of MyoD, suggesting the development of fast-twitch characteristics in previously slow-twitch fibers.

The exercise stress experiments and blood tests performed here are the first to use *Myog*-deleted mice to identify functions for myogenin in adult exercise and metabolism. This physiological approach identified a metabolic regulatory role for myogenin during exercise. Under high-intensity exercise conditions, *Myog*-deleted mice exhibited increased lactate levels at exhaustion. There is much debate regarding lactate production as the cause of muscle fatigue and acidosis. Long held views state that a virtually instantaneous and complete ionization of lactic acid is caused by the low pKa of the carboxylic acid functional group within lactic acid [32-38]. Thus the decrease in pH and discharge of a (H^+) proton from lactic acid to finally create lactate is defined as lactic acidosis [39]. Compelling evidence to the contrary indicates that metabolic acidosis is primarily brought about via alternative mechanisms such as ATP hydrolysis or increases in the glyceraldehyde-3-phosphate dehydrogenase reaction rate in glycolysis [40-44]. Furthermore, studies strongly suggest that lactate production and removal from the muscle actually retards acidosis by consuming H^+ protons [45] and concomitantly transporting H^+ across the sarcolemma [30, 46]. Lactate circulating through the blood can also be taken up and metabolized by other organs such as the kidneys, skeletal and cardiac muscle, and liver. Thus increased lactate levels may be contributing to the enhanced exercise capacity of *Myog*-deleted mice by slowing acidosis and muscle fatigue. Furthermore, this impediment to acidosis may be enabling *Myog*-deleted mice to metabolize and deplete additional glucose stores before reaching exhaustion significantly later than wild-type animals.

Myog-deleted mice also ran farther during the low-intensity exercise regimen and exhibited significantly decreased glucose levels at exhaustion, but did not display increased lactate levels. One possible explanation for this would be a difference in the expression levels of glucose transporter proteins, but no such differences were detected in the global gene expression analysis or subsequent GLUT4 transcript detection by qRT-PCR. However, the activity and arrangement of these proteins at the cell membrane have yet to be determined and could influence the uptake of glucose. Alternatively, increased lactate production may still be occurring but the mechanisms for clearing lactate from the blood in *Myog*-deleted animals may have been able to compensate.

The long-term effects of *Myog*-deficiency in the adult have yet to be elucidated, but extensive voluntary training has uncovered a role in adaptation to continuous exercise. After six months of open access to running wheels, *Myog*-deleted mice responded to exercise training 21% better than wild-type mice. The glucose and lactate advantages proposed above may be slowing the onset of fatigue during exercise, allowing *Myog*-deleted mice to run farther and for extended periods of time. Over the course of months, even a mild enhancement may translate into significant additional gains in exercise capacity. The loss of myogenin dramatically shifts fiber type proportions from type 2 to type 1 in response to long-term training. This shift in fiber type proportions suggests that *Myog*-deficiency may promote gradual changes in MyHC isoform expression and fiber contraction speed. Furthermore, significant increases in SDH abundance far beyond the increases seen in wild-type mice suggest an

enhancement in oxidative metabolism possibly through increases in mitochondrial count and distribution.

These results are also consistent with previous data suggesting alterations in glycolytic metabolism can be uncoupled from changes in MyHC fiber type [28]. *Myog*-deleted animals displaying an enhanced exercise capacity under the high-intensity regimen two weeks post-deletion did not exhibit a shift in fiber type proportions. Previous enzyme studies utilizing transgenic mice engineered to overexpress myogenin reported a shift in enzyme activity from glycolytic to oxidative metabolism, but no differences in fiber type proportions were observed. While metabolic enzyme activities determined here in wild-type and *Myog*-deleted mice did not reveal shifts in activity, the panel tested did not comprehensively cover the large number of enzymes involved in regulating metabolism.

Previous studies have shown myogenin regulates distinctly different pathways during various stages of life. During embryonic development, many genes encoding structural and contractile components are strongly downregulated in the absence of myogenin [47], whereas expression levels of factors regulating cell fusion, signaling, and adhesion are altered in adult skeletal muscle stem cells (satellite cells) [13]. Global gene expression analysis performed here in adult skeletal muscle now identifies potential roles for myogenin in the regulation of metabolic processes. Pc catalyzes the initial reaction of glycolysis of pyruvate to oxaloacetate, and when the liver detects excess lactate levels, Pc activity increases [for review, see 48]. Human Pc

deficiencies often result in increased lactate levels and/or high lactate:pyruvate ratios [49-51]. Thus, reduced expression of Pc may be contributing to increased lactate levels at exhaustion in *Myog*-deleted mice.

PFKFB3 was significantly upregulated in *Myog*-deleted mice. PFKFB3 encodes PFK2, which has been shown to regulate the activity of PFK1 and ultimately drive a rate-limiting reaction during glycolysis, the conversion of fructose-6-phosphate (F6P) to fructose-1,6-bisphosphate (F1,6BP) via PFK-1 [for review, see 52]. It is expressed in skeletal muscle, activated by hypoxic stimuli, and exhibits an approximately 400:1 kinase:phosphatase ratio to enhance glycolytic flux [53-55]. Myogenin has been shown to repress genes regulating glycolysis and upregulate genes involved in oxidative metabolism. Myogenin is known to activate HDAC4, a repressor of PFK-1 [24]. In the absence of myogenin, HDAC4 levels may decrease, deregulating PFKFB3 and increasing glycolytic activity.

The results presented here suggest that reduced myogenin expression would be advantageous to mice in the wild. Enhanced exercise capacity would presumably enable these animals to better escape from predators or become superior hunters. Thus the question remains as to why the expression of myogenin persists throughout adulthood. There are multiple possible explanations. *Myog*-deleted mice derived from laboratory stocks have been removed from the wild for many generations. They have not been subjected to natural environmental pressures and selection processes. Thus, it is possible that *Myog*-deleted mice do not display the same survival characteristics as mice

in the wild. Also, the results imply that *Myog*-deleted mice are able to further deplete their glucose stores before reaching exhaustion. This may adversely enable them to easily become hypoglycemic, which can lead to unconsciousness, neuroglycopenia, and potentially death. In wild-type mice, myogenin may act to restrain skeletal muscle activity in favor of glucose conservation. Furthermore, consistent muscle mass is achieved by a balance between the rates of protein synthesis and degradation. Recent studies performed in collaboration with the Olson laboratory at The University of Texas Southwestern Medical Center in Dallas indicate that myogenin is an essential activator of muscle atrophy. Through its role in the activation of E3 ubiquitin ligases, myogenin may act to maintain constant muscle mass by promoting muscle proteolysis.

The mechanism by which myogenin regulates different pathways during embryogenesis, postnatal development, and adult life have yet to be elucidated. Previous studies have focused on embryonic and postnatal development, when skeletal muscle is undergoing dramatic periods of stem cell proliferation and differentiation. Conversely, adult skeletal muscle is kept under a much less dynamic state of maintenance. As the requirements necessary to sustain muscle homeostasis change from one developmental time point to another, so may the functions of myogenin change to maintain a viable equilibrium. *Myog*-deleted adult mice displayed an enhanced capacity for exercise under both low-intensity and high-intensity running regimens. Myogenin may be regulating pathways that maintain adult muscle fiber character. It may act as a master

sensor of muscle stress to alter fiber metabolic properties in response to changing environmental conditions.

This research lends itself to a number of possible future directions. At the transcriptional level, elucidating the mechanisms conferring differential gene regulation by myogenin in embryonic versus adult skeletal muscle may provide a basis for establishing how this is achieved in other families of closely related factors. Furthermore, the unexpected functions for myogenin identified here may lead to more translational research projects with the ultimate goal of generating clinical applications. Blocking the expression of myogenin may provide useful to the sports medicine industry when developing strategies to aid in muscle repair and regeneration. Moreover, this research questions the role of myogenin in muscle wasting disorders. The functions for myogenin during periods of constant muscle regeneration may be best uncovered by downregulating its expression in mice harboring the Duchenne's muscular dystrophy (DMD^{mdx}) allele.

CHAPTER II:

Myogenin regulates exercise capacity but is dispensable for muscle regeneration in adult *mdx* mice

INTRODUCTION:

Muscular Dystrophy is the most prevalent childhood muscle disorder found in humans, affecting 1 in 3500 newborn males [56]. Duchenne's muscular dystrophy (DMD) is a chronic muscle wasting disease leading to progressive muscle weakness and atrophy. The disease is caused by mutations within the dystrophin gene, a critical structural component of the muscle cell membrane [57]. Physiological symptoms of this disorder become apparent within the first few years of life, and muscle strength quickly deteriorates by puberty and usually results in early mortality. Common diagnoses and signs of DMD include increased blood creatine kinase concentration, increased rates of myofiber regeneration, centrally located myofiber nuclei, mitochondrial swelling, and ultimately myofiber necrosis [58]. Animal models of DMD include the *mdx* mouse, which has been studied extensively to better understand human DMD [59-65].

DMD is associated with muscle metabolism dysfunction and muscle weakness. Neuronal nitric oxide synthase (nNOS) is a dystrophin-associated protein found near the muscle sarcolemma, and its expression is greatly reduced in *mdx* mice [66]. Recently, others have shown that the loss of interaction between nNOS and PFK contributes to glycolytic dysfunction and increased fatigability [67]. The forced expression of nNOS in *mdx* mice

enhances muscle endurance and glycogen metabolism. These experiments provide important insights into why *mdx* mice and humans with DMD experience progressive muscle weakness associated with muscle wasting and atrophy.

Mammalian muscle fibers are broadly divided into several subtypes based upon their expression of different myosin isoforms: type 1, type 2A, and type 2B (type 2X in humans) [68]. Types 1 and 2A are primarily oxidative in nature and confer increased exercise endurance with a high resistance to muscle fatigue during aerobic exercise. Type 2B fibers are glycolytic in nature and allow for anaerobic sprinting or short bursts of strength but fatigue more quickly. Type 1 fibers are commonly referred to as slow twitch whereas type 2 fibers are labeled as fast twitch. Glucose is a major energy source for all muscle metabolism, but glycolytic fibers are particularly dependent on glucose for energy production. Glucose stored as glycogen within skeletal muscle fibers is utilized to quickly meet the demands of high-intensity exercise. Fatty acids and glucose acquired from the liver via the blood stream provides the major source of energy that is utilized during low-intensity exercise. Lactate is a by-product of anaerobic metabolism and its blood concentration rises coincident with an increase in exercise intensity [69].

The maintenance and regeneration of skeletal muscle are orchestrated by the four basic helix-loop-helix Myogenic Regulatory Factors (MRFs): MyoD, Myf5, MRF4, and myogenin. Myogenin is required for embryonic skeletal muscle development and for achieving normal body size after birth [12, 13, 29]. Myogenin is primarily expressed in slow-twitch/oxidative myofibers and is

sufficient to induce a shift from glycolytic to oxidative metabolism when overexpressed [27, 28]. Recently, myogenin was discovered to transcriptionally activate the E3 ubiquitin ligases Fbxo32 and Trim63 following muscle denervation [26]. The loss of myogenin during adult life confers a resistance to denervation-induced muscle atrophy. Moreover, as described in chapter 1, myogenin plays a role in regulating metabolism and exercise endurance during adult life.

In this chapter, I address whether the loss of myogenin in adult *mdx* mice alters *mdx* muscle regeneration and performance. Surprisingly, the absence of myogenin appeared to have no adverse effects on muscle regeneration. Moreover, the exercise capacity of *mdx:Myog*-deleted adult mice was significantly improved over the *mdx* control group, nearly to the level of wild-type mice. This favorable improvement in exercise endurance was associated with significant changes in nNOS and Fbxo32 expression, implicating a potential mechanism for the improvement in muscle fatigue resistance. The results indicate that further investigation into the manipulation of *Myog* in mammals with DMD will be a worthy avenue for the development of new treatment options for this disease.

RESULTS:

***Myog* is not required for survival in adult *mdx* mice**

To determine the role of myogenin in adult skeletal muscle maintenance and regeneration, *Myog* conditional knockout mice harboring a tamoxifen-inducible Cre recombinase transgene [29] were interbred with the DMD^{mdx} mouse strain. Wild-type (tamoxifen-injected *Myog*$^{flox/flox}$) and *mdx* animals in the same mixed genetic background were also generated as controls. Cre-expressing adult animals 8-12 weeks old were then rendered *Myog*-deficient via a single injection of tamoxifen. Determination of transcript expression showed that *Myog* transcript levels in *mdx* mice were 5-fold higher than their wild-type counterparts (Figure 24). Moreover, *mdx:Myog*–deleted mice expressed equal levels of *Myog* transcripts compared to wild-type. This is expected as *mdx* mice are in a constant state of regeneration, when myogenin levels are highly upregulated. *Mdx*:*Myog*-deleted mice exhibited seemingly normal behavior and displayed no overt adverse phenotypic effects. The results indicated that *Myog* is not required for survival in adult *mdx* mice.

***Mdx*:*Myog*-deleted mice exhibit an enhanced capacity for exercise over their *mdx* counterparts**

Based on the results described in chaper 1, I reasoned that that the loss of myogenin may confer an enhanced capacity for exercise in *mdx mice.* *Mdx*, *mdx:Myog*-deleted, and wild-type mice were run on a treadmill to exhaustion under a high-intensity exercise regimen to determine their exercise capacities.

Figure 24

Reduced abundance of *Myog* transcripts in tamoxifen-injected *mdx:Myog*$^{flox/flox}$; Cre+ mice. *Myog* transcript levels in adult *mdx* mice were increased by 5 fold over wild-type levels. *Myog* transcript expression in *mdx:Myog*$^{flox/flox}$;Cre+ mice treated with a single IP injection of tamoxifen at a dose of 10mg/40g body weight was approximately equal to that of the wild-type control group. Green bar represents *mdx:Myog*-deleted values (n=3). Blue bar represents *mdx* values (n=3). Red bar represents wild-type control values (n=3). Error bars represent one standard deviation (*P<0.05).

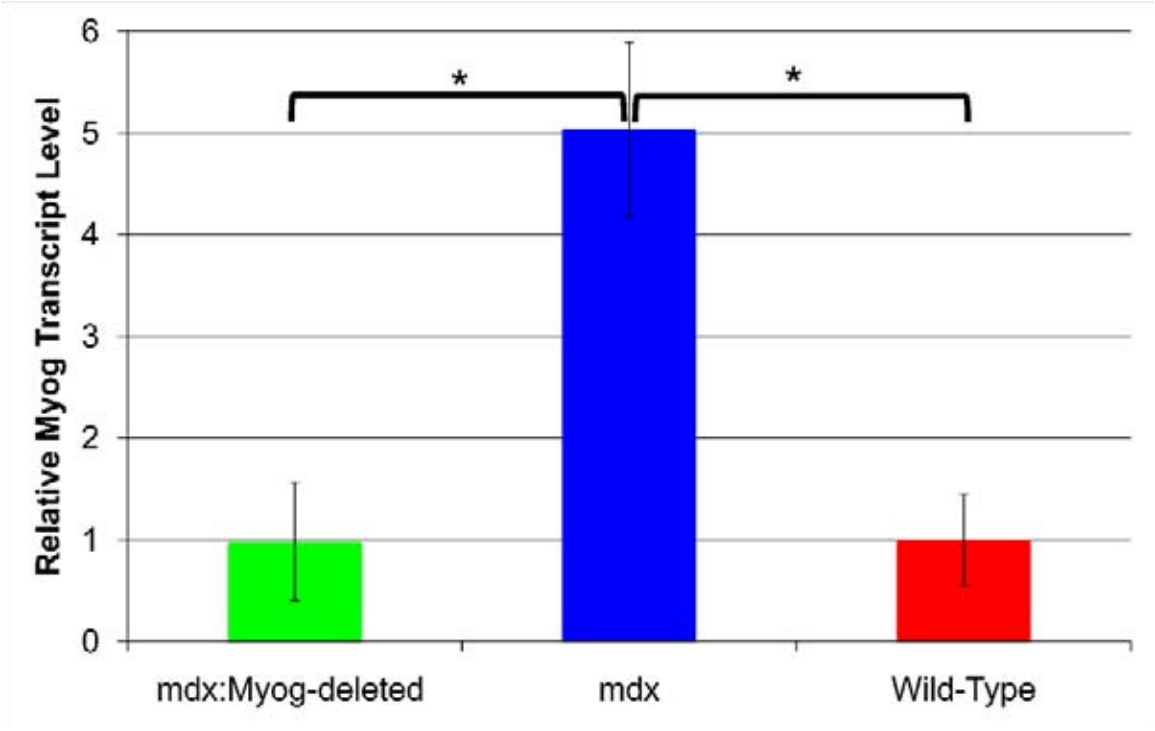
Relative Myog Transcript Level
6
5
4
3
2
1
0
*
*
mdx:Myog-deleted
mdx
Wild-Type

Over the course of 3 consecutive days of running, *mdx:Myog*-deleted mice ran on average 11% less than the wild-type group, but 37% farther than their *mdx* counterparts before reaching exhaustion (Figure 25). The results suggested that the absence of *Myog* confered a significant positive effect on exercise endurance in *mdx* mice.

The absence of myogenin alters blood metabolite concentrations during exhaustive exercise

Deletion of *Myog* enhances exercise endurance and is associated with alterations in blood metabolite concentrations. To investigate whether these phenomena also accompanied increased exercise capacity in *mdx:Myog*-deleted mice, their metabolic profiles were determined. Pre-exercise blood glucose concentrations were approximately equal between wild-type, *mdx*, and *mdx:Myog*-deleted groups. Moreover, these concentrations were virtually unchanged at exhaustion when compared to pre-exercise concentrations, and when compared between groups (Figure 26). These constant blood glucose levels indicate the use of glycolytic metabolism during this high-intensity exercise.

Lactate is a product of glycolysis, and increased blood lactate at exhaustion is a commonly used indicator of glycolytic metabolism. Virtually unchanged lactate levels would be expected during the use of oxidative metabolism. Blood lactate levels at exhaustion were significantly increased for all three test groups. However, the concentration of blood lactate in *mdx:Myog*-

Figure 25

Enhanced exercise capacity in *mdx:Myog*-deleted mice during the high-intensity exercise regimen. *mdx:Myog*-deleted mice ran on average over the course of 3 consecutive days of running 37% more than the *mdx* control group and 11% less than the wild-type mice under high-intensity exercise conditions (*mdx:Myog*-deleted, n=14; *mdx*, n=14; wild-type n=14). Green bar represents *mdx:Myog*-deleted values. Blue bar represents *mdx* values. Red bar represents wild-type control values. Error bars represent one standard deviation (*P<0.05).

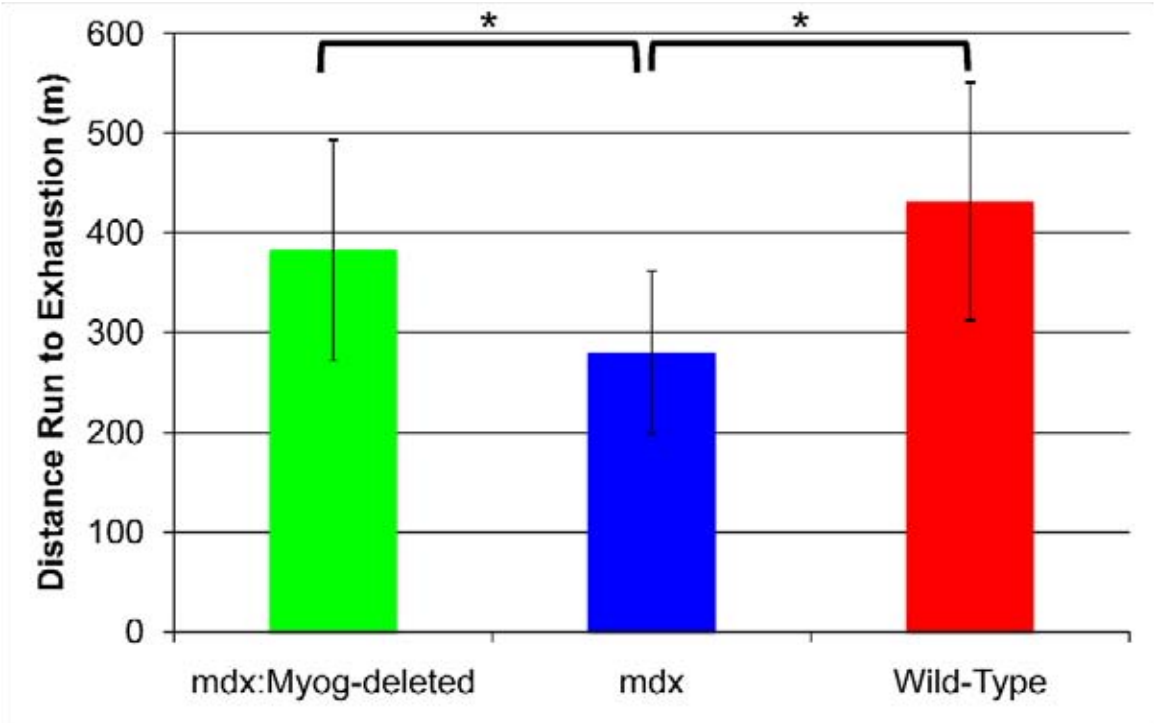
Distance Run to Exhaustion (m)
600
500
400
300
200
100
0
*
*
mdx:Myog-deleted
mdx
Wild-Type

Figure 26

Blood glucose levels in *mdx, mdx:Myog*-deleted, and wild-type mice after running to exhaustion under high-intensity exercise conditions. Baseline blood glucose levels were virtually equal for all three test groups at between 158 to 177 mg/dL (*Myog*-deleted, n=14; wild-type n=14). At exhaustion, blood glucose values remained virtually unchanged for all groups. Green bars represent *mdx:Myog*-deleted values. Blue bars represent *mdx* values. Red bars represent wild-type control values. Error bars represent one standard deviation.

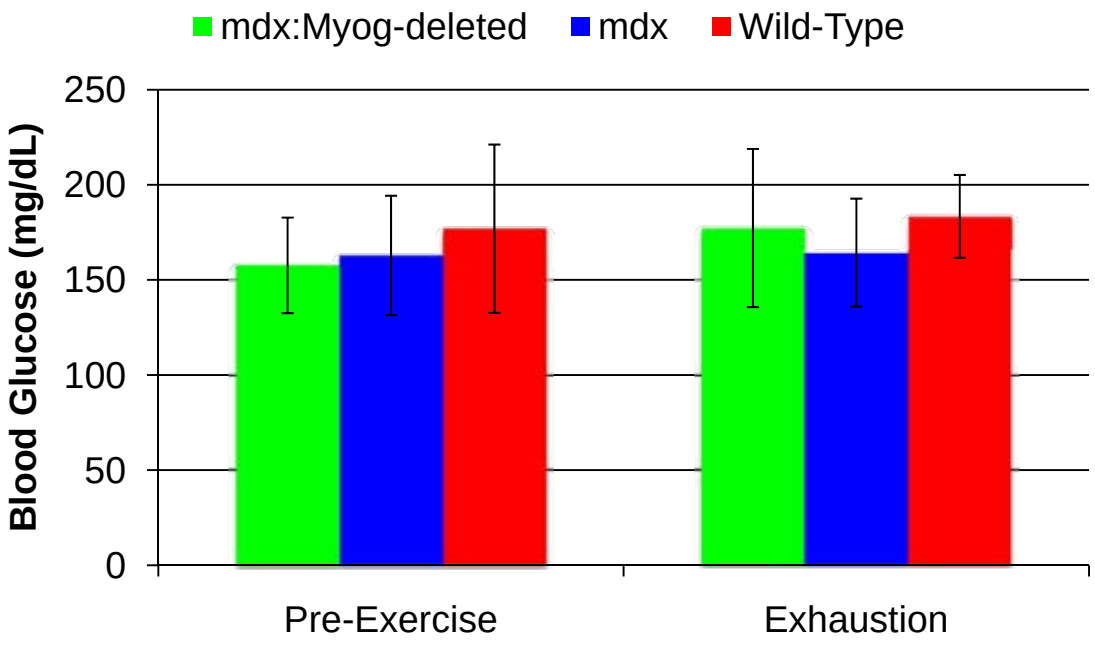
mdx:Myog-deleted
mdx
Wild-Type
Blood Glucose (mg/dL)
250
200
150
100
50
0
Pre-Exercise
Exhaustion

deleted mice was 14% greater than wild-type and 51% greater than *mdx* animals (Figure 27). The results suggested that *mdx:Myog*-deleted mice possessed a higher lactate concentration threshold before reaching exhaustion.

Myog is not required for muscle regeneration in the adult mouse

Histological analyses revealed the muscle morphology of *mdx:Myog*-deleted mice to be similar if not identical to that of *mdx* mice. Conventional signs of muscle regeneration were observed in both groups including the presence of myofibers of widely varying sizes containing centrally located nuclei (Figure 28A). Van Gieson staining for collagen and elastin also revealed similar patterns of mild fibrosis in *mdx* and *mdx:Myog*-deleted mice (Figure 28B). To determine the impact of the absence of myogenin on the dystrophin-glycoprotein complex, blood CK activity was determined. Both *mdx* and *mdx*:*Myog*-deleted mice show dramatically elevated CK levels compared to wild-type control mice (Figure 29). These results demonstrated that myogenin's absence in adult *mdx* mice did not reverse the pathological effects of muscular dystrophy in skeletal muscle. Furthermore, the absence of *Myog* in *mdx* mice did not exacerbate muscle dystrophy, indicating that *Myog* is dispensible for muscle regeneration.

Myofiber characteristics of *mdx:Myog*-deleted adult mice

The deletion of *Myog* in *mdx* mice might alter muscle properties such as fiber type proportion and glycogen content. qRT-PCR was performed to determine transcript levels for myosin type 1, type 2A, and type 2B isoforms in the

Figure 27

Increased blood lactate levels in *mdx, mdx:Myog*-deleted, and wild-type mice after running to exhaustion under high-intensity exercise conditions. Blood lactate levels were significantly elevated for all three test groups at exhaustion. Wild-type and *mdx:Mog*-deleted values were significantly greater than those of the *mdx* group. Green bar represents *mdx:Myog*-deleted values (n=12). Blue bar represents *mdx* values (n=11). Red bar represents wild-type control values (n=10). Error bars represent one standard deviation (*$P<0.05$).

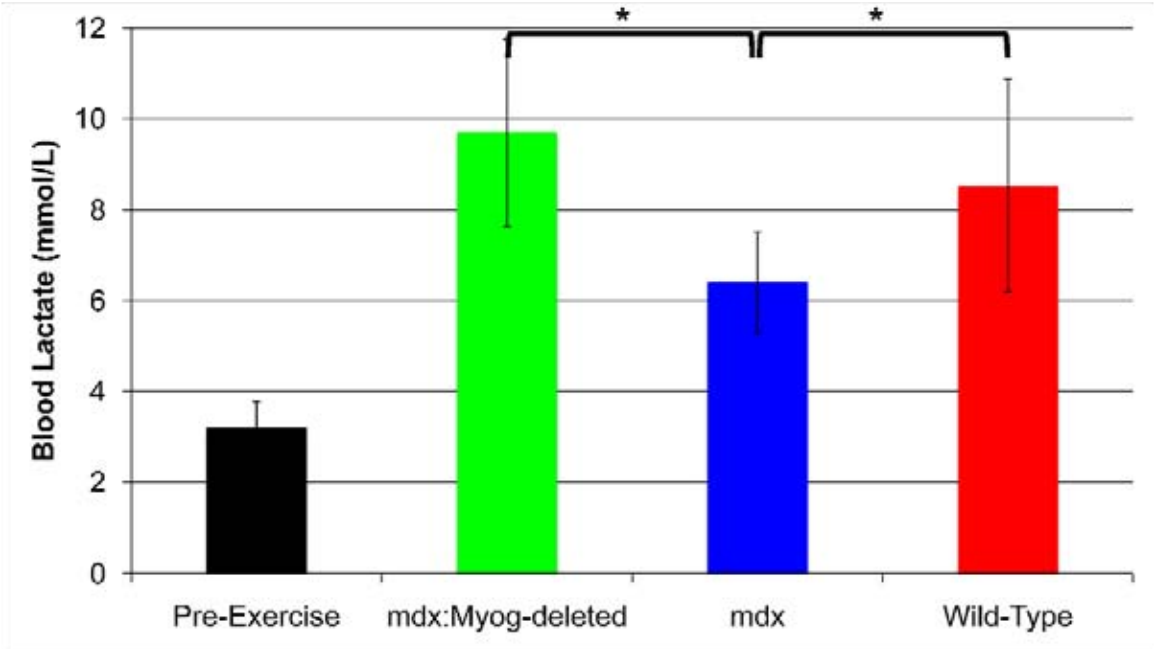
Blood Lactate (mmol/L)
12
10
8
6
4
2
0
*
*
Pre-Exercise
mdx:Myog-deleted
mdx
Wild-Type

Figure 28

Histological evaluation of *mdx, mdx:Myog*-deleted, and wild-type hindlimb muscle. (A) Hematoxylin and eosin stained *mdx and mdx:Myog*-deleted muscle sections both displayed classic characteristics of regeneration including wide variations in fiber caliber and centrally located nuclei that were not observed in wild-type samples. (B) Staining for collagen and elastin reveals similar levels of fibrosis in *mdx and mdx:Myog*-deleted muscle sections that are not observed in wild-type samples.

A

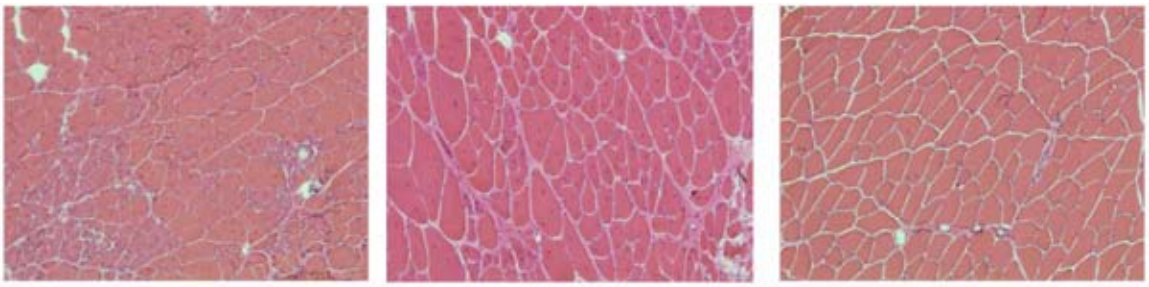
mdx:Mvoa-deleted
mdx
Wild-Type

B

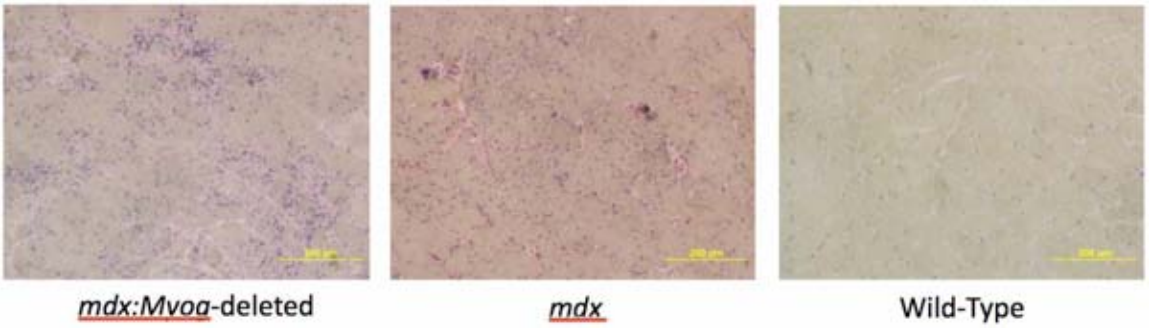
mdx:Mvoa-deleted
mdx
Wild-Type

Figure 29

Increased concentration of blood creatine kinase in *mdx* and *mdx:Myog*-deleted mice. Blood creatine kinase levels were significantly elevated for both *mdx* and *mdx:Myog*-deleted mice compared to the wild-type control group, but there was no significant difference between the *mdx* and *mdx:Myog*-deleted groups. Green bar represents *mdx:Myog*-deleted values (n=9). Blue bar represents *mdx* values (n=10). Red bar represents wild-type control values (n=6). Error bars represent one standard deviation (*$P<0.05$).

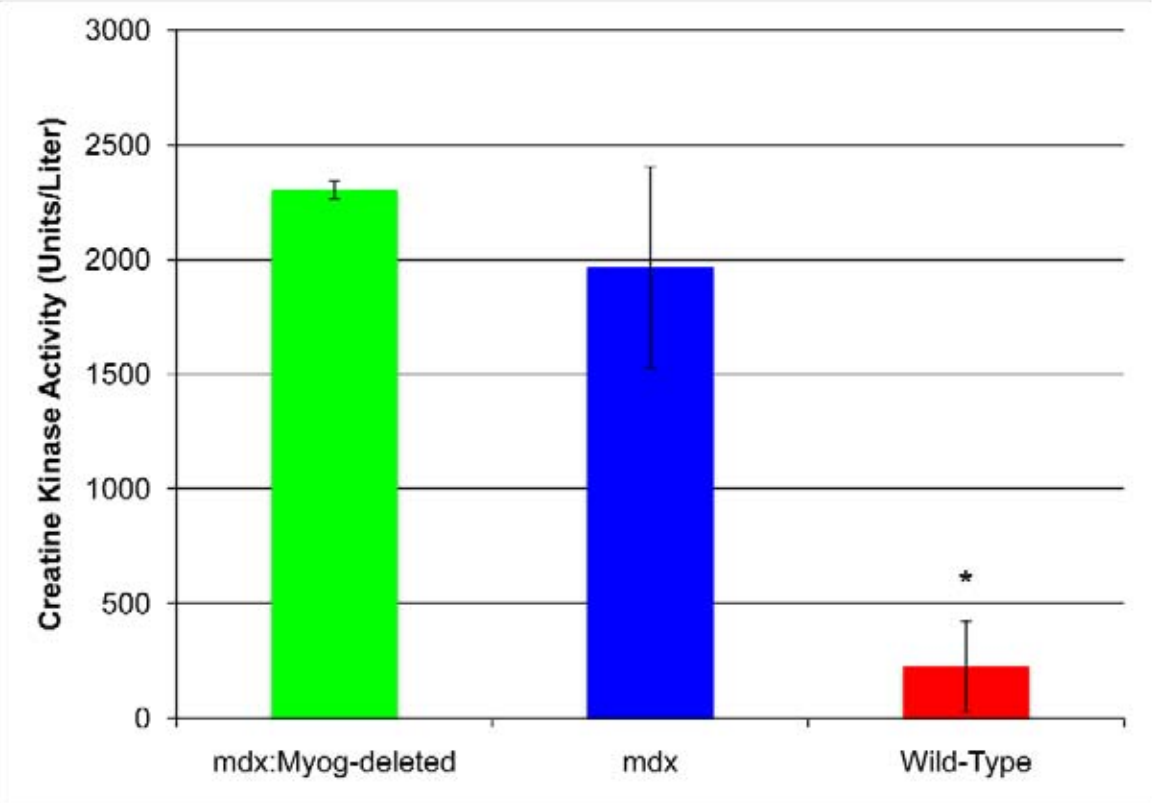
Creatine Kinase Activity (Units/Liter)
3000
2500
2000
1500
1000
500
0
*
mdx:Myog-deleted
mdx
Wild-Type

gastrocnemius muscles of *mdx*, *mdx*:*Myog*-deleted, and wild-type control mice. No significant changes in the expression of these transcripts between *mdx* and *mdx*:*Myog*-deleted mice were detected (Figure 30).

Glycogen staining of muscle sections revealed a dramatic increase in glycogen content in *mdx*:*Myog*-deleted muscle compared to *mdx* and wild-type muscle samples (Figure 31A). However, attempts to quantify the data using whole muscle homogenates with a glycogen biochemical assay were unable to confirm the significance of this observation (Figure 31B). The results indicated that the deletion of *Myog* from *mdx* mice did not alter myosin isoform distribution but may have increased glycogen abundance.

Expression levels of genes regulating muscle fatigue, metabolism, and proteolysis are altered in *mdx:Myog*-deleted adult mice

To begin elucidating the mechanisms driving the observed enhanced exercise capacity of *mdx:Myog*-deleted mice over their mdx counterparts, putative myogenin target genes were identified in adult skeletal muscle. Transcript levels of genes regulating muscle development, metabolic processes and muscle proteolysis such as nNOS, Pfk, Hdac4, Trim63, Fbxo32, glycogen synthase, and muscle glycogen phosphorylase were measured. Of these genes, the expression of nNOS and Fbxo32 were significantly altered in the absence of myogenin (Figure 32). These changes in expression may contribute to the observed enhanced exercise capacity in *mdx:Myog*-deleted mice over the *mdx*

Figure 30

Myosin expression levels in *mdx, mdx:Myog*-deleted, and wild-type hindlimb muscle. No significant changes in transcript expression values, as assessed by qRT-PCR, for myosins type 1, 2A, and 2B were observed between the *mdx* and *mdx:Myog*-deleted groups. Slight but significant alterations in myosins types 2A and 2B were detected between wild-type and *mdx:Myog*-deleted mice. Green bars represent *mdx:Myog*-deleted values (n=3). Blue bars represent *mdx* values (n=3). Red bars represent wild-type control values (n=3). Error bars represent standard error of the mean.

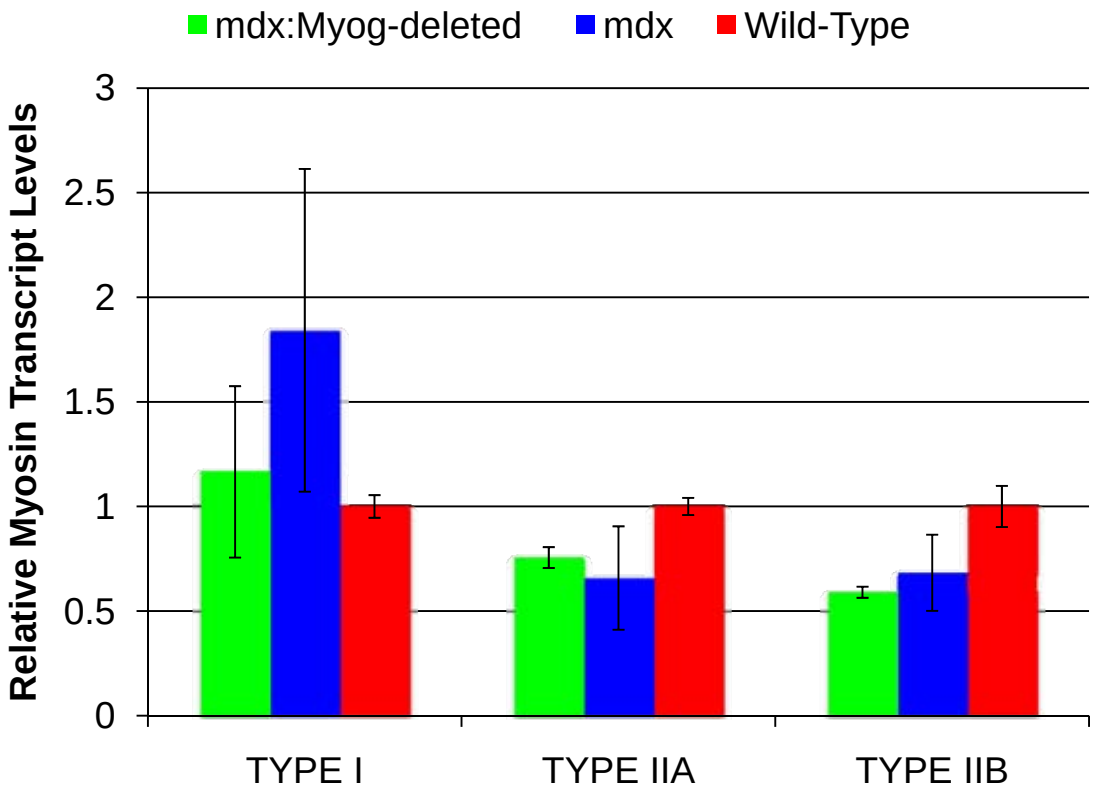
mdx:Myog-deleted
mdx
Wild-Type
Relative Myosin Transcript Levels
3
2.5
2
1.5
1
0.5
0
TYPE I
TYPE IIA
TYPE IIB

Figure 31

Glycogen content in wild-type and *Myog*-deleted hindlimb muscle. (A) PAS staining for glycogen in the gastrocnemius reveals similar levels of glycogen in *mdx* and wild-type samples, but suggests the *mdx:Myog*-deleted sections may harbor increased glycogen content. (B) Biochemical data suggests a nonstatistical trend toward increased glycogen content in the soleus and EDL muscles of *mdx:Myog*-deleted mice. Green bars represent *mdx:Myog*-deleted values (n=3). Blue bars represent *mdx* values (n=3). Red bars represent wild-type control values (n=3). Error bars represent standard error of the mean (*P<0.05).

A.

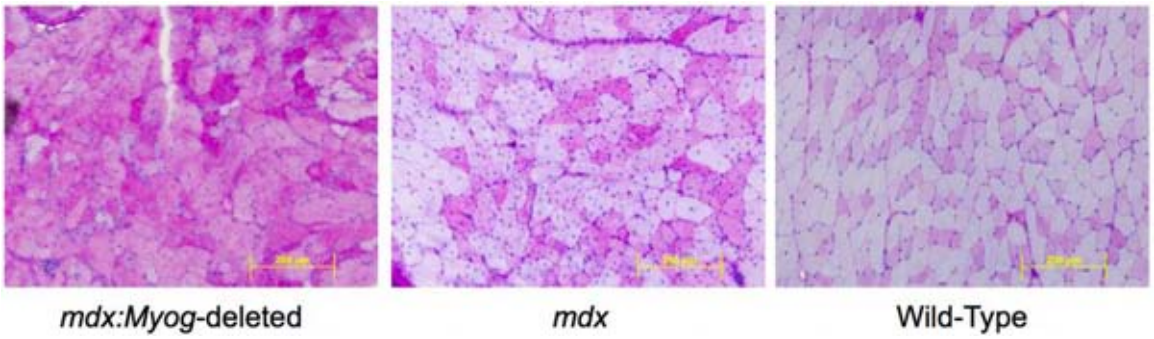
mdx:Myog-deleted
mdx
Wild-Type

B.

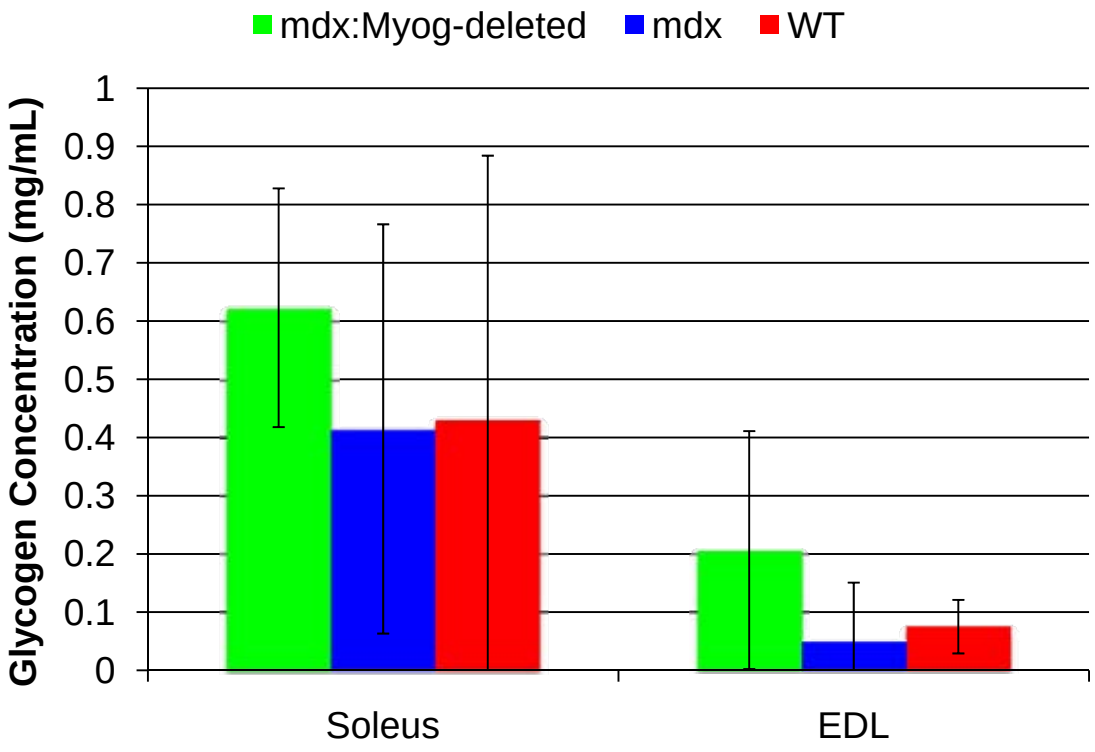
mdx:Myog-deleted
mdx
WT
Glycogen Concentration (mg/mL)
1
0.9
0.8
0.7
0.6
0.5
0.4
0.3
0.2
0.1
0
Soleus
EDL

Figure 32

Altered expression of nNOS and Fbxo32 in *mdx, mdx:Myog*-deleted, and wild-type hindlimb muscle. As verified by qRT-PCR, transcript levels of nNOS were dramatically reduced in *mdx* mice. Expression of nNOS was increased by 2.2 fold in *mdx:Myog*-deleted mice over their *mdx* counterparts. Fbxo32 expression was determined to be significantly increased in *mdx* mice over the *mdx:Myog*-deleted group and showed a trend toward increased expression over wild-type mice. Green bars represent *mdx:Myog*-deleted values (n=3). Blue bars represent *mdx* values (n=3). Red bars represent wild-type control values (n=3). Error bars represent one standard deviation (*P<0.05).

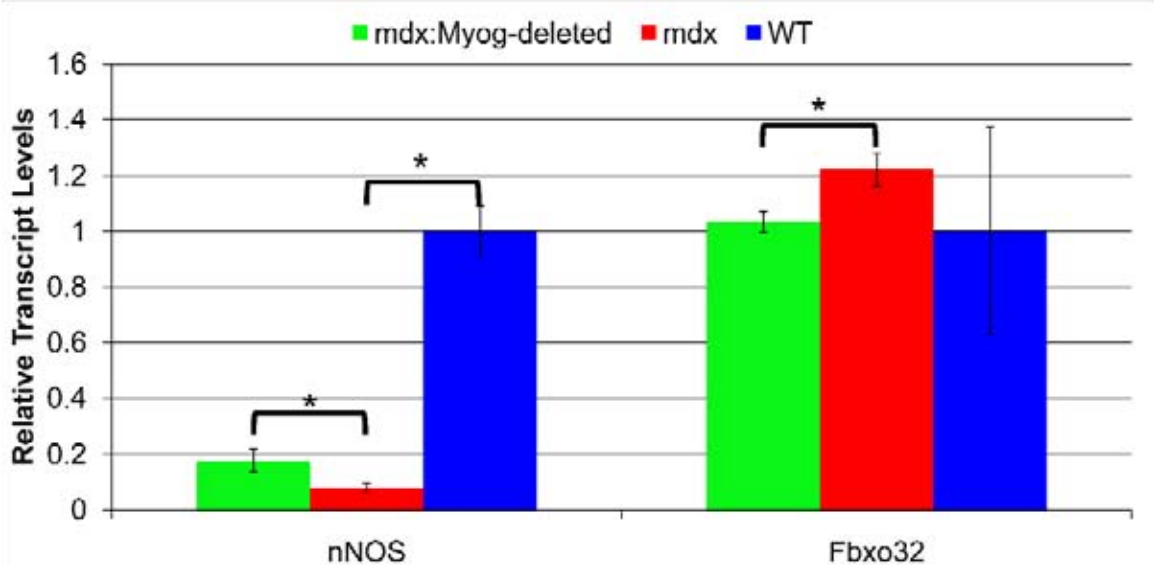
mdx:Myog-deleted
mdx
WT
Relative Transcript Levels
1.6
1.4
1.2
1
0.8
0.6
0.4
0.2
0
*
*
*
nNOS
Fbxo32

group and could provide insight into the mechanisms by which myogenin exerts its effects.

DISCUSSION:

Myogenin is an essential transcription factor involved in the development of muscle fibers during embryogenesis [12, 29, 70]. Myogenin's role in the maintenance and regeneration of adult skeletal muscle has been long speculated but not tested in model systems where muscle regeneration is genetically compromised. In this study, essential coding and regulatory regions of the *Myog* locus were conditionally deleted from *mdx* adult mice. Efficient deletion of *Myog* was achieved after tamoxifen-induced Cre-mediated recombination. *Mdx:Myog*-deleted mice exhibited no remarkable differences in their behavior or mobility when compared to wild-type controls. These results are consistent with previous studies indicating that *Myog* is dispensable during adult life [13, 29]**.**

Given that *Myog* is activated upon muscle injury to help facilitate muscle repair and regeneration, and *mdx* mice exist in a constant state of muscle regeneration [71], I expected that *Myog* transcripts would be upregulated in muscle from *mdx* mice. *Myog* transcript levels were dramatically increased in *mdx* mice while *mdx:Myog*-deleted mice exhibited levels much closer to wild-type controls. As skeletal muscle stem cells are activated to repair and fuse with existing muscle fibers, myogenin expression increases in the latter stages of differentiation. These compensatory events in *mdx* mice result in muscle hypertrophy characterized by increases in muscle mass, fiber count, centrally located nuclei, and distribution of the fiber calibers in *mdx* mice [60, 72, 73]. The results described in this chapter confirm previously published studies indicating

that myogenin expression is elevated in *mdx* mice [74]. The efficient deletion of *Myog* and its subsequent downregulation in *mdx* mice resulted in no noticeable adverse effects and indicates that *Myog* is not required for survival or normal muscle function in these animals.

Since dystrophic muscle exists in a constant state of damage repair [62, 63, 65, 75], I hypothesized that vigorously exercised *mdx* mice would exhibit a dramatic reduction in exercise capacity compared to wild-type mice. Under high-intensity exercise conditions, *mdx* mice ran 35% less than wild-type controls. *Mdx:Myog*-deleted mice ran 36% farther than the *mdx* control group, nearly equaling the distances achieved by wild-type control mice. These data agree with previous findings described in chapter I and indicate that *mdx* mice, like wild-type mice, benefit from the loss of myogenin and exhibit similar gains in exercise capacity following *Myog*-deletion.

Results described in chapter I indicated that the deletion of *Myog* enhanced exercise endurance by altering skeletal muscle metabolism. The metabolic changes were evidenced by alterations in blood glucose and lactate concentrations following exercise. While blood glucose was significantly depleted below wild-type levels in *Myog*-deleted mice following high-intensity exercise, *mdx:Myog*-deleted mice exhibited blood glucose levels equal to that of the wild-type and *mdx* control groups. This result is expected as the high-intensity exercise regimen is designed to employ the use of glycolytic metabolism, which primarily utilizes muscle glycogen as a fuel source. *Mdx:Myog*-deleted mice often reach exhaustion before metabolizing significant

amounts of liver glycogen, thus leaving blood glucose concentrations at normal levels. The lack of observable blood glucose depletion in *mdx:Myog*-deleted mice suggests that the inherent muscle weakness of *mdx* mice limits exercise endurance, thus preventing their blood glucose levels from dropping below those of wild-type mice. Blood lactate concentrations were significantly elevated in *mdx:Myog*-deleted mice compared to the *mdx* control group following high-intensity exercise. These results suggest that the loss of myogenin in *mdx* mice confers an increased lactate threshold before reaching exhaustion.

As discussed in chapter I, lactate production may actually retard muscle acidosis. The conversion of pyruvate to lactate by lactate dehydrogenase also generates NAD+. This aids in sustaining the NAD+/NADH cytosolic redox potential which promotes substrate flux through glycolysis and ultimately enables the glycolytic production of ATP [30]. Furthermore, this reaction consumes an additional proton from the cytosol and is thus alkalizing to the muscles. The discharge of lactate from the muscle is facilitated by monocarboxylate transporter [32, 76-79], a known symport for proton removal from muscle fibers. The transport of lactate out of the muscle by this mechanism is stoichiometrically accompanied by the removal of protons. In fact, published data suggests the rate of proton removal outpaces the rate of lactate removal in active muscle [80]. Thus, increased blood lactate levels may contribute to the observed increase in exercise capacity.

Mdx mice exhibit defects in muscle regeneration due to the absence of dystrophin at the sarcolemma [81]. These defects in muscle regeneration are

readily apparent after bouts of intense exercise and generally result in chronic muscle weakness. As *mdx:Myog*-deleted mice exhibited enhanced exercise endurance, I determined whether their muscles displayed signs of improved muscle function. No remarkable changes were detected in the muscle pathology of *mdx:Myog*-deleted mice when compared to the *mdx* control group. Characteristic signs of muscle regeneration such as centrally located nuclei and wide variations in myofiber diameter were observed in both *mdx:Myog*-deleted and *mdx* mice. *Mdx* muscles are also particularly prone to fibrosis due to the increased production of connective tissue that is coincident with defective muscle regeneration and muscle atrophy [58]. No differences were detected in the abundance of fibrotic tissue from the muscles of *mdx:Myog*-deleted mice compared to the *mdx* control group. Elevated blood CK levels resulting from the leakage of CK through the damaged sarcolemma are also characteristic of dystrophic muscle [82]. Dramatically elevated blood CK levels were observed in both *mdx:Myog*-deleted mice and the *mdx* control group when compared to wild-type. Given that CK levels remained elevated in *mdx:Myog*-deleted mice, the sarcolemmal defects normally associated with dystrophin deficiency are likely unrepaired in these animals. Although *mdx:Myog*-deleted mice display enhanced exercise endurance, the pathology of these mice resembles that of the *mdx* control group.

Surprisingly, *mdx* mice did not display an increased penetrance of muscular dystrophy following the deletion of *Myog*. The mice displayed no overt adverse phenotypic characteristics with seemingly normal activity levels. This is

unexpected since *mdx:MyoD(*-/-) mice are known to exhibit a severe dorsal-ventral curvature of the spine, become progressively less activity, and incur premature death [83]. This suggests that the loss of myogenin neither enhances nor impairs muscle regeneration and is thus dispensable for these processes.

In mammalian muscle, enhanced exercise endurance is typically associated with increases in type 1 and type 2A muscle fibers as well as increases in muscle glycogen content [84]. To determine whether a change in muscle fiber type or glycogen content was conferring the observed enhanced exercise capacity in *mdx:Myog*-deleted mice, histological, biochemical, and gene expression analyses were performed. Selected hindlimb muscles from *mdx:Myog*-deleted mice displayed no significant differences in myosin isoform expression when compared to the *mdx* control mice. The staining of muscle for glycogen abundance suggested there was increased glycogen content in *mdx:Myog*-deleted samples. Biochemical analyses of whole muscle glycogen content also revealed a trend toward increased glycogen in *mdx:Myog*-deleted muscle. The results indicated that myofibers of *mdx:Myog*-deleted mice may contain more glycogen than their *mdx* counterparts, but display many other characteristics similar to that of *mdx* mice.

Dystrophin deficiency confers a complex pathophysiology in *mdx* mice due to the secondary loss of other dystrophin-glycoprotein complex factors [67]. In fact, 80-90% of all dystrophin-glycoprotein associated factors are absent in *mdx* mice [66, 85]. These proteins are synthesized as normal, but without dystrophin they are unable to incorporate into the sarcolemma properly and are

thus targeted for degradation [86]. One of these factors is nNOS. Mice deficient for nNOS are unable to oppose vasoconstriction resulting in ischemia and increased fatiguability [87, 88]. Furthermore, nitric oxide has been shown to regulate neuromuscular transmission [89] as well as enhance mitochondrial biogenesis [90] and GLUT4 production and transport [91], suggesting that reduced nitric oxide production could contribute to the early onset of fatigue [92].

Recently, Wehling-Henricks et al. showed that a loss of interaction between nNOS and PFK contributes to glycolysis defects and increased fatigability in *mdx* mice [67]. Given these results, I determined whether nNOS and PFK expression would be affected by the deletion of myogenin from *mdx* mice. The results confirmed a dramatic decrease in nNOS expression in *mdx* muscle compared to wild-type and detected a 2.2-fold increase in nNOS expression in *mdx:Myog*-deleted muscle compared to *mdx* samples; PFK expression remained unchanged. The increase in nNOS expression in *mdx:Myog*-deleted mice could contribute to their reduced fatigability and may help explain their enhanced exercise endurance compared to the *mdx* control group.

Recently, Moresi et al. showed that *Myog*-deleted mice are resistant to denervation-induced muscle atrophy [26]. Myogenin was found to activate Trim63 and Fbxo32, E3 ubiquitin ligases involved in muscle proteolysis and atrophy. Trim63 and Fbxo32 are normally upregulated in various models of muscle wasting, and a deficiency of these factors protects against muscle atrophy. The loss of myogenin was associated with preserved muscle mass

following denervation and diminished expression of Trim63 and Fbxo32. Their results suggest the involvement of myogenin in a molecular pathway responsible for muscle wasting disorders and prompted us to determine Trim63 and Fbxo32 expression levels in *mdx* mice lacking myogenin. Although no changes in Trim63 expression were observed, a significant reduction in Fbxo32 expression in *mdx:Myog*-deleted mice was detected. This result is consistent with the study described above and suggests that the loss of myogenin may downregulate Fbxo32 activity. The reduction in Fbxo32 expression may help protect against the inherent and chronic muscle atrophy found in dystrophic muscle.

In humans, DMD is a chronic muscle disease leading to progressive muscle weakness and muscle wasting. The *mdx* mouse model described here reliably demonstrates that the exercise capacity of *mdx* mice is considerably less than that of wild-type control mice. The observed decrease in exercise capacity of *mdx* mice is similar to the muscle weakness typically observed in humans with DMD and is likely caused by similar mechanisms. When *Myog* was deleted from *mdx* mice, significant increases in exercise endurance were observed that are associated with changes in the expression of nNOS and Fbxo32. While *mdx:Myog*-deleted mice exhibited an enhanced capacity for exercise, no differences were detected in the histopathology of their muscles compared to the *mdx* control group. Thus, the loss of myogenin from *mdx* mice may rescue their inherent glycolytic dysfunction and muscle weakness, allowing for increased muscle endurance.

Currently, there are no effective treatments to stop the progression or reverse the effects of DMD. Therapies and treatments for this disease, such as corticosteriods and orthotics, are limited and only serve to delay the onset of progressive muscle weakness and eventually death. New therapeutic strategies aim to treat DMD at the molecular level, such as gene replacement therapy and exon skipping. Our results suggest that reducing *Myog* expression in *mdx* mice could contribute to the development of new therapeutic strategies for human DMD. Future directions could include the development of an RNAi delivery system targeting *Myog* transcripts in adult *mdx* mice. If similar enhancements in exercise capacity are observed in those animals, a more translational research approach may be warranted to apply this strategy to larger animals with the ultimate goal of developing therapies for humans with DMD.

APPENDIX:

Elucidating the mechanisms conferring selective target gene activation by myogenin

INTRODUCTION:

Developmental diversity is regarded, in part, to be the evolutionary result of individual transcription factor family members taking on specific roles in regulating selective gene targets [93]. Little is known about how closely related transcription factors distinguish their respective target genes. Elucidating mechanisms that confer this selectivity will provide insight into how this is achieved in transcription factor families composed of closely related members. As gene duplications are a major feature of the human genome, understanding the mechanisms by which this functional specialization is obtained is especially pertinent [94].

As discussed in chapters 1 and 2, the roles of the myogenic regulatory factors (MRFs), MyoD [1], Myf5 [2], MRF4 [3-5], and myogenin [6, 7], have been well established in embryonic skeletal muscle development. Of special interest to this investigation are myogenin and MyoD. The functions of these two factors during embryogenesis are markedly different, yet they share nearly indistinguishable basic helix-loop-helix DNA binding sequences and remarkable homology in other domains [95]. The transcriptional mechanisms enabling MyoD and myogenin to selectively activate specific sets of target genes are still largely unknown. MyoD and myogenin both bind to sequence consensus sites called E-boxes (CANNTG) found in the transcriptional control regions (TCRs) of

muscle-specific genes. MyoD regulates the initial stages of limb skeletal muscle development during the early determination of myoblasts, embryonic skeletal muscle stem cells. The expression of MyoD also persists into the differentiation stages of myogenesis. Myogenin is upregulated in the latter stages of myogenesis and is required for the terminal differentiation of myoblasts into myofibers [96, 97].

Myogenin selectively activates target genes such that MyoD cannot compensate for the loss of myogenin. Although myogenin and MyoD share significant sequence homology, in *Myog*-null myoblasts, MyoD cannot activate the transcription of many myogenin target genes. *Myog*-null mice exhibit skeletal muscle precursor cells expressing MyoD, but possess few or no functional myofibers and die pernatally due to a severe skeletal muscle deficiency [12, 70, 98, 99]. Thus myogenin activates its own unique set of target genes. Discerning how this mode of selectivity is achieved is an important step in obtaining a comprehensive understanding of the myogenic regulatory network. Extensive knowledge of the myogenic regulatory network makes the skeletal muscle gene regulatory system a valuable model for determining how closely related transcription factors regulate selective clusters of target genes [100, 101].

Both chromatin modifications and cofactors have been shown to play important roles in regulating skeletal muscle-specific gene activation. For example, histones H3 and H4 are acetylated following the recruitment of the histone acetyltransferase p300 to the promoter of muscle-specific genes [96].

Cofactors such as E12/47 and MEF2C are critical for synergistically activating muscle-specific genes [102-104], and E-boxes and MEF2 binding sites are often found in very close proximity [105]. Elements such as these may play a role in conferring target gene selectivity.

Recent investigations have attempted to explain how myogenin and MyoD may utilize their functional differences to work in concert during the activation of late-expressing genes in myogenesis [96, 106, 107]. MyoD is known to bind at the TCR's of muscle-specific genes and activate the expression of early-expressing factors [108-110]. It's expression also persists into the differentiation stages of myogenesis where it binds to and initiates chromatin remodeling in late-expressing genes through the recruitment of factors such as HAT3/4 and BRG1 , although it is thought to be insufficient for the activation of these factors [106, 108]. Myogenin is highly upregulated in the latter differentiation phases of myogenesis and activates the transcription of late-expressing genes. However, myogenin appears to be incapable of binding to the TCRs of many muscle-specific genes in the absence of MyoD. Ohkawa et al speculate that myogenin replaces MyoD at the E-box to initiate transcription in late-expressing genes whereas others hypothesize MyoD is required to first bind and initiate the remodeling of chromatin in order to allow the concomitant binding of myogenin at the TCR and activate transcription [106, 108-110]. These models discerning MyoD- from myogenin-mediated gene activation fail to address the mechanisms by which binding to gene regulatory regions early in myogenesis differs from binding to regulatory regions late in myogenesis.

Myogenin and MyoD share significant sequence similarities, yet they function in different capacities. The mechanisms conferring the specific activation of early- or late- expressing genes in myogenesis have yet to be identified. I hypothesize that myogenin acts as a selective activator of transcription through a regulatory network composed of both chromatin modifications and cofactors that are distinct from those employed by MyoD, thereby allowing it to activate specific sets of target genes.

In this appendix, I describe the creation of a Tet-On *Myog*-inducible cell culture system. This system allows for the activation and deactivation of *Myog* in myoblasts under either proliferating or differentiating conditions. Once established, these cells will be used as a tool to elucidate the mechanisms responsible for conferring target gene specificity.

Results

Myog-null myoblasts were isolated and characterized from the tongue tissue of *Myog*$^{-/-}$ E15.5 mouse embryos. Embryos were isolated and tongue tissue was dissected. Tissue samples were then finely minced, treated with collagenase, and grown in culture. Cells from separate embryos were pooled after genotyping confirmed the absence of myogenin. Pre-platings were performed to remove fibroblasts and other contaminating cells. Genotyping performed after pooling and pre-plating indicated both the absence of the wild type allele and the presence of a neomycin cassette (as a result of generating the knockout mouse) (Figure 33). Immunofluorescence using primary antibodies against markers for skeletal muscle stem cells indicated that the cells expressed these markers (Figure 34). When placed in differentiation media for 24 hours, cells began to elongate and fuse together, classic signs of differentiation (Figure 35). This analysis verified that the isolated cells were embryonic skeletal muscle stem cells.

The Retro-X Tet-On Advanced Inducible Expression System from Clontech (www.clontech.com) was employed to generate *Myog*-null myoblasts stably infected with an inducible form of myogenin. The system requires the generation of a double-stable cell line. First, the cells must be stably infected with the vector coding for the tetracycline-controlled transactivator (pRetroX-Tet-On Advanced). The cells are then infected with the vector containing the gene of interest (pRetroX-Tight-Pur).

Figure 33

Genotype verification of isolated *Myog*-null cells. Putative myoblasts isolated from *Myog*-null E15.5 tongue tissue exhibit both the absence of the wild type allele (A) and the presence of a neomycin cassette (B) (as a result of generating the knockout mouse).

A.

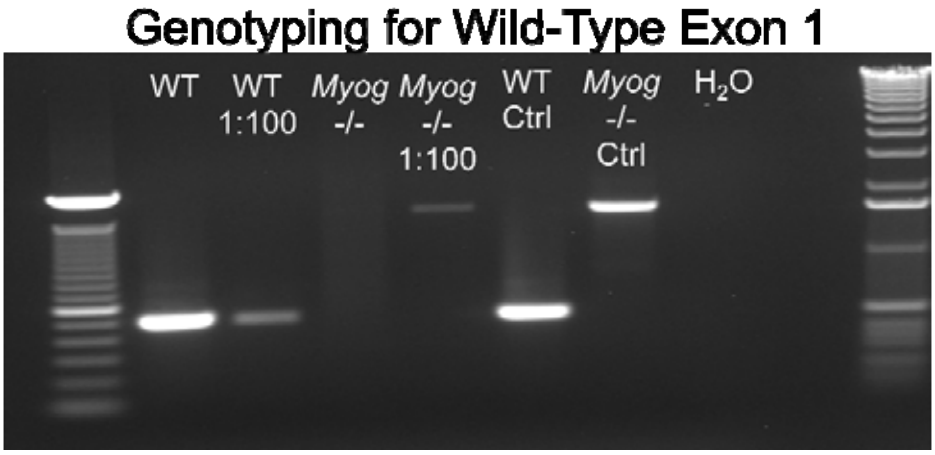
Genotyping for Wild-Type Exon 1
WT
WT 1:100
Myog -/-
Myog -/- 1:100
WT Ctrl
Myog -/- Ctrl
H2O

B.

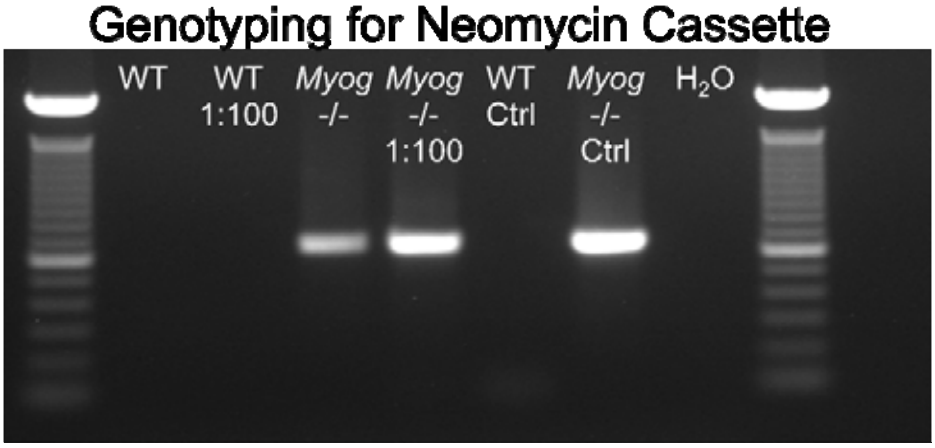
Genotyping for Neomycin Cassette
WT
WT 1:100
Myog -/-
Myog -/- 1:100
WT Ctrl
Myog -/- Ctrl
H2O

Figure 34

Differentiation of putative myoblasts into myotubes. Putative myoblasts isolated from *Myog*-null E15.5 tongue tissue proliferate continually in high-concentration fetal bovine serum (FBS) media. When switched to low-concentration horse serum media for 24 hours, cells cease proliferation and begin to differentiate, elongating and fusing together to form myotubes.

Proliferation

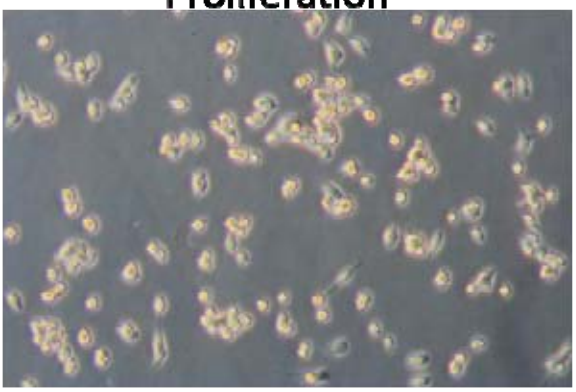

24hrs Differentiation

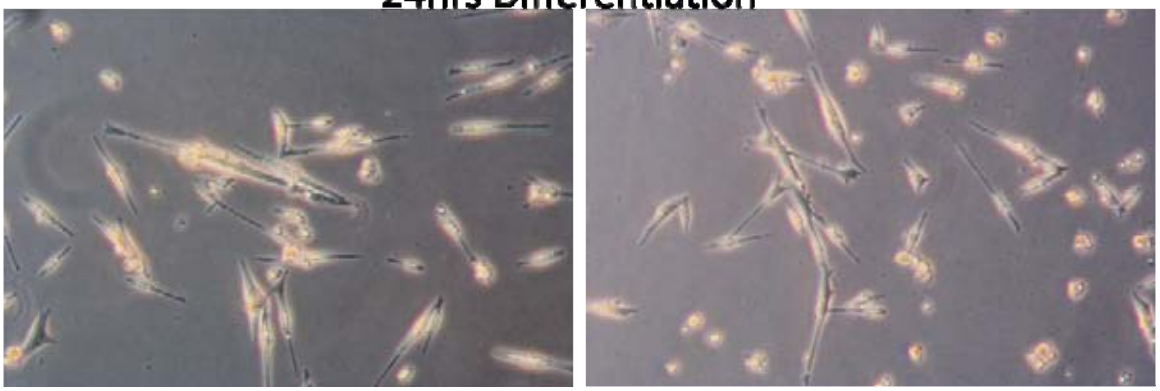

Figure 35

Verification of expression of skeletal muscle stem cell markers.

Immunofluorescence using primary antibodies against markers for skeletal muscle stem cells (MyoD, C-met, Pax3, M-cadherin, and Desmin) indicated the isolated cells do express these markers.

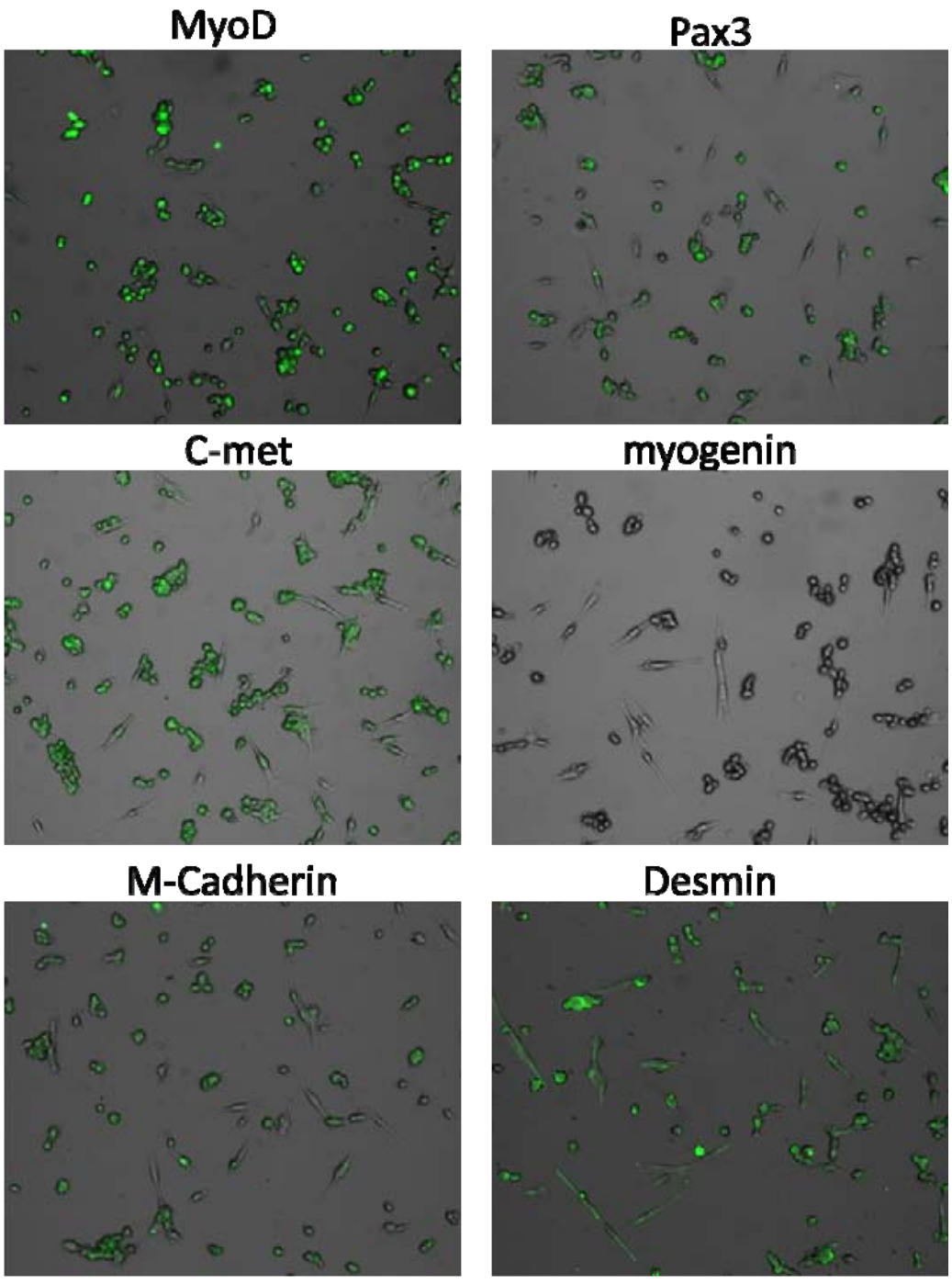
MyoD
Pax3
C-met
myogenin
M-Cadherin
Desmin

The pRetroX-Tet-On Advanced vector utilizes a neomycin cassette so that stably infected cells can be selected for using G418 in drug selection. Because *Myog*-null myoblasts already expressed a neomycin cassette as a result of generating the null line, the vector was engineered with an alternate method for drug selection. The neomycin cassette was excised and a blasticidin cassette from another vector was subcloned in its place (Figure 36).

Myog cDNA followed by an IRES-GFP cassette was subcloned into the pRetroX-Tight-Pur vector (Figure 37). This was achieved by generating a *Myog*-GFP topovector, removing the *Myog*-GFP sequence, and ligating into the linear pRetroX-Tight-Pur vector to create the final pRetroX-Tight-Pur-*Myog-GFP* vector. This vector was later sequenced to verify the orientation and the absence of mutations.

Both vectors described above were transiently transfected into Eco-Pack 293 packaging cells to generate retrovirus stocks. Virus-containing medium was collected and the viral titer was determined by colony formation.

A death curve for the *Myog*-null myoblasts with varying concentrations of blasticidin & puromycin was performed to determine the minimal concentrations necessary to eradicate all the cells. These concentrations were then used for drug selection.

A single-stable RetroX-Tet-On Advanced cell line was then generated by infecting *Myog*-null myoblasts with the RetroX-Tet-On Advanced vector. The infection was allowed to proceed for 24 hours. Blasticidin was then added to the plates and 40 colonies were isolated using cloning discs.

Figure 36

Verification of replacement of Neomycin cassette for Blasticidin cassette in the pRetroX-Tet-On Advanced vector. The neomycin cassette was excised and subcloned in its place was a blasticidin cassette. Restriction digestions indicate the insertions were of the expected sizes.

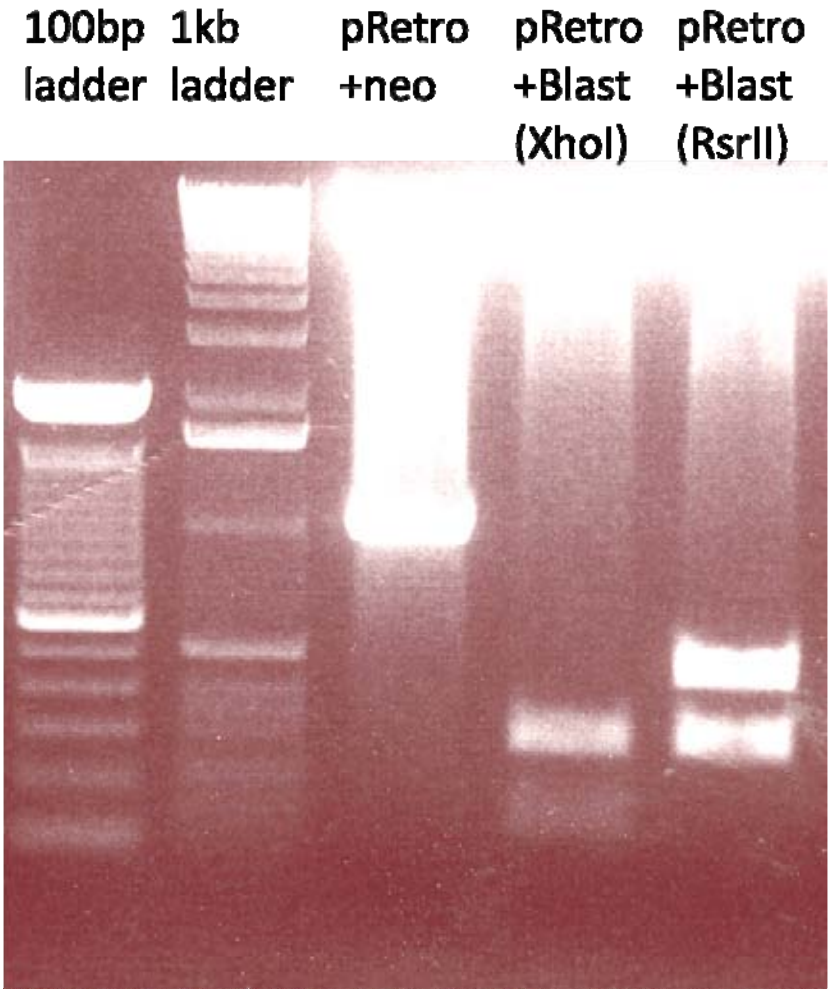
100bp ladder
1kb ladder
pRetro +neo
pRetro +Blast (XhoI)
pRetro +Blast (RsrII)

Figure 37

Verification of *Myog*-GFP cassette insertion into the pRetroX-Tight vector. *Myog* cDNA followed by an IRES-GFP cassette was subcloned into the pRetroX-Tight-Pur vector. Restriction digestions indicate the insertions were of the expected sizes.

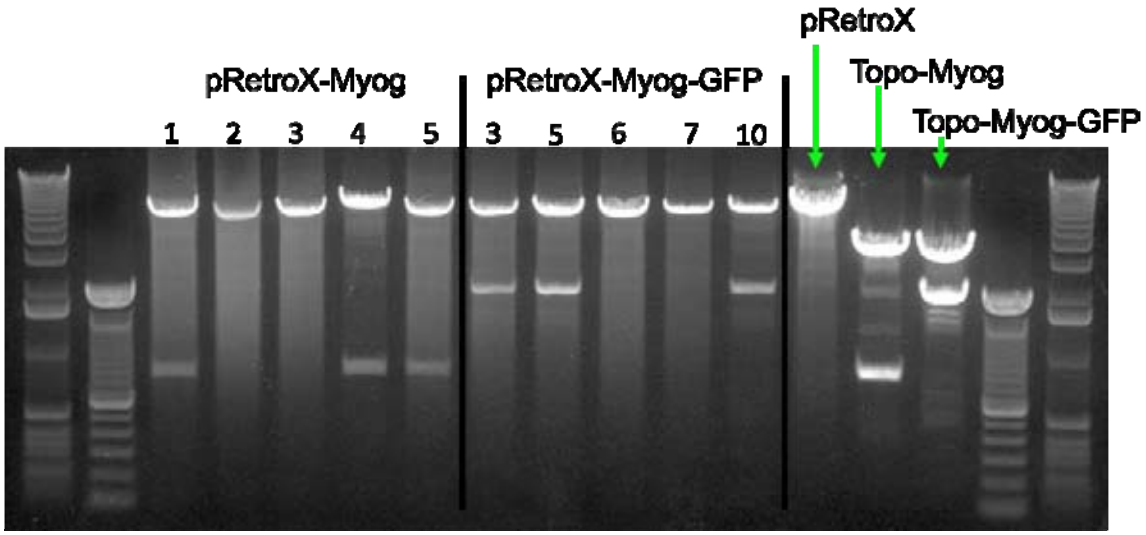
pRetroX
pRetroX-Myog
pRetroX-Myog-GFP
Topo-Myog
Topo-Myog-GFP
1
2
3
4
5
3
5
6
7
10

The viability of the RetroX-Tet-On Advanced clones was tested by infecting them with a luciferase reporter vector that is activated by the tetracycline-controlled transactivator encoded by the RetroX-Tet-On Advanced vector. Each clone was then treated with 500 ng/ml of Doxycycline (Dox) and the fold induction was determined. Clones exhibiting 20- to 50-fold induction were chosen to generate double-stable lines (Figure 38).

To accomplish this, single-stable *Myog*-null myoblasts were infected with the pRetroX-Tight-Pur-*Myog*-*GFP* vector to generate double-stable lines. The infection was allowed to proceed for 24 hours. Puromycin was added to the plates and colonies were isolated using cloning discs.

Double-stable cell lines were then screened by qRT-PCR for the presence of *Myog* transcripts in the presence and absence of Dox at 500 ng/ml. Multiple lines exhibiting significant induction in the presence of Dox and little to no induction in the absence of Dox (Figure 39) were frozen in liquid nitrogen. Cell line 11 was chosen as the primary line for further study.

Since the pRetroX-Tight-Pur vector contained *Myog* cDNA followed by an IRES-GFP cassette, induced double-stable *Myog*-null myoblasts expressed GFP (Figure 40). Furthermore, double immunostaining showed the presence of myogenin in the nucleus and GFP in the cytoplasm of the same cells (Figure 41).

To more accurately reflect the endogenous expression of myogenin that is observed in wild-type differentiating myoblasts, I attempted to determine the concentration of Dox required to induced *Myog* expression to wild-type levels in

Figure 38

Luciferase activity of selected single stable myoblast colonies. Subpopulations of cells infected with the RetroX-Tet-On Advanced vector and a luciferase reporter vector that is activated by the tetracycline-controlled transactivator encoded by the RetroX-Tet-On Advanced vector displayed varying levels of reporter activity. Clones exhibiting 20- to 50-fold induction were chosen to continue making double-stable lines with.

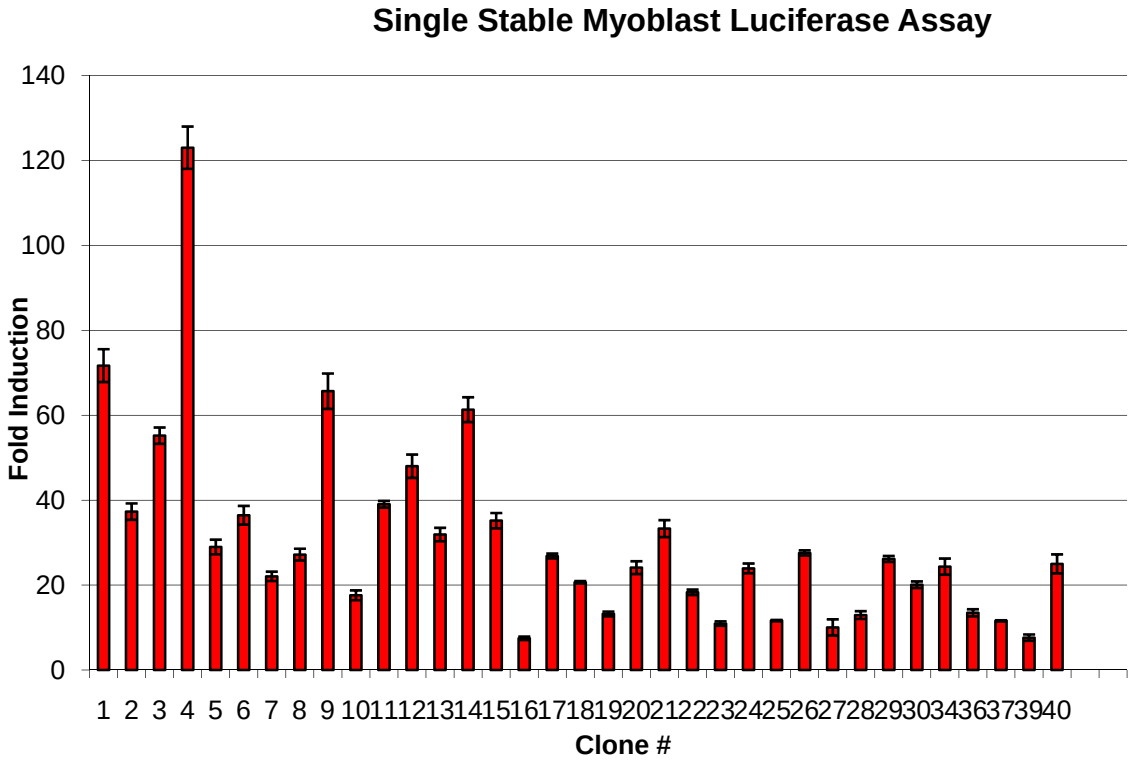
Single Stable Myoblast Luciferase Assay
Fold Induction
0
20
40
60
80
100
120
140
1 2 3 4 5 6 7 8 9 10 11 12 13 14 15 16 17 18 19 20 21 22 23 24 25 26 27 28 29 30 34 36 37 39 40
Clone #

Figure 39

Doxycyclin induction of *Myog* expression in double-stable myoblasts. Subpopulations of cells infected with the RetroX-Tet-On Advanced vector and pRetroX-Tight-Pur-Myog vector displayed varying levels of *Myog* activation in the presence of Doxycyclin. Clones exhibiting high *Myog* expression in the presence of Dox and little to no *Myog* expression in the absence of Dox were chosen for further experiments.

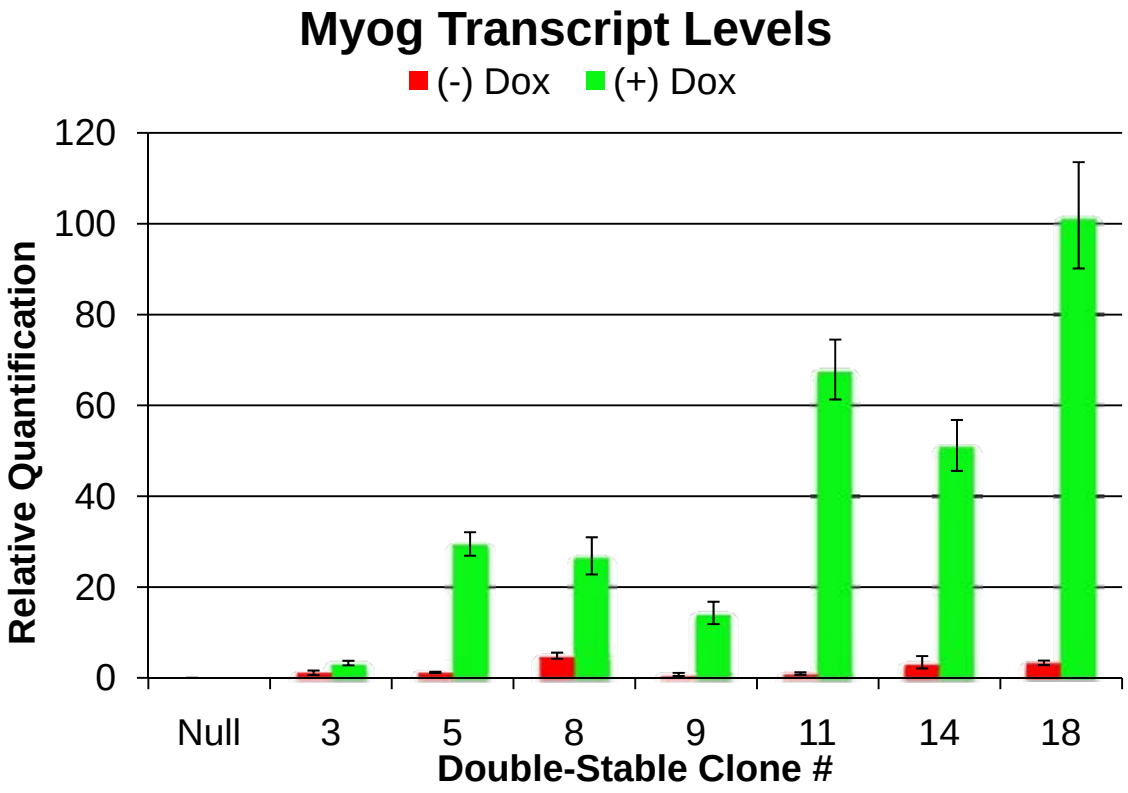
Myog Transcript Levels
(-) Dox
(+) Dox
Relative Quantification
120
100
80
60
40
20
0
Null
3
5
8
9
11
14
18
Double-Stable Clone #

Figure 40

GFP reporter expression in double-stable myoblasts in the presence and absence of Dox. Double-stable myoblasts fluoresce green only in the presence of Dox indicating the induction of myogenin.

(-) DOX

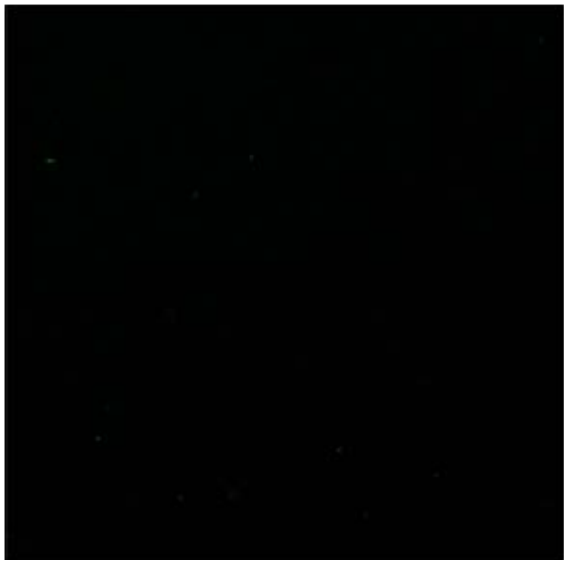

(+) DOX – 48hrs

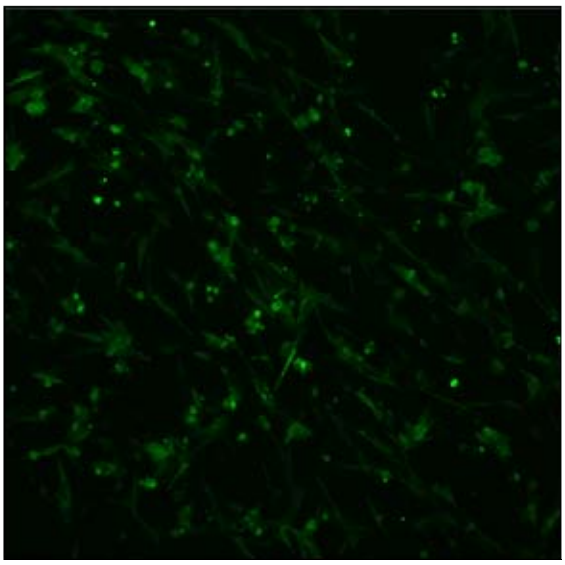

Figure 41

Expression of myogenin and GFP in the same cells in the presence of Dox. Immunofluorescence indicates the nuclear expression of myogenin and the cytoplasmic expression of GFP in the same cells only in the presence of Dox.

(-) DOX

(+) DOX – 48hrs

myogenin GFP

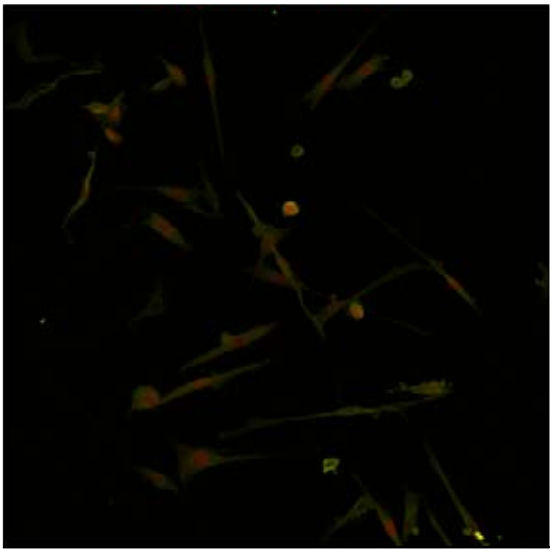

double-stable myobalsts. To accomplish this, a primary culture of wild-type embryonic myoblasts was required. However, numerous attempts to isolate and establish a wild-type line were unsuccessful due to technical difficulties such as bacterial or yeast contaminations, unsuccessful preplatings due to an overabundance of fibroblasts, and unviable populations of myoblasts either dying or not proliferating. In attempts to circumvent these issues, I determined whether an established line of commercially available C2C12 myoblasts would be an acceptable substitute. qRT-PCR was used to determine the *Myog* transcript levels in C2C12 myoblasts compared to other control myogenic cell lines (Figure 42). C2C12 myoblasts possessed fewer *Myog* transcripts than either wild-type satellite cells (adult skeletal muscle stem cells) or *Myog*-deleted satellite cells. Furthermore, they had little more *Myog* than *Myog*-null myoblasts. I therefore concluded that C2C12 myoblasts were an unacceptable alternative for wild-type myoblasts.

Figure 42

Expression of *Myog* in various populations of skeletal muscle stem cells. *Myog* expression levels in C2C12 myoblasts are similar to that of *Myog*-deleted satellite cells or *Myog*-null myoblasts and are far less than that of wild-type satellite cells.

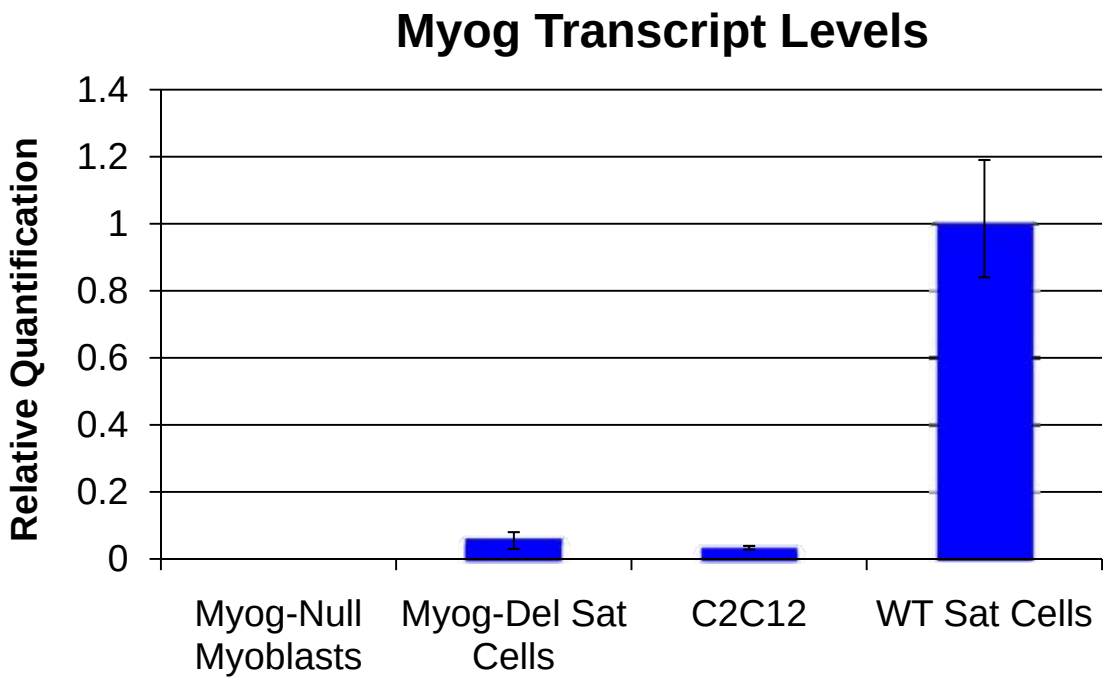
Myog Transcript Levels
Relative Quantification
1.4
1.2
1
0.8
0.6
0.4
0.2
0
Myog-Null Myoblasts
Myog-Del Sat Cells
C2C12
WT Sat Cells

Future Directions

To proceed with this project, several control experiments are necessary. The concentration of Dox required to recapitulate endogenous wild-type myogenin levels must be determined. In addition, the expression patterns of genes previously determined to be either embryonic-specific [47] or adult-specific [13] must be determined in the presence of myogenin to demonstrate that they recapitulate the gene activity patterns observed in the wild-type scenario. If these experiments are successfully completed, this system will provide a unique opportunity to identify the associated cofactors and chromatin marks in the presence and absence of myogenin using chromatin immunoprecipitation and MALDI-TOF mass spectrometry. With these approaches, we can begin elucidating the mechanisms conferring myogenin's selective target gene activation.

MATERIALS AND METHODS

Generation of *Myog*-deleted Mice

Mice used for this research were homozygous for the *Myog*^{flox} allele and harbored the CAGGCre-ER transgene [29, 111]. These animals consisted of a C57BL/6 and 129 mixed background. Efficient deletion of *Myog* genomic DNA in ~10 week old mice was achieved by a single injection of tamoxifen dissolved in corn oil at a concentration of 10mg/40g body weight. All experimental procedures described below followed the U.S. Public Health Service Policy on Human Care and Use of Laboratory Animals and were approved by the Institutional Animal Care and Use Committee at the The University of Texas M.D. Anderson Cancer Center. In chapter 1, wild-type mice are defined as tamoxifen-injected Myog$^{flox/flox}$ animals not harboring the Cre-recombinase gene. In chapter 2, wild-type mice are defined as tamoxifen-injected mdx:Myog$^{flox/flox}$ animals not harboring the Cre-recombinase gene.

Maximal Exercise Capacity

Involuntary Treadmill Running: Treadmill exercise regimes we derived from previously published protocols [112]. Adult wild-type and Myog-deleted mice were run on a rodent treadmill (Columbus Instruments Animal Treadmill: Exer 3/6). This treadmill is equipped with a rear electrical stimulus grid set to deliver 0.2 mA, an uncomfortable but not physically harmful shock. Mice were determined to have reached the point of exhaustion when they made contact

with the grid for a period of 10 seconds. The stimulus was then shut off in the lane of the exhausted mouse.

The low-intensity exercise regime consisted of mice warming up for a period of 30 minutes at 10 m/min (0° incline). The speed was then increased to 20m/min (0° incline), and mice were allowed to run to exhaustion. Exercise duration and distance were recorded at exhaustion.

The high-intensity exercise regime consisted of mice warming up for a period of 10 minutes at 10m/min on a 10° incline. The speed was then increased by 2 m/min every 2 minutes while maintaining a 10° incline until exhaustion. Exercise duration, distance, and maximum speed were recorded at exhaustion.

Voluntary Wheel Running: Cages containing exercise wheels were built in-house. Exercise wheels were suspended in the center of the cage and held in place by wires fastened to the cage top and base. One mouse was housed in each cage. Running wheels were connected to sensors recording time, average speed, maximum speed, and distance ran since the last reset.

Assay for Blood Glucose and Blood Lactate

Blood glucose concentration was determined by using a Precision Xtra glucometer (Abbott) at rest and within 30 seconds of reaching exhaustion. Blood lactate concentration was determined by using a Lactate Pro blood lactate test meter (Arkray) at rest and within 30 seconds of reaching exhaustion.

Histological Assays

Hind-limb muscles were dissected and snap frozen in LN_2-cooled isopentane. Ten to 12 μm fresh-frozen sections were then cut on a Cryostat.

Fiber Typing ATP Staining Protocol: A protocol from Washington University's Neuromuscular Disease Center (http://neuromuscular.wustl.edu/pathol/histol/atp.htm) was utilized to perform this assay. Sections were incubated for 5 min in pre-incubation solution pH 4.6 (5.0 mL Barbital Acetate Solution [1.47 g sodium barbital, 0.97 g sodium acetate, 50 mL final volume in H_2O], 10 mL 0.1N HCl, 4.0 mL H_2O), rinsed with H2O, and then incubated for 25 min in ATP solution H 9.4 (60 mg ATP powder, 6.0 mL of 0.1 M sodium barbital, 21.0 mL of H_2O, 3.0 mL of 0.18 M Calcium Chloride). Sections were washed with 3 exchanges of 1% calcium chloride for 10 min total, 2% cobalt chloride for 10 min, and 4 exchanges of 1:20 solution of 0.1M sodium barbital, 5 exchanges of H_2O. Sections were then exposed to 2% ammonium sulfide for 20-30 seconds, washed with 5 exchanges of H_2O, dehydrated in ascending alcohols, cleared with xylene, and mounted with canada balsam.

Succinate Dehydrogenase Enzyme Stain: A modified protocol [113] from the Universty of Nottingham Medical School was utilized for this assay (http://www.nottingham.ac.uk/pathology/protocols/sdh.html). Sections were incubated for 5 minutes in medium containing 0.2 mL of 500 mM sodium succinate, 0.7 mg phenazine methosulphate, and 2.0 mL NBT Solution (6.5 mg KCN, 185 mg EDTA, 100 mg Nitroblue tetrazolium, 100 mL 100mM phosphate buffer pH 7.6 {12 mL of Solution A [1.36g KH_2PO_4 in 100mL H_20] and 88 mL of

Solution B [1.42g Na_2HPO_4/100mL H_2O]}). Sections were then washed, fixed for 15 minutes in formaline, dehydrated in ascending alcohols, cleared with xylene, and mounted.

Glycogen Stain: The Periodic Acid-Schiff Staining System from Sigma-Aldrich was utilized for this assay. Sections were hydrated with deionized water, fixed with 10% neutral buffered formalin for 30 minutes, and then incubated in Periodic Acid Solution for 5 minutes at room temperature. Sections were then rinsed in distilled water and incubated in Schiff's Reagent for 15 minutes at room temperature. Slides were then washed in running tap water for 5 minutes and counterstained in Hematoxylin Solution for 90 seconds. Slides were again washed in running tap water, dehydrated in ascending alcohols, clear with 2 exchanges of Xylene, and mounted.

Fibrosis stain for Collagen and Elastin: Muscle sections were hydrated with deionized water and then fixed for 30 minutes in neutral buffered formalin. Slides were then incubated in Working Elastic Stain Solution for 10 minutes (20 mL Hematoxylin Solution, 3 mL Ferric Cholride Solution, 8mL Weigert's Iodine Solution, 5 mL Deionized water). Slides were then washed in deionized water and incubated in Wokring Ferric Chloride Solution for 1 minute (3mL Ferric Chloride Solution, 37 mL deionized water). Sections were then washed in tap water followed by rinsing in 95% alcohol. Slides were then rinsed in deionized water, incubated in Van Gieson Solution for 5 minutes, rinsed in 95% alcohol, dehydrated in ascending alcohols, cleared with 2 exchanges of Xylene, and mounted.

Affymetrix Gene Microarray Hybridization and Analysis

Hindlimb muscles of trained wild-type and *Myog*-deleted mice were treated with Trizol and used to isolate RNA from. Methods for this assay have been described previously [13]. Hybridization probes were prepared from 100 ng of total RNA from each sample. Three samples from each group tested were then utilized in standard Affymetrix protocols to yield biotin labeled cRNA fragments hybridized to Mouse Genome 430 2.0 GeneChips (Affymetrix, Santa Clara, CA). Affymetrix GCOS software with Robust Multi-chip Averaging normalization was employed to scan hybridized genechips [114]. For statistical analysis, two-tailed pooled t-tests were conducted with the minimum significance value set to $P<0.05$. Genes exhibiting expression changes greater than 1.4 fold were retained for additional experimentation. The microarray data discussed in this dissertation are MIAME compliant have been deposited in NCBI's Gene Expression Omnibus [115] and are accessible through GEO Series accession number GSE22046, (http://www.ncbi.nlm.nih.gov/geo/query/acc.cgi?acc=GSE22046).

RNA Isolation and qRT-PCR

RNA was isolated from hind-limb skeletal muscle of trained mice using the Qiagen RNeasy Plus kit protocol. Reverse transcription was performed as previously described [47]. TaqMan Gene Expression Assays (Applied Biosystems) were utilized to determine cDNA abundance for each gene assayed.

Enzymatic Analysis

Enzymatic analysis was performed on Soleus, Extensor Digitorum Longus (EDL), and Plantaris muscles from wild-type and *Myog*-deleted mice. An abbreviated protocol includes the following steps: fast- and slow-twitch muscles were isolated and snap frozen in LN_2. Muscle was homogenized in stabilizing medium at a 1:100 dilution based on wet weight. Stabilizing medium consists of 50% glycerol, 20 mM phosphate buffer, pH 7.4, 5 mM beta-mercaptoethanol, 0.5 mM EDTA, 0.02% BSA [28].

Assays performed include: Pyruvate Kinase (PK, EC 2.7.1.40), Hexokinase (HK, EC 2.7.1.1), Lactic Dehydrogenase (LDH, EC 1.1.1.27), Glycerophosphate Dehydrogenase (GOPDH, EC 1.1.1.8), Glycogen Phosphorylase (PHRL, EC 2.4.1.1), Fructose-6-Phosphate Kinase (PFK, EC 2.7.1.11), Adenylate Kinase (AK, EC 2.7.4.3), β-Hydroxybutyrate Dehydrogenase (BDH, EC 1.1.1.30), Carnitine Acetyltransferase (CAT, EC 2.3.1.7), Pyruvate Carboxylase (PC, EC 6.4.1.1), Citrate Synthase (Cit-Syn, (EC 4.1.3.7), β-Hydroxyacyl-CoA Dehydrogenase (BOAC, EC 1.1.1.35), and Malic Dehydrogenase (MDH, EC 1.1.1.37).

Cuvettes were prepared with the buffer and substrates required for the particular assay and monitored with a spectrophotometer at A_{340nm} until constant. Diluted homogenates were then added to each cuvette in duplicate and monitored with continuous spectrophotometric rate determination, recording the change in A_{340nm} for approximately 10 minutes at 25°C. The change in A_{340nm}/minute was determined using the maximum linear rate for both the test

and the blank. Enzyme activities are given as $mmol \cdot kg^{-1} \cdot min^{-1}$. Detailed protocol information is available from the Sigma Aldrich Enzyme Explorer Assay Library (http://www.sigmaaldrich.com/life-science/metabolomics/enzyme-explorer.html).

Biochemical determination of glycogen content

Soleus and extensor digitorum longus (EDL) muscles were harvested from wild-type, *mdx*, and *mdx:Myog*-deleted mice. An abbreviated protocol followed from MBL International Corporation (www.mblintl.com) includes the following steps: muscles were isolated and snap frozen in liquid nitrogen. Muscle was homogenized in dH_2O, boiled for 5 minutes, and centrifuged at 13,000rpm for 5min. Glucoamylase hydrolysis enzyme mix was then added to the supernatants. A master mix of development buffer, development enzyme mix, and OxiRed probe were then added to the samples and left to incubate at room temperature protected from light for 30 minutes. Samples were then measured colorimetrically using a spectrophotometer at a wavelength of 570nm. Non-hydrolysis control readings were then subtracted from the experimental raw values, and glycogen concentration was determined by applying the final values to a standard curve.

Statistical Analysis

Statistical analyses were performed using 2-tailed pooled student's *t*-tests in Microsoft Excel 2008. A confidence level of $p<0.05$ was considered to be

statistically significant. Error bars represent one standard deviation from the mean.

Increased Training Response: Thanks to the Department of Biostatistics for their help in the statistical analysis of this data. A general linear model was fitted to evaluate the effects of marker (wild-type vs. *Myog*-deleted), training status, and their interaction on dependent variable distance. Analysis indicates that when comparing to marker wild-type group, the difference in distance between the training and non-training groups is significantly different.

REFERENCES

1. Davis, R.L., H. Weintraub, and A.B. Lassar, *Expression of a single transfected cDNA converts fibroblasts to myoblasts.* Cell, 1987. **51**(6): p. 987-1000.

2. Braun, T., G. Buschhausen-Denker, E. Bober, E. Tannich, and H.H. Arnold, *A novel human muscle factor related to but distinct from MyoD1 induces myogenic conversion in 10T1/2 fibroblasts.* EMBO J, 1989. **8**(3): p. 701-9.

3. Braun, T., E. Bober, B. Winter, N. Rosenthal, and H.H. Arnold, *Myf-6, a new member of the human gene family of myogenic determination factors: evidence for a gene cluster on chromosome 12.* EMBO J, 1990. **9**(3): p. 821-31.

4. Miner, J.H. and B. Wold, *Herculin, a fourth member of the MyoD family of myogenic regulatory genes.* Proc Natl Acad Sci U S A, 1990. **87**(3): p. 1089-93.

5. Rhodes, S.J. and S.F. Konieczny, *Identification of MRF4: a new member of the muscle regulatory factor gene family.* Genes Dev, 1989. **3**(12B): p. 2050-61.

6. Edmondson, D.G. and E.N. Olson, *A gene with homology to the myc similarity region of MyoD1 is expressed during myogenesis and is sufficient to activate the muscle differentiation program.* Genes Dev, 1989. **3**(5): p. 628-40.

7. Wright, W.E., D.A. Sassoon, and V.K. Lin, *Myogenin, a factor regulating myogenesis, has a domain homologous to MyoD.* Cell, 1989. **56**(4): p. 607-17.

8. Molkentin, J.D. and E.N. Olson, *Defining the regulatory networks for muscle development.* Curr Opin Genet Dev, 1996. **6**(4): p. 445-53.

9. Braun, T., E. Bober, M.A. Rudnicki, R. Jaenisch, and H.H. Arnold, *MyoD expression marks the onset of skeletal myogenesis in Myf-5 mutant mice.* Development, 1994. **120**(11): p. 3083-92.

10. Braun, T., M.A. Rudnicki, H.H. Arnold, and R. Jaenisch, *Targeted inactivation of the muscle regulatory gene Myf-5 results in abnormal rib development and perinatal death.* Cell, 1992. **71**(3): p. 369-82.

11. Rudnicki, M.A., P.N. Schnegelsberg, R.H. Stead, T. Braun, H.H. Arnold, and R. Jaenisch, *MyoD or Myf-5 is required for the formation of skeletal muscle.* Cell, 1993. **75**(7): p. 1351-9.

12. Hasty, P., A. Bradley, J.H. Morris, D.G. Edmondson, J.M. Venuti, E.N. Olson, and W.H. Klein, *Muscle deficiency and neonatal death in mice with a targeted mutation in the myogenin gene.* Nature, 1993. **364**(6437): p. 501-6.

13. Meadows, E., J.H. Cho, J.M. Flynn, and W.H. Klein, *Myogenin regulates a distinct genetic program in adult muscle stem cells.* Dev Biol, 2008. **322**(2): p. 406-14.

14. Sherwood, L., *Human Physiology: From Cells to Systems*. 5th ed. 2004, Belmont, CA: Thomson Learning Inc. - Brooks/Cole. 256-299.

15. Bassel-Duby, R. and E.N. Olson, *Signaling pathways in skeletal muscle remodeling.* Annu Rev Biochem, 2006. **75**: p. 19-37.

16. Schiaffino, S., L. Gorza, S. Sartore, L. Saggin, S. Ausoni, M. Vianello, K. Gundersen, and T. Lomo, *Three myosin heavy chain isoforms in type 2 skeletal muscle fibres.* J Muscle Res Cell Motil, 1989. **10**(3): p. 197-205.

17. Bottinelli, R., R. Betto, S. Schiaffino, and C. Reggiani, *Unloaded shortening velocity and myosin heavy chain and alkali light chain isoform composition in rat skeletal muscle fibres.* J Physiol, 1994. **478 (Pt 2)**: p. 341-9.

18. Reiser, P.J., R.L. Moss, G.G. Giulian, and M.L. Greaser, *Shortening velocity in single fibers from adult rabbit soleus muscles is correlated with myosin heavy chain composition.* J Biol Chem, 1985. **260**(16): p. 9077-80.

19. Gorza, L., K. Gundersen, T. Lomo, S. Schiaffino, and R.H. Westgaard, *Slow-to-fast transformation of denervated soleus muscles by chronic high-frequency stimulation in the rat.* J Physiol, 1988. **402**: p. 627-49.

20. Mayne, C.N., T. Mokrusch, J.C. Jarvis, S.J. Gilroy, and S. Salmons, *Stimulation-induced expression of slow muscle myosin in a fast muscle of the rat. Evidence of an unrestricted adaptive capacity.* FEBS Lett, 1993. **327**(3): p. 297-300.

21. Windisch, A., K. Gundersen, M.J. Szabolcs, H. Gruber, and T. Lomo, *Fast to slow transformation of denervated and electrically stimulated rat muscle.* J Physiol, 1998. **510 (Pt 2)**: p. 623-32.

22. Gundersen, K., *Determination of muscle contractile properties: the importance of the nerve.* Acta Physiol Scand, 1998. **162**(3): p. 333-41.

23. Fitts, R.H. and J.J. Widrick, *Muscle mechanics: adaptations with exercise-training.* Exerc Sport Sci Rev, 1996. **24**: p. 427-73.

24. Tang, H., P. Macpherson, M. Marvin, E. Meadows, W.H. Klein, X.J. Yang, and D. Goldman, *A histone deacetylase 4/myogenin positive feedback loop coordinates denervation-dependent gene induction and suppression.* Mol Biol Cell, 2009. **20**(4): p. 1120-31.

25. Tang, H. and D. Goldman, *Activity-dependent gene regulation in skeletal muscle is mediated by a histone deacetylase (HDAC)-Dach2-myogenin signal transduction cascade.* Proc Natl Acad Sci U S A, 2006. **103**(45): p. 16977-82.

26. Moresi, V., *Myogenin and class II HDACs trigger skeletal muscle atrophy by inducing E3 ubiquitin ligases* 2010.

27. Hughes, S.M., J.M. Taylor, S.J. Tapscott, C.M. Gurley, W.J. Carter, and C.A. Peterson, *Selective accumulation of MyoD and myogenin mRNAs in fast and slow adult skeletal muscle is controlled by innervation and hormones.* Development, 1993. **118**(4): p. 1137-47.

28. Hughes, S.M., M.M. Chi, O.H. Lowry, and K. Gundersen, *Myogenin induces a shift of enzyme activity from glycolytic to oxidative metabolism in muscles of transgenic mice.* J Cell Biol, 1999. **145**(3): p. 633-42.

29. Knapp, J.R., J.K. Davie, A. Myer, E. Meadows, E.N. Olson, and W.H. Klein, *Loss of myogenin in postnatal life leads to normal skeletal muscle but reduced body size.* Development, 2006. **133**(4): p. 601-10.

30. Robergs, R.A., F. Ghiasvand, and D. Parker, *Biochemistry of exercise-induced metabolic acidosis.* Am J Physiol Regul Integr Comp Physiol, 2004. **287**(3): p. R502-16.

31. Hood, D.A., *Mechanisms of exercise-induced mitochondrial biogenesis in skeletal muscle.* Appl Physiol Nutr Metab, 2009. **34**(3): p. 465-72.

32. Hagberg, H., *Intracellular pH during ischemia in skeletal muscle: relationship to membrane potential, extracellular pH, tissue lactic acid and ATP.* Pflugers Arch, 1985. **404**(4): p. 342-7.

33. Sahlin, K., *Metabolic Changes Limiting Muscle Performance*, in *Biochemistry of Exercise VI*, B. Saltin, Editor. 1986, Human Kinetics Publishers: Champaign, IL. p. 323-343.

34. Sahlin, K., L. Edstrom, H. Sjoholm, and E. Hultman, *Effects of lactic acid accumulation and ATP decrease on muscle tension and relaxation.* Am J Physiol, 1981. **240**(3): p. C121-6.

35. Sahlin, K., R.C. Harris, B. Nylind, and E. Hultman, *Lactate content and pH in muscle obtained after dynamic exercise.* Pflugers Arch, 1976. **367**(2): p. 143-9.

36. Sahlin, K. and J. Henriksson, *Buffer capacity and lactate accumulation in skeletal muscle of trained and untrained men.* Acta Physiol Scand, 1984. **122**(3): p. 331-9.

37. Sahlin, K., A. Katz, and J. Henriksson, *Redox state and lactate accumulation in human skeletal muscle during dynamic exercise.* Biochem J, 1987. **245**(2): p. 551-6.

38. Sahlin, K., M. Tonkonogi, and K. Soderlund, *Energy supply and muscle fatigue in humans.* Acta Physiol Scand, 1998. **162**(3): p. 261-6.

39. Laski, M.W., DE, *Lactic Acidosis*, in *Acid-Base Electrolyte Disorders: A Companion to Brenner and Rector's The Kidney*, T.H. DuBose, LL, Editor. 2002, Saunders: Philadelphia, PA. p. 83-107.

40. Busa, W.B. and R. Nuccitelli, *Metabolic regulation via intracellular pH.* Am J Physiol, 1984. **246**(4 Pt 2): p. R409-38.

41. Gevers, W., *Generation of Protons by Metabolic Processes Other Than Glycolysis in Muscle-Cells - Critical-View - Reply.* Journal of Molecular and Cellular Cardiology, 1979. **11**(3): p. 328-330.

42. Gevers, W., *Generation of protons by metabolic processes in heart cells.* J Mol Cell Cardiol, 1977. **9**(11): p. 867-74.

43. Hochachka, P.W. and T.P. Mommsen, *Protons and anaerobiosis.* Science, 1983. **219**(4591): p. 1391-7.

44. Smith, G.L., P. Donoso, C.J. Bauer, and D.A. Eisner, *Relationship between intracellular pH and metabolite concentrations during metabolic inhibition in isolated ferret heart.* J Physiol, 1993. **472**: p. 11-22.

45. Toffaletti, J.G., *Blood lactate: biochemistry, laboratory methods, and clinical interpretation.* Crit Rev Clin Lab Sci, 1991. **28**(4): p. 253-68.

46. Noakes, T.D., *1996 J.B. Wolffe Memorial Lecture. Challenging beliefs: ex Africa semper aliquid novi.* Med Sci Sports Exerc, 1997. **29**(5): p. 571-90.

47. Davie, J.K., J.H. Cho, E. Meadows, J.M. Flynn, J.R. Knapp, and W.H. Klein, *Target gene selectivity of the myogenic basic helix-loop-helix*

transcription factor myogenin in embryonic muscle. Dev Biol, 2007. **311**(2): p. 650-64.

48. Robinson, B.H., *Lactic acidemia and mitochondrial disease.* Mol Genet Metab, 2006. **89**(1-2): p. 3-13.

49. Carbone, M.A., D.A. Applegarth, and B.H. Robinson, *Intron retention and frameshift mutations result in severe pyruvate carboxylase deficiency in two male siblings.* Hum Mutat, 2002. **20**(1): p. 48-56.

50. Robinson, B.H., J. Oei, J.M. Saudubray, C. Marsac, K. Bartlett, F. Quan, and R. Gravel, *The French and North American phenotypes of pyruvate carboxylase deficiency, correlation with biotin containing protein by 3H-biotin incorporation, 35S-streptavidin labeling, and Northern blotting with a cloned cDNA probe.* Am J Hum Genet, 1987. **40**(1): p. 50-9.

51. Robinson, B.H., J. Oei, W.G. Sherwood, D. Applegarth, L. Wong, J. Haworth, P. Goodyer, R. Casey, and L.A. Zaleski, *The molecular basis for the two different clinical presentations of classical pyruvate carboxylase deficiency.* Am J Hum Genet, 1984. **36**(2): p. 283-94.

52. Yalcin, A., S. Telang, B. Clem, and J. Chesney, *Regulation of glucose metabolism by 6-phosphofructo-2-kinase/fructose-2,6-bisphosphatases in cancer.* Exp Mol Pathol, 2009. **86**(3): p. 174-9.

53. Atsumi, T., J. Chesney, C. Metz, L. Leng, S. Donnelly, Z. Makita, R. Mitchell, and R. Bucala, *High expression of inducible 6-phosphofructo-2-kinase/fructose-2,6-bisphosphatase (iPFK-2; PFKFB3) in human cancers.* Cancer Res, 2002. **62**(20): p. 5881-7.

54. Kurland, I.J., L. Li, A.J. Lange, J.J. Correia, M.R. el-Maghrabi, and S.J. Pilkis, *Regulation of rat 6-phosphofructo-2-kinase/fructose-2,6-bisphosphatase. Role of the NH2-terminal region.* J Biol Chem, 1993. **268**(19): p. 14056-64.

55. Marsin, A.S., C. Bouzin, L. Bertrand, and L. Hue, *The stimulation of glycolysis by hypoxia in activated monocytes is mediated by AMP-activated protein kinase and inducible 6-phosphofructo-2-kinase.* J Biol Chem, 2002. **277**(34): p. 30778-83.

56. Emery, A.E., *Population frequencies of inherited neuromuscular diseases--a world survey.* Neuromuscul Disord, 1991. **1**(1): p. 19-29.

57. Hoffman, E.P., R.H. Brown, Jr., and L.M. Kunkel, *Dystrophin: the protein product of the Duchenne muscular dystrophy locus.* Cell, 1987. **51**(6): p. 919-28.

58. Engel, A., Franzini-Armstrong, C, *Myology: basic and clinical*. 2004, New York, NY: McGraw-Hill Medical Pub. Division.

59. Bulfield, G., W.G. Siller, P.A. Wight, and K.J. Moore, *X chromosome-linked muscular dystrophy (mdx) in the mouse.* Proc Natl Acad Sci U S A, 1984. **81**(4): p. 1189-92.

60. Carnwath, J.W. and D.M. Shotton, *Muscular dystrophy in the mdx mouse: histopathology of the soleus and extensor digitorum longus muscles.* J Neurol Sci, 1987. **80**(1): p. 39-54.

61. Chamberlain, J.S., J.A. Pearlman, D.M. Muzny, R.A. Gibbs, J.E. Ranier, C.T. Caskey, and A.A. Reeves, *Expression of the murine Duchenne muscular dystrophy gene in muscle and brain.* Science, 1988. **239**(4846): p. 1416-8.

62. Dangain, J. and G. Vrbova, *Muscle development in mdx mutant mice.* Muscle Nerve, 1984. **7**(9): p. 700-4.

63. Head, S.I., D.A. Williams, and D.G. Stephenson, *Abnormalities in structure and function of limb skeletal muscle fibres of dystrophic mdx mice.* Proc Biol Sci, 1992. **248**(1322): p. 163-9.

64. Sicinski, P., Y. Geng, A.S. Ryder-Cook, E.A. Barnard, M.G. Darlison, and P.J. Barnard, *The molecular basis of muscular dystrophy in the mdx mouse: a point mutation.* Science, 1989. **244**(4912): p. 1578-80.

65. Tanabe, Y., K. Esaki, and T. Nomura, *Skeletal muscle pathology in X chromosome-linked muscular dystrophy (mdx) mouse.* Acta Neuropathol, 1986. **69**(1-2): p. 91-5.

66. De la Porte, S., S. Morin, and J. Koenig, *Characteristics of skeletal muscle in mdx mutant mice.* Int Rev Cytol, 1999. **191**: p. 99-148.

67. Wehling-Henricks, M., M. Oltmann, C. Rinaldi, K.H. Myung, and J.G. Tidball, *Loss of positive allosteric interactions between neuronal nitric oxide synthase and phosphofructokinase contributes to defects in glycolysis and increased fatigability in muscular dystrophy.* Hum Mol Genet, 2009. **18**(18): p. 3439-51.

68. Schiaffino, S., M. Sandri, and M. Murgia, *Activity-dependent signaling pathways controlling muscle diversity and plasticity.* Physiology (Bethesda), 2007. **22**: p. 269-78.

69. Gladden, L.B., *A lactatic perspective on metabolism.* Med Sci Sports Exerc, 2008. **40**(3): p. 477-85.

70. Venuti, J.M., J.H. Morris, J.L. Vivian, E.N. Olson, and W.H. Klein, *Myogenin is required for late but not early aspects of myogenesis during mouse development.* J Cell Biol, 1995. **128**(4): p. 563-76.

71. Sabourin, L.A. and M.A. Rudnicki, *The molecular regulation of myogenesis.* Clin Genet, 2000. **57**(1): p. 16-25.

72. Anderson, J.E., W.K. Ovalle, and B.H. Bressler, *Electron microscopic and autoradiographic characterization of hindlimb muscle regeneration in the mdx mouse.* Anat Rec, 1987. **219**(3): p. 243-57.

73. Coulton, G.R., J.E. Morgan, T.A. Partridge, and J.C. Sloper, *The mdx mouse skeletal muscle myopathy: I. A histological, morphometric and biochemical investigation.* Neuropathol Appl Neurobiol, 1988. **14**(1): p. 53-70.

74. Jin, Y., N. Murakami, Y. Saito, Y. Goto, K. Koishi, and I. Nonaka, *Expression of MyoD and myogenin in dystrophic mice, mdx and dy, during regeneration.* Acta Neuropathol, 2000. **99**(6): p. 619-27.

75. Torres, L.F. and L.W. Duchen, *The mutant mdx: inherited myopathy in the mouse. Morphological studies of nerves, muscles and end-plates.* Brain, 1987. **110 (Pt 2)**: p. 269-99.

76. Juel, C., *Lactate/proton co-transport in skeletal muscle: regulation and importance for pH homeostasis.* Acta Physiol Scand, 1996. **156**(3): p. 369-74.

77. Lindinger, M.I. and G.J. Heigenhauser, *The roles of ion fluxes in skeletal muscle fatigue.* Can J Physiol Pharmacol, 1991. **69**(2): p. 246-53.

78. Roth, D.A. and G.A. Brooks, *Lactate transport is mediated by a membrane-bound carrier in rat skeletal muscle sarcolemmal vesicles.* Arch Biochem Biophys, 1990. **279**(2): p. 377-85.

79. Wilson, M.C., V.N. Jackson, C. Heddle, N.T. Price, H. Pilegaard, C. Juel, A. Bonen, I. Montgomery, O.F. Hutter, and A.P. Halestrap, *Lactic acid efflux from white skeletal muscle is catalyzed by the monocarboxylate transporter isoform MCT3.* J Biol Chem, 1998. **273**(26): p. 15920-6.

80. Juel, C., C. Klarskov, J.J. Nielsen, P. Krustrup, M. Mohr, and J. Bangsbo, *Effect of high-intensity intermittent training on lactate and H+ release from human skeletal muscle.* Am J Physiol Endocrinol Metab, 2004. **286**(2): p. E245-51.

81. Arahata, K., S. Ishiura, T. Ishiguro, T. Tsukahara, Y. Suhara, C. Eguchi, T. Ishihara, I. Nonaka, E. Ozawa, and H. Sugita, *Immunostaining of skeletal and cardiac muscle surface membrane with antibody against Duchenne muscular dystrophy peptide.* Nature, 1988. **333**(6176): p. 861-3.

82. Glesby, M.J., E. Rosenmann, E.G. Nylen, and K. Wrogemann, *Serum CK, calcium, magnesium, and oxidative phosphorylation in mdx mouse muscular dystrophy.* Muscle Nerve, 1988. **11**(8): p. 852-6.

83. Megeney, L.A., B. Kablar, K. Garrett, J.E. Anderson, and M.A. Rudnicki, *MyoD is required for myogenic stem cell function in adult skeletal muscle.* Genes Dev, 1996. **10**(10): p. 1173-83.

84. Booth, F.W. and D.B. Thomason, *Molecular and cellular adaptation of muscle in response to exercise: perspectives of various models.* Physiol Rev, 1991. **71**(2): p. 541-85.

85. Ohlendieck, K. and K.P. Campbell, *Dystrophin-associated proteins are greatly reduced in skeletal muscle from mdx mice.* J Cell Biol, 1991. **115**(6): p. 1685-94.

86. Matsumura, K. and K.P. Campbell, *Dystrophin-glycoprotein complex: its role in the molecular pathogenesis of muscular dystrophies.* Muscle Nerve, 1994. **17**(1): p. 2-15.

87. Sander, M., B. Chavoshan, S.A. Harris, S.T. Iannaccone, J.T. Stull, G.D. Thomas, and R.G. Victor, *Functional muscle ischemia in neuronal nitric oxide synthase-deficient skeletal muscle of children with Duchenne muscular dystrophy.* Proc Natl Acad Sci U S A, 2000. **97**(25): p. 13818-23.

88. Thomas, G.D., M. Sander, K.S. Lau, P.L. Huang, J.T. Stull, and R.G. Victor, *Impaired metabolic modulation of alpha-adrenergic vasoconstriction in dystrophin-deficient skeletal muscle.* Proc Natl Acad Sci U S A, 1998. **95**(25): p. 15090-5.

89. Zhu, X., L.M. Heunks, L. Ennen, H.A. Machiels, H.F. Van Der Heijden, and P.N. Dekhuijzen, *Nitric oxide modulates neuromuscular transmission during hypoxia in rat diaphragm.* Muscle Nerve, 2006. **33**(1): p. 104-12.

90. Nisoli, E., E. Clementi, C. Paolucci, V. Cozzi, C. Tonello, C. Sciorati, R. Bracale, A. Valerio, M. Francolini, S. Moncada, and M.O. Carruba, *Mitochondrial biogenesis in mammals: the role of endogenous nitric oxide.* Science, 2003. **299**(5608): p. 896-9.

91. Lira, V.A., Q.A. Soltow, J.H. Long, J.L. Betters, J.E. Sellman, and D.S. Criswell, *Nitric oxide increases GLUT4 expression and regulates AMPK signaling in skeletal muscle.* Am J Physiol Endocrinol Metab, 2007. **293**(4): p. E1062-8.

92. Percival, J.M., K.N. Anderson, P. Gregorevic, J.S. Chamberlain, and S.C. Froehner, *Functional deficits in nNOSmu-deficient skeletal muscle: myopathy in nNOS knockout mice.* PLoS One, 2008. **3**(10): p. e3387.

93. Kirschner, M. and J. Gerhart, *Evolvability.* Proc Natl Acad Sci U S A, 1998. **95**(15): p. 8420-7.

94. Taylor, J.S. and J. Raes, *Duplication and divergence: the evolution of new genes and old ideas.* Annu Rev Genet, 2004. **38**: p. 615-43.

95. Bergstrom, D.A. and S.J. Tapscott, *Molecular distinction between specification and differentiation in the myogenic basic helix-loop-helix transcription factor family.* Mol Cell Biol, 2001. **21**(7): p. 2404-12.

96. Berkes, C.A. and S.J. Tapscott, *MyoD and the transcriptional control of myogenesis.* Semin Cell Dev Biol, 2005. **16**(4-5): p. 585-95.

97. Buckingham, M., L. Bajard, T. Chang, P. Daubas, J. Hadchouel, S. Meilhac, D. Montarras, D. Rocancourt, and F. Relaix, *The formation of skeletal muscle: from somite to limb.* J Anat, 2003. **202**(1): p. 59-68.

98. Nabeshima, Y., K. Hanaoka, M. Hayasaka, E. Esumi, S. Li, and I. Nonaka, *Myogenin gene disruption results in perinatal lethality because of severe muscle defect.* Nature, 1993. **364**(6437): p. 532-5.

99. Rawls, A., J.H. Morris, M. Rudnicki, T. Braun, H.H. Arnold, W.H. Klein, and E.N. Olson, *Myogenin's functions do not overlap with those of MyoD or Myf-5 during mouse embryogenesis.* Dev Biol, 1995. **172**(1): p. 37-50.

100. Black, B.L. and E.N. Olson, *Transcriptional control of muscle development by myocyte enhancer factor-2 (MEF2) proteins.* Annu Rev Cell Dev Biol, 1998. **14**: p. 167-96.

101. Olson, E.N. and W.H. Klein, *bHLH factors in muscle development: dead lines and commitments, what to leave in and what to leave out.* Genes Dev, 1994. **8**(1): p. 1-8.

102. Lassar, A.B., R.L. Davis, W.E. Wright, T. Kadesch, C. Murre, A. Voronova, D. Baltimore, and H. Weintraub, *Functional activity of myogenic HLH proteins requires hetero-oligomerization with E12/E47-like proteins in vivo.* Cell, 1991. **66**(2): p. 305-15.

103. Molkentin, J.D., B.L. Black, J.F. Martin, and E.N. Olson, *Cooperative activation of muscle gene expression by MEF2 and myogenic bHLH proteins.* Cell, 1995. **83**(7): p. 1125-36.

104. Murre, C., P.S. McCaw, H. Vaessin, M. Caudy, L.Y. Jan, Y.N. Jan, C.V. Cabrera, J.N. Buskin, S.D. Hauschka, A.B. Lassar, and et al., *Interactions between heterologous helix-loop-helix proteins generate complexes that bind specifically to a common DNA sequence.* Cell, 1989. **58**(3): p. 537-44.

105. Wasserman, W.W. and J.W. Fickett, *Identification of regulatory regions which confer muscle-specific gene expression.* J Mol Biol, 1998. **278**(1): p. 167-81.

106. de la Serna, I.L., Y. Ohkawa, C.A. Berkes, D.A. Bergstrom, C.S. Dacwag, S.J. Tapscott, and A.N. Imbalzano, *MyoD targets chromatin remodeling complexes to the myogenin locus prior to forming a stable DNA-bound complex.* Mol Cell Biol, 2005. **25**(10): p. 3997-4009.

107. Tapscott, S.J., *The circuitry of a master switch: Myod and the regulation of skeletal muscle gene transcription.* Development, 2005. **132**(12): p. 2685-95.

108. Cao, Y., R.M. Kumar, B.H. Penn, C.A. Berkes, C. Kooperberg, L.A. Boyer, R.A. Young, and S.J. Tapscott, *Global and gene-specific analyses show distinct roles for Myod and Myog at a common set of promoters.* EMBO J, 2006. **25**(3): p. 502-11.

109. Ohkawa, Y., C.G. Marfella, and A.N. Imbalzano, *Skeletal muscle specification by myogenin and Mef2D via the SWI/SNF ATPase Brg1.* EMBO J, 2006. **25**(3): p. 490-501.

110. Ohkawa, Y., S. Yoshimura, C. Higashi, C.G. Marfella, C.S. Dacwag, T. Tachibana, and A.N. Imbalzano, *Myogenin and the SWI/SNF ATPase Brg1 maintain myogenic gene expression at different stages of skeletal myogenesis.* J Biol Chem, 2007. **282**(9): p. 6564-70.

111. Hayashi, S. and A.P. McMahon, *Efficient recombination in diverse tissues by a tamoxifen-inducible form of Cre: a tool for temporally regulated gene activation/inactivation in the mouse.* Dev Biol, 2002. **244**(2): p. 305-18.

112. Hakimi, P., J. Yang, G. Casadesus, D. Massillon, F. Tolentino-Silva, C.K. Nye, M.E. Cabrera, D.R. Hagen, C.B. Utter, Y. Baghdy, D.H. Johnson, D.L. Wilson, J.P. Kirwan, S.C. Kalhan, and R.W. Hanson, *Overexpression of the cytosolic form of phosphoenolpyruvate carboxykinase (GTP) in skeletal muscle repatterns energy metabolism in the mouse.* J Biol Chem, 2007. **282**(45): p. 32844-55.

113. Pette, D. and K.R. Tyler, *Response of succinate dehydrogenase activity in fibres of rabbit tibialis anterior muscle to chronic nerve stimulation.* J Physiol, 1983. **338**: p. 1-9.

114. Katz, S., R.A. Irizarry, X. Lin, M. Tripputi, and M.W. Porter, *A summarization approach for Affymetrix GeneChip data using a reference training set from a large, biologically diverse database.* BMC Bioinformatics, 2006. **7**: p. 464.

115. Edgar, R., M. Domrachev, and A.E. Lash, *Gene Expression Omnibus: NCBI gene expression and hybridization array data repository.* Nucleic Acids Res, 2002. **30**(1): p. 207-10.

Vita

Jesse Michael James Flynn was born in Roswell, New Mexico on May, 26, 1982, the son of Kerry and Patti Flynn. After completing his work at Gregory-Portland High School, Portland, Texas in 2000, he entered Texas A&M University in College Station, Texas. He received the degree of Bachelor of Sciences with a major in biomedical sciences from Texas A&M in May, 2004. For the next year, he worked as a research technician in the Department of Biochemistry at Texas A&M University. In September of 2005 he entered The University of Texas Health Science Center at Houston Graduate School of Biomedical Sciences.

Permanent address:

11910 Fortune Park Dr

Houston, Texas 77047